Nanotechnology

PURPOSE-LED PUBLISHING™

TOPICAL REVIEW • OPEN ACCESS

Recent advances in nanofabrication strategies for biosensors: from precision nanopatterning to scalable, flexible, and AI-assisted manufacturing

To cite this article: Meryem Beyza Avci *et al* 2026 *Nanotechnology* **37** 422003

View the article online for updates and enhancements.

You may also like

- Advanced Microfabricated Biosensing Platforms for Healthcare and Research Applications
Zongqi Liu and Kaiyu Fu
- Nanoimprint lithography-based replication techniques for fabrication of metal and polymer biomimetic nanostructures for biosensor surface functionalization
Bharat Nowduri, Anette Britz-Grell, Monika Saumer et al.
- Fully printed and flexible multi-material electrochemical aptasensor platform enabled by selective graphene biofunctionalization
Shay Goff Wallace, Michael C Brothers, Zachary E Brooks et al.

This content was downloaded from IP address 161.9.131.30 on 26/10/2026 at 21:10

Nanotechnology

Check for updates

TOPICAL REVIEW

OPEN ACCESS

RECEIVED
23 August 2026

REVISED
22 September 2026

ACCEPTED FOR PUBLICATION
7 October 2026

PUBLISHED
21 October 2026

Original content from this work may be used under the terms of the Creative Commons Attribution 4.0 licence.

Any further distribution of this work must maintain attribution to the author(s) and the title of the work, journal citation and DOI.

Recent advances in nanofabrication strategies for biosensors: from precision nanopatterning to scalable, flexible, and AI-assisted manufacturing

Meryem Beyza Avci[1,2,4,6], **Furkan Kocer**[1,6], **Seda Nur Topkaya**[1,2], **Konstantinos Papatryfonos**[3] and **Arif E Cetin**[1,2,4,5,*]

[1] Izmir Biomedicine and Genome Center, Balcova, Izmir 35340, Türkiye
[2] Izmir International Biomedicine and Genome Institute, Dokuz Eylul University, Balcova, Izmir 35340, Türkiye
[3] Institute of Electronics, Microelectronics and Nanotechnology (IEMN), UMR CNRS 8520, University of Lille, Avenue Poincare, 59650 Villeneuve d'Ascq, France
[4] Department of Biophysics, Faculty of Medicine, Dokuz Eylul University, Balcova, Izmir 35340, Türkiye
[5] Department of Electrical and Electronics Engineering, Istanbul Atlas University, Kagithane, Istanbul 34408, Türkiye
[6] These authors contributed equally.
[*] Author to whom any correspondence should be addressed.

E-mail: arifengin.cetin@ibg.edu.tr

Keywords: biosensors, nanofabrication, nanolithography, scalable manufacturing, self-assembly, AI-assisted manufacturing

Abstract

Nanofabrication has become central to the development of high-performance biosensors by enabling precise control over sensing interfaces, enhanced signal transduction, and integration across optical, electrochemical, microfluidic, and wearable platforms. This review examines the evolution of biosensor nanofabrication from deterministic top-down patterning toward scalable and integrated manufacturing strategies. Top-down approaches, including electron-beam lithography, focused ion beam milling, nanoimprint lithography, reactive ion etching, and laser-based fabrication, are discussed alongside replication and transfer processes, soft lithography, lithography-free plasmonic structuring, and additive three-dimensional fabrication. Bottom-up strategies based on nanoparticle assembly, DNA nanotechnology, block-copolymer and nanoporous templating, and stimuli-responsive materials are further considered as routes to programmable nanoscale organization and functional biointerfaces. Particular attention is given to flexible and wearable biosensors, where substrate mechanics, conductive-interface fabrication, textile integration, epidermal microfluidics, packaging, power management, and wireless communication introduce manufacturing requirements beyond conventional rigid devices. Across these approaches, the review emphasizes that analytical sensitivity alone is insufficient for translation; nanoscale precision must be accompanied by reproducibility, scalable processing, stable biofunctionalization, antifouling performance, packaging, storage stability, and device-level quality control. Emerging AI-assisted fabrication and process optimization strategies are also discussed as tools for linking manufacturing parameters with structural and analytical performance. Overall, the review provides a manufacturing-oriented perspective on how hybrid nanofabrication strategies can bridge high-performance laboratory biosensors with reproducible, scalable, and application-ready sensing systems.

1. Introduction

Biosensors have become indispensable analytical platforms for healthcare, environmental monitoring, food safety, agriculture, and biodefense because they enable rapid, selective, and increasingly decentralized detection of biological and chemical targets. Advances in molecular biology, materials science, microelectronics, and nanotechnology have dramatically expanded the range of detectable biomarkers, from nucleic acids, proteins, and metabolites to pathogens, extracellular vesicles, and whole cells. At the

© 2026 The Author(s). Published by IOP Publishing Ltd

same time, the growing demand for point-of-care diagnostics, continuous health monitoring, wearable sensing, and personalized medicine has shifted biosensor development beyond laboratory-based analytical devices toward portable, integrated, and manufacturable sensing systems. Nanofabrication has played a central role in this transformation. By engineering structures with dimensions comparable to optical wavelengths, electron transport lengths, and biomolecular interaction scales, nanofabrication enables sensing mechanisms that are difficult or impossible to achieve using conventional microfabrication alone. Precisely controlled nanostructures can manipulate localized electromagnetic fields, increase effective surface area, regulate charge transport, control molecular transport, and create highly engineered biointerfaces. Consequently, advances in nanofabrication have driven major improvements across a wide range of biosensing technologies, including surface plasmon resonance (SPR), localized SPR (LSPR), surface-enhanced Raman scattering (SERS), photonic crystal and metasurface biosensors, field-effect transistor (FET) biosensors, electrochemical sensors, fluorescence-based platforms, and integrated optofluidic systems.

Traditionally, progress in biosensor nanofabrication has been evaluated primarily in terms of fabrication resolution and analytical performance. Considerable effort has been devoted to producing increasingly smaller feature sizes, narrower plasmonic gaps, higher-aspect-ratio nanostructures, denser nanoparticle assemblies, and stronger electromagnetic hotspots to improve sensitivity and lower limits of detection. While these advances have substantially improved device performance under laboratory conditions, they have also highlighted an important limitation: exceptional analytical performance does not necessarily translate into practical biosensor technologies. Many proof-of-concept devices demonstrate remarkable sensitivity but remain difficult to reproduce, expensive to manufacture, incompatible with scalable production, or challenging to integrate with biofunctionalization, packaging, and real-world sample analysis. Accordingly, the field has gradually shifted from pursuing nanostructure precision alone toward developing manufacturing-oriented fabrication strategies. Rather than considering nanofabrication as an isolated patterning process, recent studies increasingly treat it as part of a complete manufacturing workflow that includes material synthesis, scalable pattern replication, process control, microfluidic integration, surface functionalization, quality assurance, packaging, and system-level validation. In this context, manufacturing-related metrics, including process reproducibility, dimensional fidelity, fabrication tolerance, batch-to-batch consistency, yield, scalability, cost, and compatibility with downstream integration, have become as important as analytical sensitivity itself. This evolution reflects the broader transition of biosensors from academic demonstrations toward deployable diagnostic and monitoring technologies.

The rapid diversification of fabrication technologies during the last five years has further accelerated this transition. Conventional deterministic top-down approaches such as electron-beam lithography (EBL), focused ion beam (FIB) milling, photolithography, nanoimprint lithography (NIL), laser interference lithography (LIL), and plasma-based etching continue to provide precise control over nanoscale architectures while increasingly supporting scalable replication through master-template strategies. In parallel, hybrid manufacturing approaches have expanded to include transfer printing, roll-to-roll processing, soft lithography, additive manufacturing, laser-written conductive architectures, and three-dimensional microfabrication, enabling biosensors on flexible, wearable, and application-specific substrates. Bottom-up self-assembly has likewise evolved from simple nanoparticle aggregation toward programmable molecular architectures based on colloidal assembly, DNA nanotechnology, block copolymers, and bioinspired interfaces that complement deterministic fabrication with molecular-level organization. More recently, artificial intelligence has begun to influence fabrication through inverse design, process optimization, defect prediction, quality control, autonomous materials synthesis, and data-driven manufacturing workflows, providing new opportunities to improve reproducibility and manufacturing efficiency. Despite these advances, the literature remains highly fragmented. Most reviews focus on individual fabrication techniques, specific sensing mechanisms, or particular classes of biosensors. Reviews dedicated to EBL, NIL, soft lithography, additive manufacturing, plasmonic nanostructures, wearable biosensors, or self-assembled nanomaterials provide valuable technical insight but often discuss fabrication methods independently of their manufacturing implications. Conversely, reviews emphasizing biosensor performance frequently prioritize sensitivity, limit of detection, or selectivity while giving comparatively limited attention to reproducibility, manufacturability, process integration, quality control, and translational readiness. As a result, it remains difficult for readers to understand how different nanofabrication strategies compare within a common manufacturing framework or how individual fabrication decisions influence the practical deployment of biosensor technologies.

This review addresses this gap by examining nanofabrication strategies from a manufacturing-oriented perspective. Rather than ranking fabrication methods solely according to resolution or analytical performance, we discuss how each approach contributes to reproducibility, scalability, process integration, device robustness, and translational potential. We first examine deterministic top-down

nanofabrication and scalable lithographic techniques before discussing hybrid manufacturing routes, bottom-up and self-assembled architectures, flexible and wearable fabrication strategies, and the emerging role of artificial intelligence in fabrication-aware design, process optimization, quality control, and autonomous manufacturing. Finally, we consider the key translational challenges that continue to limit the widespread adoption of nanofabricated biosensors, including reproducibility, manufacturing variability, quality assurance, biofunctionalization, packaging, regulatory considerations, and real-world validation. The conceptual evolution of these fabrication strategies is summarized in figure 1(A), highlighting the transition from conventional nanopatterning toward scalable, three-dimensional, and AI-assisted manufacturing approaches for advanced biosensors. The growing commercial relevance of biochip technologies further reinforces the need for scalable and manufacturing-ready fabrication strategies. Based on the reported forecast growth and compound annual growth rate (CAGR), the global biochips market is estimated to increase from approximately USD 25.6 billion in 2023 to USD 97.9 billion by 2028, corresponding to an overall increase of USD 72.27 billion and a CAGR of 30.73% over the forecast period (figure 1(B)) [1]. This substantial market expansion further emphasizes the need to translate laboratory-scale biosensor concepts into reproducible, high-throughput, and economically viable manufacturing processes. Accordingly, process scalability, device-to-device consistency, material compatibility, quality control, and system integration are becoming increasingly important alongside conventional analytical performance metrics.

Because nanofabrication encompasses both nanoscale transducer formation and the micro- to macroscale processes required for device integration, packaging, and operation, this review adopts a manufacturing-oriented perspective that extends beyond nanoscale patterning alone. Enabling fabrication studies are included when they provide clear and transferable insights into biosensor design, reproducibility, integration, or scale-up, while direct biosensor demonstrations are distinguished from relevant advances in adjacent fields such as photonics, semiconductor processing, flexible electronics, and autonomous materials synthesis. The review focuses primarily on literature published between 2021 and 2026, supplemented by selected earlier studies where necessary to establish foundational fabrication principles. To enable systematic comparison across the diverse approaches considered, each fabrication strategy is evaluated in terms of feature control, achievable area and throughput, design freedom, material and substrate compatibility, biofunctionalization compatibility, dominant sources of variability, metrology and quality-control requirements, integration burden, typical manufacturing role, and readiness for scale-up. These criteria are consolidated in table 1, which provides a comparative framework and roadmap for the method-specific discussions that follow.

2. Application-driven device requirements and fabrication selection

Selection of a nanofabrication strategy should begin with the functional requirements of the intended biosensing application rather than with fabrication resolution alone. Different sensing modalities impose distinct constraints on geometry, material composition, surface architecture, mechanical properties, and system integration. Accordingly, the intended application first defines the device-level requirements, which subsequently guide the selection of appropriate structures and materials and, ultimately, the fabrication strategy. Within this framework, the optimal fabrication route is not necessarily the method that provides the smallest feature size, but rather the one that can reproducibly realize the structural and material characteristics required by the sensing mechanism while remaining compatible with sample handling, biofunctionalization, readout, and the intended manufacturing scale.

Optical biosensors provide a clear example of this application-driven relationship. In SERS, fluorescence, LSPR/SPR, photonic, and metasurface-based sensing, the operating wavelength must be considered together with the optical properties of the biological environment. Absorption, scattering, and autofluorescence are wavelength dependent, making the spectral characteristics of biological samples important constraints on excitation and emission wavelengths, particularly in bioimaging and *in vivo* applications [52]. These spectral requirements subsequently influence material selection, resonance conditions, and nanostructure geometry. In SERS, fabrication must additionally provide strong and reproducible electromagnetic hotspots, making nanogap dimensions, particle spacing, surface morphology, and hotspot uniformity critical manufacturing variables. Deterministic methods such as EBL and FIB are therefore valuable when precise nanoscale geometry is required, whereas NIL, LIL, and template-assisted approaches become increasingly attractive when similar optical responses must be reproduced over larger areas and

Table 1. Comparison of representative nanofabrication strategies for biosensor manufacturing, including fabrication principles, representative biosensor architectures, major advantages, limitations, scalability, typical manufacturing roles, and representative recent references.

Photolithography	UV mask-based or maskless exposure of photoresist followed by development, lift-off, or etch transfer.	Microfluidic biochips; SU-8 molds; PDMS lab-on-chip devices; patterned electrode arrays; polymer-based biochips; organ-on-chip biosensors.	Mature, repeatable, high-throughput, and compatible with semiconductor and microfluidic workflows.	Limited deep-nanoscale resolution; multistep processing; cleanroom dependence; limited flexibility for rapid design iteration.	High for wafer-scale and batch microfabrication; moderate for rapid prototyping.	Wafer-scale microstructures; electrode definition; SU-8 master fabrication; microfluidic channel layouts; polymer biochip workflows.	[11–14]
Electron-beam lithography (EBL)	Direct-write focused electron beam exposure of resist, followed by development, metal lift-off, or etch transfer.	Plasmonic nanohole arrays; nanogaps; SERS metasurfaces; photonic crystals; nanophotonic biosensors; SiNW-FET-related test structures; NIL master molds.	Nanometer-scale precision; arbitrary geometry; excellent control over pitch, gap size, shape, and alignment.	Serial writing; high cost; low throughput; limited large-area manufacturability.	Low throughput; best for research-scale devices, reference structures, and master molds.	High-resolution plasmonic/nanophotonic patterning; mechanistic studies; reference devices; master fabrication for replication methods.	[15–17]
Focused ion beam processing (FIB)	Maskless, site-specific ion-beam milling, sputtering, trimming, or direct nanostructure modification.	Plasmonic nanoapertures; nanogaps; nanopores; SERS-active templates; optical-fiber nanostructures; localized nanophotonic prototypes.	Resist-free direct writing; site-specific modification; suitable for difficult or nonplanar substrates; useful for rapid prototyping and local trimming.	Ion implantation; amorphization; redeposition; surface contamination; low throughput; high cost.	Low throughput; localized prototyping and template fabrication rather than mass production.	Precision prototyping; localized modification; plasmonic nanoaperture fabrication; SERS template fabrication; optical-fiber integration.	[18–21]
Laser interference lithography (LIL)	Interference of coherent laser beams creates periodic exposure patterns over large areas.	Periodic plasmonic arrays; gratings; photonic crystals; SERS substrates; metamaterial absorbers; guided-mode resonance or objective-free optical biosensors.	Parallel large-area patterning; rapid fabrication of periodic nanostructures; lower cost than serial direct-write methods.	Mainly limited to periodic or quasi-periodic geometries; poor suitability for arbitrary layouts and complex multiplexed designs.	High for periodic large-area strulctures.	Large-area periodic templates; optical biosensor surfaces; plasmonic/SERS arrays; photonic crystal structures.	[13, 22–24] .

(Continued.)

Table 1. (Continued.)

Nanoimprint lithography (NIL)	Mechanical, thermal, or UV-assisted replication of a nanostructured master into imprint resist.	Disposable plasmonic chips; photonic crystal biosensors; metasurface sensors; large-area optical biosensor platforms; replicated nanostructured biochips.	High-resolution replication; high throughput after master fabrication; suitable for disposable and large-area devices.	Requires high-quality master mold, defect control, stamp durability, and re-fabrication of the mold for design changes.	High after master fabrication; suitable for replication and batch manufacturing.	Replication of EBL/FIB-defined masters; disposable optical biosensor chips; photonic and plasmonic nanostructure copying.	[13, 25–27]
RIE/ICP-RIE/DRIE	Plasma-based anisotropic dry etching transfers lithographically defined patterns into silicon, dielectric, or hard-material substrates.	SiNW-FETs; vertical silicon nanowire arrays; photonic crystals; waveguides; silicon nitride resonators; nanochannels; microfluidic channels; high-aspect-ratio vias.	Strong pattern transfer; high-aspect-ratio structuring; semiconductor compatibility; essential for silicon and photonic biosensor fabrication.	Etch lag; scalloping; sidewall tapering; microtrenching; mask erosion; plasma damage; roughness; process sensitivity.	Moderate to high; compatible with wafer-scale processing but process-dependent.	Pattern transfer; etch-depth control; sidewall definition; Si/SiN photonic device fabrication; microfluidic and nanofluidic channel formation.	[28–32]
Soft lithography (replica molding)	Replica molding or casting, typically using PDMS on a micro/nanostructured master, to form microfluidic channels and structured polymer devices.	PDMS microfluidic biochips; lab-on-chip devices; fluidic integration around optical/electrochemical sensing interfaces.	Rapid prototyping; relatively low cost after master fabrication; optical transparency; straightforward integration with microfluidics.	Master fabrication requirements; PDMS deformation and material limitations; curing incompatibility with some 3D-printed mold resins.	Moderate to high for prototyping and small-batch fabrication.	Fabrication of fluid-handling structures and polymer device layers surrounding biosensing interfaces.	[33–35]
Roll-to-roll (R2R) manufacturing	Continuous web-based imprinting, coating, printing, or functional-layer deposition onto flexible substrates.	Foil-based diagnostic chips; flexible sensor substrates; large-area printed or replicated sensing layers.	Very high throughput; low unit cost; continuous large-area processing; compatibility with flexible substrates.	Registration and alignment control; defect propagation; layer uniformity; strong dependence on in-line metrology and process control.	Very high; suitable for industrial-scale continuous manufacturing.	Mass manufacturing of flexible biochips, replicated micro/nanostructures, electrode layers, and sensing substrates.	[36, 37]

(Continued.)

Table 1. (Continued.)

Additive manufacturing (3D printing)	Layer-by-layer digital fabrication using FFF/FDM, extrusion, material jetting, SLA/DLP, or related additive processes.	3D electrochemical biosensors; microfluidic devices; customized sensor bodies and electrodes.	High design freedom; rapid and tool-free iteration; customizable 3D geometries; potential integration of microfluidics and electrodes.	Lower resolution than advanced lithography; surface roughness; material and biocompatibility constraints; post-processing requirements.	Moderate; best suited to rapid prototyping, customized devices, and low-volume production.	Rapid prototyping, personalized biosensor fabrication, complex microfluidic structures, and low-volume production.	[35, 38]
Two-photon polymerization/two-photon lithography	Nonlinear localized photopolymerization enables direct writing of high-resolution three-dimensional micro/nanostructures.	Bioelectronic 3D microstructures; high-resolution molds and 3D architectures relevant to biosensing.	High three-dimensional design freedom; substantially finer resolution than conventional 3D printing; fabrication of complex freeform structures.	Serial writing; limited throughput and build volume; photosensitive-material and post-processing constraints.	Low to moderate; specialized high-resolution prototyping rather than high-throughput manufacturing.	Specialized high-resolution prototyping, 3D biointerfaces, and master/mold fabrication.	[34, 39]
Colloidal nanoparticle self-assembly	Spontaneous or directed organization of nanoparticles through interfacial, ligand-mediated, electrostatic, capillary, or DNA-programmed interactions.	Ordered plasmonic/photonic nanoparticle assemblies and hotspot-rich sensing interfaces.	Mask-free and solution-processable; programmable nanoparticle spacing and composition; compatible with multicomponent assembly.	Assembly kinetics and efficiency; domain defects; particle dispersity; limited arbitrary pattern placement and batch reproducibility.	Moderate; potentially large-area but strongly process-dependent.	Bottom-up generation of ordered nanoparticle sensing interfaces and plasmonic/photonic architectures.	[40, 41]
DNA origami	Watson-Crick base pairing folds DNA scaffolds into addressable nanostructures that position nanoparticles, reporters, and recognition elements with nanoscale precision.	LFIA signal-amplification systems; nanopore, optical, and plasmonic nanosensing architectures.	Extremely high programmability and addressability; nanometer-scale spatial control; multivalent signal amplification and dynamic functionality.	Oligonucleotide cost; structural stability; nuclease and ionic-condition sensitivity; assembly-yield and device-integration challenges.	Low to moderate; solution-based batch assembly and primarily research-scale manufacturing.	Molecular-scale organization of receptors and reporters; signal amplification; programmable nanosensing architectures.	[42, 43]

(Continued.)

Table 1. (Continued.)

Block copolymer self-assembly	Microphase separation of chemically distinct polymer blocks creates periodic nanoscale domains that can serve as functional interfaces or templates.	Nanobiosensor surfaces; biomolecule-patterning interfaces; periodic nanoscale templates.	Parallel nanoscale patterning; potentially sub-10-nm dimensions; low-cost large-area organization; tunable feature periodicity.	Defect density; domain orientation and registration; dependence on polymer chemistry, solvent, annealing, and pattern-transfer conditions.	Moderate to high for periodic large-area nanopatterning.	Creation of nanoscale templates, high-density biomolecular interfaces, and directed nanostructure organization.	[44, 45]
Template-assisted nanostructuring (AAO, nanosphere/ colloidal, and sacrificial templates)	Preformed or self-assembled templates define nanoscale pores, masks, or removable scaffolds for deposition, etching, or material growth	Nanowire/nanorod arrays, nanoporous electrodes, nanohole/nanoring arrays, SERS/LSPR substrates, nanochannel sensors	Low-cost nanoscale patterning; high surface area; tunable pore/feature geometry; compatible with large-area fabrication	Template defects and transfer/removal steps; AAO barrier-layer processing; self-assembly defects; geometry dependent on template quality	Moderate-High; cm2-scale colloidal patterning and large-area AAO possible	Scalable alternative to serial lithography for ordered, porous, and high-surface-area sensing interfaces	[46–51]

Note: Scalability/throughput classifications represent qualitative assessments based on the fabrication characteristics and manufacturing considerations reported in the cited literature.

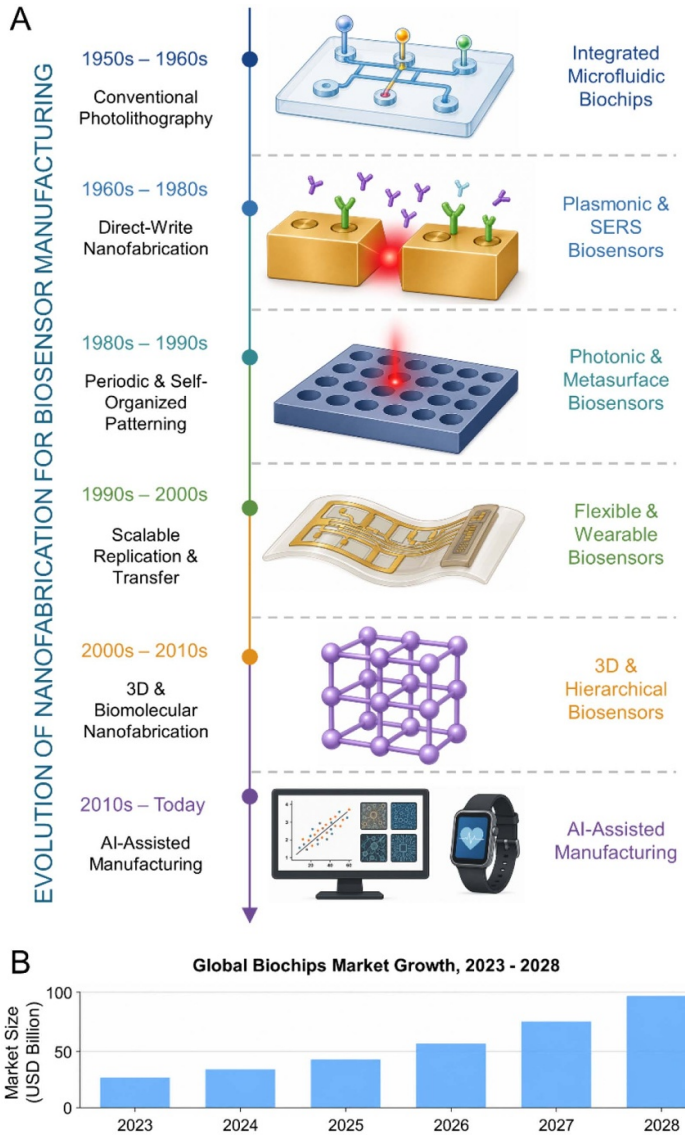


Figure 1. Evolution of nanofabrication strategies for biosensor manufacturing. (A) The timeline summarizes major milestones from photolithography, EBL, FIB, and LIL to self-assembly, NIL, block-copolymer patterning, multiphoton lithography, transfer-based fabrication, and AI-assisted manufacturing. Rather than defining strict historical generations, it illustrates the expansion of nanofabrication from precision patterning toward scalable replication, molecular and three-dimensional organization, flexible-device integration, and data-driven manufacturing [2–10]. (B) Estimated global biochips market growth from 2023 to 2028, with annual market-size values derived from the reported USD 72.27 billion increase and a compound annual growth rate (CAGR) of 30.73% over the forecast period [1].

at higher throughput. Recent optical nanobiosensor studies further emphasize that portability, integration with microfluidics, reproducibility, and scalable manufacturing become increasingly important when optical sensing is translated toward point-of-care applications [53, 54].

Electrical biosensors impose a different set of requirements. In FET-based biosensors, device performance is strongly influenced by channel geometry, transducing material, dielectric and interface properties, ionic screening, surface functionalization, and electrical noise. In particular, Debye screening in physiological environments directly affects the coupling of biomolecular binding events to the transistor channel and therefore becomes an important consideration in device and interface design. Consequently, nanowire, nanosheet, and two-dimensional-material FET architectures require fabrication strategies capable of controlling channel dimensions and interfaces while maintaining compatibility with subsequent biofunctionalization. Lithographic patterning combined with controlled plasma etching is particularly suitable for such semiconductor-compatible architectures [55, 56]. In electrochemical biosensors, by contrast, high electrochemically active surface area and efficient analyte transport may be more important than deterministic nanoscale placement. Porous, nanoparticle-modified, and three-dimensional electrodes can therefore benefit from printing, electrodeposition, templating, or additive fabrication, provided that conductivity, surface chemistry, and device-to-device reproducibility are maintained.

For microfluidic and point-of-care biosensors, fabrication requirements increasingly extend beyond the sensing interface to the complete sample-to-answer architecture. Sample volume, analyte transport, assay time, reagent handling, multiplexing, sealing, alignment, disposability, and cost can influence practical performance as strongly as the nanoscale transducer itself. A handheld optofluidic SPR platform, for example, combined a compact microfluidic architecture with cleanroom-free chamber fabrication and high-throughput nanohole-array fabrication to address portability and scalability requirements [57]. Accordingly, photolithography and soft lithography remain useful for controlled microfluidic prototyping, whereas molding, thermoplastic replication, printing, and roll-to-roll-compatible processes become increasingly relevant when low-cost disposable production is required. The fabrication strategy should therefore be selected jointly for the sensing interface and the surrounding sample-handling architecture rather than optimized independently.

Flexible and wearable biosensors introduce additional mechanical and biointerface constraints. Devices intended for skin-interfaced or continuous monitoring must maintain sensing performance during bending, stretching, repeated motion, biofluid exposure, and prolonged contact with biological surfaces. Conformability, elastic modulus, stretchability, fatigue resistance, adhesion, encapsulation, and integration with electronics therefore become explicit device-level requirements. Recent analyses emphasize that wearable biosensor development requires the coupled consideration of mechanics, structural design, biointerface engineering, and fabrication rather than optimization of the sensing material in isolation [58]. These requirements favor compliant polymeric or textile substrates, stretchable interconnects, printed or transferred functional materials, and laser-based fabrication strategies. Recent literature similarly links wearable sensing requirements to material flexibility, biofluid collection, scalable fabrication, and standardized device validation [59, 60].

Taken together, these examples demonstrate that nanofabrication strategies should be evaluated according to their ability to satisfy application-specific device requirements, rather than through resolution or throughput alone. The same fabrication method may therefore serve different roles across sensing modalities, while similar analytical targets may require different manufacturing routes depending on the biological matrix, transduction mechanism, production volume, and operating environment. Table 2 summarizes this application-driven selection framework and provides a practical link between biosensor requirements and the fabrication strategies discussed in the following sections.

3. Top-down nanofabrication for high-performance biosensors

Top-down methods remain essential when biosensor performance depends on deterministic control of geometry, alignment, and material interfaces. While earlier studies primarily emphasized achieving the smallest possible feature sizes, recent developments increasingly prioritize manufacturing-oriented metrics, including pattern-transfer fidelity, process reproducibility, scalable replication, semiconductor compatibility, and integration with biofunctionalization and readout systems. This evolution reflects a broader shift in biosensor engineering from demonstrating isolated high-performance devices toward developing robust, manufacturable sensing platforms. Fabrication quality directly influences biosensor performance because variations in nanoscale geometry and material interfaces can alter optical, electrical, and fluidic responses. This sensitivity makes dimensional fidelity and process uniformity central considerations in top-down biosensor fabrication. This section examines these complementary top-down routes from the perspective of fabrication precision, scalability, process integration, and biosensor manufacturability (figure 2).

3.1. Deterministic high-resolution patterning: EBL, FIB, and silicon-compatible nanostructures

EBL and FIB milling remain the benchmark techniques for deterministic nanofabrication when biosensor performance depends on precise control of nanoscale geometry, alignment, and electromagnetic field confinement. Their direct-write capability enables the fabrication of plasmonic nanohole arrays, engineered nanogaps, photonic crystals, metasurfaces, nanodot antennas, and silicon nanowire field-effect transistor (SiNW-FET) biosensors with feature dimensions and spatial arrangements that directly govern resonance wavelength, hotspot localization, linewidth, optical coupling, and refractive-index sensitivity. For nanophotonic biosensors, deterministic patterning has enabled systematic investigation of plasmonic, dielectric, and hybrid nanostructures for label-free sensing, fluorescence enhancement, SERS, SPR/LSPR, and metasurface-based detection. Because these sensing mechanisms rely on highly localized light–matter interactions, structural reproducibility across the sensing surface is essential for quantitative measurements [15]. Consequently, EBL and FIB increasingly function as upstream fabrication tools

Table 2. Application-driven framework for selecting nanofabrication strategies for biosensors.

Application	Primary device requirement	Structure/material implication	Critical fabrication requirement	Suitable strategies	References
SERS	High electromagnetic enhancement; reproducible hotspots; operation in complex samples	Au/Ag nanogaps, nanoarrays, hotspot-rich surfaces	Nanogap and morphology control; hotspot uniformity and reproducibility	EBL, FIB, NIL, template-assisted nanostructuring	[52, 61]
Fluorescence/Bioimaging	Spectral compatibility; low background; efficient excitation/emission; appropriate optical penetration	Plasmonic antennas, metasurfaces, photonic structures; wavelength-compatible materials	Resonance and dimensional control; optical/material compatibility	EBL, NIL, LIL, template-assisted fabrication	[53, 54]
FET	High surface sensitivity; low noise; operation under ionic screening	Nanowire/nanosheet/2D channels; controlled dielectric and biointerface	Channel and interface control; process uniformity; biofunctionalization compatibility	Lithography, RIE/ICP-RIE, semiconductor processing	[55, 56]
Electrochemical	High active area; conductivity; efficient mass transport	Porous, nanoparticle-modified, or 3D electrodes	Surface/material reproducibility; electrical continuity	Printing, electrodeposition, templating, additive fabrication	[62, 63]
POC/microfluidic	Low sample volume; rapid transport; multiplexing; disposability; low cost	Integrated channels, chambers, and sensing interfaces	Bonding, alignment, sealing, scalable replication and transducer integration	Photolithography, soft lithography, molding, printing, R2R	[53, 57, 63]
Wearable	Conformability; stretchability; adhesion; mechanical durability; biofluid compatibility	Compliant substrates, stretchable conductors and interconnects	Mechanical reliability; encapsulation; substrate/process compatibility	Transfer printing, screen/inkjet printing, laser fabrication, textile processing	[58–60]

for producing reference devices, validating nanoscale design rules, and generating master templates for subsequent large-area replication rather than as standalone manufacturing technologies (figure 3).

A recent example of this fabrication logic is the resonant quantum-tunneling plasmonic biosensor reported by Lee *et al*, in which lithographically defined Au nanowires with widths of approximately 92 nm and a period of 400 nm were integrated on a metal–insulator–metal tunneling structure containing an approximately 5 nm Al_2O_3 barrier [64]. The device architecture combined nanoscale plasmonic patterning with a precisely controlled tunneling junction, allowing the metasurface itself to serve as both the electrically driven light-emitting structure and the biosensing interface. The corresponding device geometry and cross-sectional nanoscale characterization are shown in figure 3(A), illustrating how deterministic lithography can be used not only to define resonant nanostructures, but also to integrate optical excitation, transduction, and sensing within a single nanofabricated platform. For SiNW-FET biosensors, the principal advantage of top-down fabrication lies in its compatibility with established semiconductor manufacturing processes. Precise control of nanowire dimensions, doping profiles, oxide thickness, and array architecture enables reproducible electrical characteristics and facilitates large-scale integration. However, recent studies indicate that the major challenge has shifted from nanowire fabrication itself to controlling process variability across large sensor arrays. Variations in nanowire width, line-edge roughness, oxide quality, and surface functionalization can alter threshold voltage, transconductance, electrical noise, and biosensing performance, making process uniformity a key limitation for practical implementation [28].

FIB complements EBL by enabling direct maskless milling, trimming, and modification of nanostructures without resist processing. Its localized fabrication capability makes it particularly valuable for rapid prototyping, optical-fiber integration, post-fabrication optimization, and site-specific fabrication of plasmonic and SERS-active nanostructures. For example, Yang *et al* fabricated arrays containing more

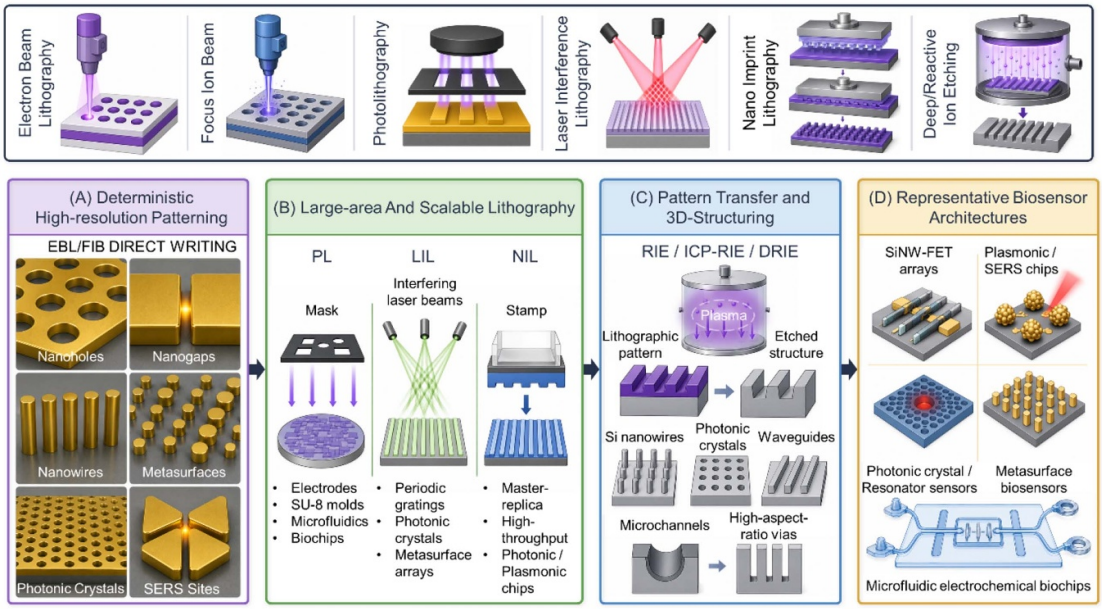


Figure 2. Top-down nanofabrication strategies for high-performance biosensors. The schematic summarizes deterministic nanopatterning by electron-beam lithography (EBL) and focused ion beam (FIB), scalable patterning by photolithography, laser interference lithography (LIL), and nanoimprint lithography (NIL), and plasma-based pattern transfer by reactive-ion etching (RIE) and deep reactive-ion etching (DRIE). Together, these approaches support silicon nanowire FETs, plasmonic and SERS substrates, photonic and metasurface biosensors, and microfluidic electrochemical platforms.

than 64 inverted-bowtie plasmonic nanoapertures with gap sizes of 10–20 nm and single-nanometer fabrication variation using FIB milling [20]. The resulting nanoapertures enabled label-free trapping and interrogation of individual proteins for observation times on the order of minutes, demonstrating the capability of deterministic FIB fabrication for single-molecule biosensing (figure 3(B)). FIB-defined templates have also been used for controlled assembly of SERS-active nanoparticle dimers [21]. Nevertheless, beam-induced damage, including ion implantation, amorphization, redeposition, and surface contamination, together with inherently low throughput remains a significant limitation. Accordingly, recent roadmaps emphasize that future advances will depend on improved automation, contamination control, damage mitigation, and integration with complementary nanofabrication processes [19]. Despite their unmatched precision, EBL and FIB remain primarily valuable for prototype fabrication and master-template generation because their serial nature limits direct high-volume manufacturing.

3.2. Scalable lithography: photolithography, LIL, NIL, and high-throughput patterning

Scalable fabrication has become a central requirement for translating nanofabricated biosensors from laboratory prototypes to practical devices. Many optical biosensors, including plasmonic chips, photonic crystals, guided-mode resonance sensors, metasurfaces, SERS substrates, and SPR/LSPR arrays, require uniform nanostructures over centimeter- or wafer-scale areas to ensure consistent performance under macroscopic illumination, multiplexed readout, or low-cost imaging systems. Consequently, the key challenge has shifted from achieving the smallest possible feature size to reproducibly replicating functional nanostructures over large sensing areas. Conventional photolithography remains one of the most mature manufacturing technologies because of its high throughput, precise alignment capability, and seamless compatibility with semiconductor processing and microfluidic integration. Rather than competing with direct-write nanolithography, it increasingly serves as the manufacturing backbone for electrodes, SU-8 molds, microfluidic components, patterned biointerfaces, and hybrid biochip architectures, where reproducibility and multilayer integration are generally more important than ultimate nanoscale resolution [13, 14, 59, 65]. Recent work has further expanded conventional photolithography to wearable biosensors. Wang *et al* combined polymer-assisted metal deposition with double-sided photolithography to fabricate permeable textile electronics with sub-100 μm patterning resolution, 10 000-cycle bending stability, and 20-cycle washing durability while preserving fabric breathability. The platform enabled integrated multiplexed sweat biosensing, illustrating how photolithography can be extended beyond rigid substrates toward scalable wearable biosensor manufacturing (figure 3(C)) [66].

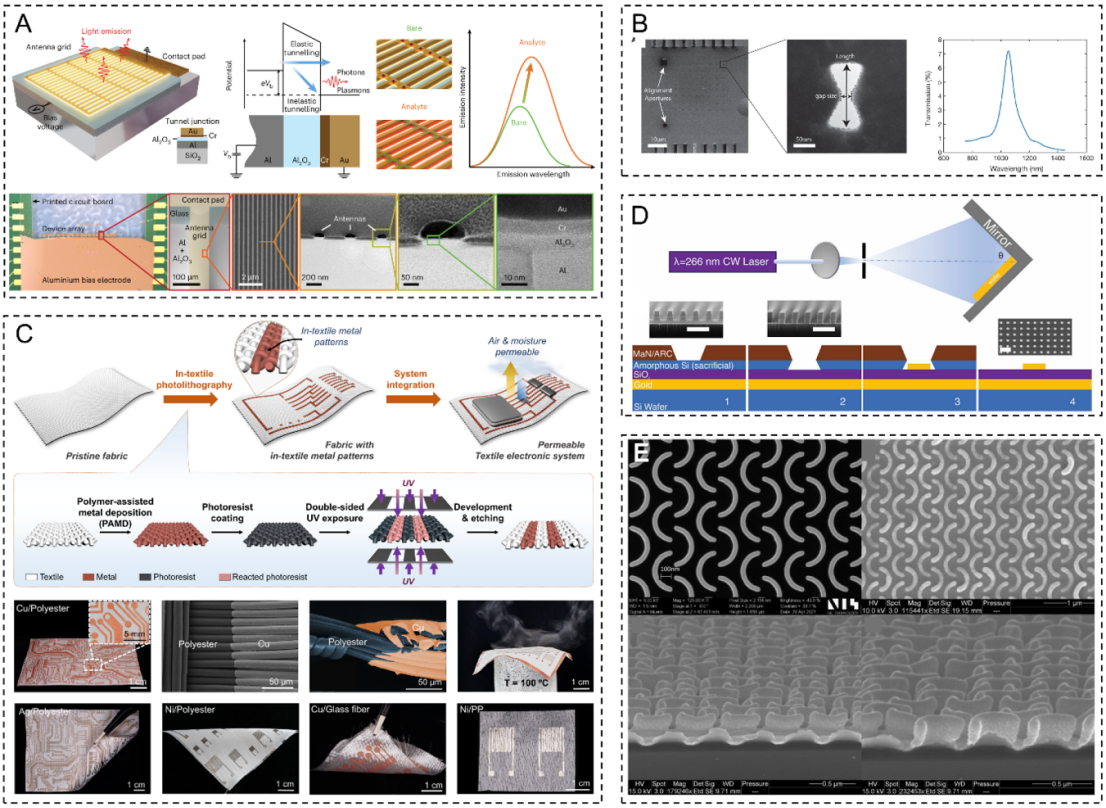


Figure 3. Representative lithographic patterning strategies for biosensor-oriented micro- and nanofabrication. (A) Resonant quantum-tunneling plasmonic metasurface integrating a metal–insulator–metal tunneling junction with optical and electron-microscopy characterization for biosensing. Adapted from [64], Copyright© 2025 Springer Nature. (B) FIB-milled inverted-bowtie nanoapertures fabricated in a 100 nm Au film on a freestanding SiN membrane for label-free single-protein trapping, with SEM/TEM characterization and simulated optical transmission. Adapted from [20]. Copyright© 2021 Elsevier. (C) In-textile photolithography of Cu, Ag, and Ni circuits on polyester, glass-fiber, and non-woven PP substrates, demonstrating lithographic integration with wearable electronics. Adapted from [66], Copyright© 2024 Springer Nature. (D) Laser interference lithography for large-area periodic metamaterial biosensors, including interference exposure, pattern transfer, metallization, lift-off, and SEM characterization. Adapted from [23], Copyright© 2024 American Chemical Society. (E) UV-NIL replication of C-shaped plasmonic SERS nanopatterns from a Si master to Au-coated imprinted substrates. Adapted from [69], Copyright© 2023, MDPI.

LIL addresses large-area nanopatterning through the parallel exposure of periodic structures using coherent laser interference. Because exposure time is largely independent of patterned area, LIL is particularly attractive for photonic crystals, diffraction gratings, plasmonic arrays, and metasurface biosensors. Recent demonstrations include centimeter-scale metamaterial absorber arrays fabricated within minutes for label-free protein detection and reusable optical sensing, together with deep-UV LIL platforms capable of producing 75 nm half-pitch periodic nanostructures over large areas [23, 24]. For example, Koç *et al* fabricated 4 cm^2 plasmonic metamaterial surfaces exhibiting a refractive-index sensitivity of 685 nm RIU^{-1}, radius variation of only ±6 nm, and resonance wavelength deviations below 1% across the sensing area, demonstrating that LIL can achieve centimeter-scale structural and optical uniformity while maintaining optical performance comparable to EBL-fabricated structures (figure 3(D)) [23]. However, LIL remains largely restricted to periodic architectures and offers limited flexibility for arbitrary nanostructure layouts.

NIL provides a complementary solution by replicating nanoscale patterns from a high-resolution master mold into polymer resists. This master-replica strategy converts the cost of serial nanofabrication into an efficient high-throughput manufacturing process and enables reproducible optical and interfacial nanostructures over useful device areas, making NIL particularly attractive for plasmonic chips, photonic crystal biosensors, metasurfaces, SERS substrates, biomimetic interfaces, and disposable optical sensors [67, 68]. A representative example was reported by Milenko *et al*, who developed UV-NIL-fabricated C-shaped plasmonic nanopatterns optimized for 785 nm excitation [69]. By directly coating gold onto the replicated resist structures, the process eliminated silicon etching, reducing process complexity and manufacturing cost while supporting reproducible, high-throughput fabrication of SERS substrates (figure 3(E)). Recent studies demonstrate that NIL-fabricated photonic crystal slabs can support

quasi-bound-state-in-the-continuum resonances suitable for label-free biosensing, highlighting that large-area replication can preserve high optical performance while significantly improving manufacturability [26]. Each scalable lithographic technique offers distinct advantages. Photolithography provides excellent alignment accuracy and compatibility with semiconductor manufacturing, but is limited in nanoscale resolution. LIL enables rapid, low-cost fabrication of periodic nanostructures over large areas but offers limited design flexibility. NIL combines high resolution with large-area replication but remains dependent on master-mold quality, stamp durability, residual-layer control, and defect accumulation during repeated imprinting. Method selection therefore depends on the required architecture, area, and process compatibility.

Several additional lithographic techniques, including deep-UV, EUV, immersion, and x-ray lithography, together with scanning probe, edge, and near-field lithography, extend the capabilities of conventional patterning but remain largely confined to specialized research or semiconductor manufacturing because of their cost, infrastructure requirements, or limited throughput [27, 70, 71]. Other methods such as soft lithography, stereolithography, two-photon lithography, block copolymer lithography, nanosphere lithography, electrohydrodynamic lithography, capillary force lithography, magnetolithography, magnetorheological drawing lithography, and nanotransfer printing are discussed in later sections where flexible substrates, additive manufacturing, hybrid fabrication, or self-assembly become the primary focus [71–73]. These patterned structures must subsequently be transferred into functional device architectures through controlled etching processes.

3.3. Plasma-based pattern transfer: RIE/DRIE for silicon, photonic, and microfluidic biosensors

Reactive-ion etching (RIE), inductively coupled plasma RIE (ICP-RIE), cryogenic RIE, and deep RIE (DRIE) transform lithographically defined patterns into functional silicon, dielectric, photonic, and microfluidic structures. Beyond simple material removal, these processes determine etch depth, sidewall angle, surface roughness, aspect ratio, and dimensional fidelity, directly influencing electrical, optical, and fluidic performance. For resonant sensing structures, fabrication roughness can impose a performance ceiling rather than merely introduce a small perturbation [74]. Modeling of optical and nanoacoustic DBR cavities has shown that nanometer-scale top-layer roughness or material inhomogeneities can broaden resonances, limit the maximum achievable quality factor, and reduce the ability of open resonators to resolve stimulus-induced frequency shifts; the same analysis highlights polishing and planarization as possible mitigation strategies [75]. Topological interface-state designs may provide an additional route toward fabrication-tolerant resonators, as they have demonstrated enhanced robustness to layer-thickness disorder compared with conventional Fabry–Perot cavities, [76, 77] whether this robustness extends to surface-roughness-induced degradation in sensing architectures remains to be established. Related sensing-oriented semiconductor-photonic work illustrates how e-beam pattern definition, RIE chemistry, etch depth, duty cycle, sidewall quality, and grating-to-waveguide spacing jointly determine optical coupling and loss [74]. In a regrowth-free laterally-coupled DFB laser platform developed for absorption-spectroscopy applications, optimization of high-duty-cycle etched gratings produced strong feedback while avoiding the additional loss associated with metallic gratings [74, 78]. Plasma-based etching should therefore be regarded as a performance-defining stage of biosensor fabrication rather than merely a post-lithography processing step. In silicon nanowire field-effect transistor (SiNW-FET) biosensors, RIE defines nanowire geometry and substantially influences threshold voltage, transconductance, electrical noise, and surface-charge sensitivity. Process-induced variations in nanowire width, line-edge roughness, oxide quality, and interface chemistry remain major sources of device-to-device variability [28]. Wafer-scale fabrication of ultrasmall silicon nanowires for cystatin C detection further illustrates how precise etch control directly contributes to clinically relevant sensing performance [79].

Cryogenic DRIE extends these capabilities by producing vertical silicon nanowire arrays and other high-aspect-ratio structures with tunable morphology and smooth sidewalls [29]. Although primarily demonstrated as a fabrication study, this work is directly relevant because nanowire geometry determines sensing surface area, analyte accessibility, electric-field distribution, and measurement reproducibility in many biosensor platforms. In integrated photonic biosensors, plasma etching critically determines waveguide dimensions, sidewall roughness, and resonance quality. CMOS-compatible photonic biosensors rely on highly controlled etching to maintain low optical loss and stable resonance characteristics [80]. Representative examples include inverse-designed silicon-on-insulator waveguide biosensors fabricated using EBL followed by plasma etching, [32] ICP-RIE optimization of tantalum oxide photonic crystal waveguides, [81] and silicon nitride photonic crystal-assisted microring resonators, where nanoscale fabrication precision directly governs Fano resonance behavior [82].

Plasma etching also underpins the fabrication of microfluidic and nanofluidic biosensors by producing anisotropic channels, chambers, vias, and other high-aspect-ratio structures that regulate analyte transport, residence time, mixing efficiency, and hydraulic resistance [30, 83]. Accordingly, DRIE contributes not only to nanoscale sensing elements but also to the sample-handling architectures essential for practical biosensor operation. For plasmonic, SERS, and metasurface biosensors, the importance of RIE depends on device architecture. While metallic nanostructures are often fabricated by lift-off or direct lithography, plasma etching becomes indispensable whenever nanoholes, nanopillars, dielectric resonators, or photonic slabs must be transferred into semiconductor or dielectric substrates. These examples collectively demonstrate that reproducible nanoscale geometry is fundamental to achieving reliable optical performance [17, 84]. Despite its versatility, plasma etching remains highly process-sensitive. Etch lag, aspect-ratio dependence, sidewall tapering, microtrenching, scalloping, plasma-induced damage, and surface roughness can degrade electrical characteristics, broaden optical resonances, increase leakage, or alter fluidic performance. Future advances will therefore depend on improved etch uniformity, sidewall control, damage mitigation, and integration with scalable lithography, in-line metrology, and AI-assisted process monitoring. Plasma-based pattern transfer thus represents a critical link between lithographic pattern definition and manufacturable biosensor performance.

4. Scalable, hybrid, and three-dimensional nanofabrication approaches

While deterministic top-down nanofabrication provides the precision required for high-performance biosensors, practical sensing platforms also demand scalability, cost efficiency, substrate compatibility, and integration with large-area or three-dimensional device architectures. These requirements become particularly important for disposable diagnostics, point-of-care testing, wearable monitoring, microfluidic systems, and multiplexed arrays, where fabrication must reproduce functional sensing structures over technologically useful areas and on application-compatible substrates. Recent manufacturing strategies increasingly combine scalable replication, substrate transfer, polymer processing, self-assembly, and additive fabrication to translate nanoscale sensing functionality into application-compatible device formats (figure 4).

4.1. Replication and transfer-based manufacturing: NIL, roll-to-roll, and nanotransfer printing

Roll-to-roll NIL extends this concept from batch replication to continuous manufacturing. Khumwan *et al* translated a COVID-19 serology assay from injection-molded microfluidic chips to foil-based lateral-flow devices fabricated using UV-NIL and extrusion coating, illustrating the potential of web-compatible imprinting for scalable point-of-care production, as shown in figure 4(A) [36]. Continuous patterning on flexible polymer webs is particularly attractive for disposable, wearable, and large-area optical biosensors, although practical implementation depends on web registration, mold durability, substrate deformation, and repeated pattern fidelity [60, 85, 86]. Nanotransfer printing addresses a complementary challenge by decoupling nanostructure fabrication from the final substrate. Metallic, dielectric, semiconductor, or plasmonic features can first be prepared on a donor and subsequently transferred to flexible, textile, elastomeric, or polymeric receivers using adhesion-controlled printing or stamping. This enables high-resolution structures to be integrated onto substrates that cannot tolerate aggressive lithography, solvents, vacuum processing, or etching [87]. Together, NIL, roll-to-roll processing, and nanotransfer printing shift nanofabrication from one-time pattern definition toward repeated and substrate-flexible device production. Their translational limitations arise primarily from master degradation, defect propagation, residual-layer control, stamp deformation, adhesion, overlay accuracy, and loss of nanoscale fidelity during repeated replication or transfer [71, 88–90]. Successful replication ultimately depends on yield, structural fidelity, and device-level stability.

4.2. Lithography-free and template-assisted plasmonic nanostructures

Lithography-free and template-assisted approaches provide cost-effective alternatives to serial EBL or FIB for producing plasmonic biosensor surfaces over relatively large areas. The manufacturing routes considered here include evaporation-driven colloidal deposition, nanoparticle aggregation, thin-film dewetting, nanosphere lithography, and template-guided formation of ordered plasmonic structures. Their principal trade-off is reduced dependence on direct nanoscale pattern writing versus less deterministic control over feature size, interparticle gaps, long-range order, and hotspot distribution. This distinction is particularly important for SERS and LSPR sensing, where morphology directly determines field enhancement and quantitative reproducibility [25]. The molecular mechanisms underlying colloidal and block-copolymer self-assembly are discussed separately in sections 4.1 and 4.3.

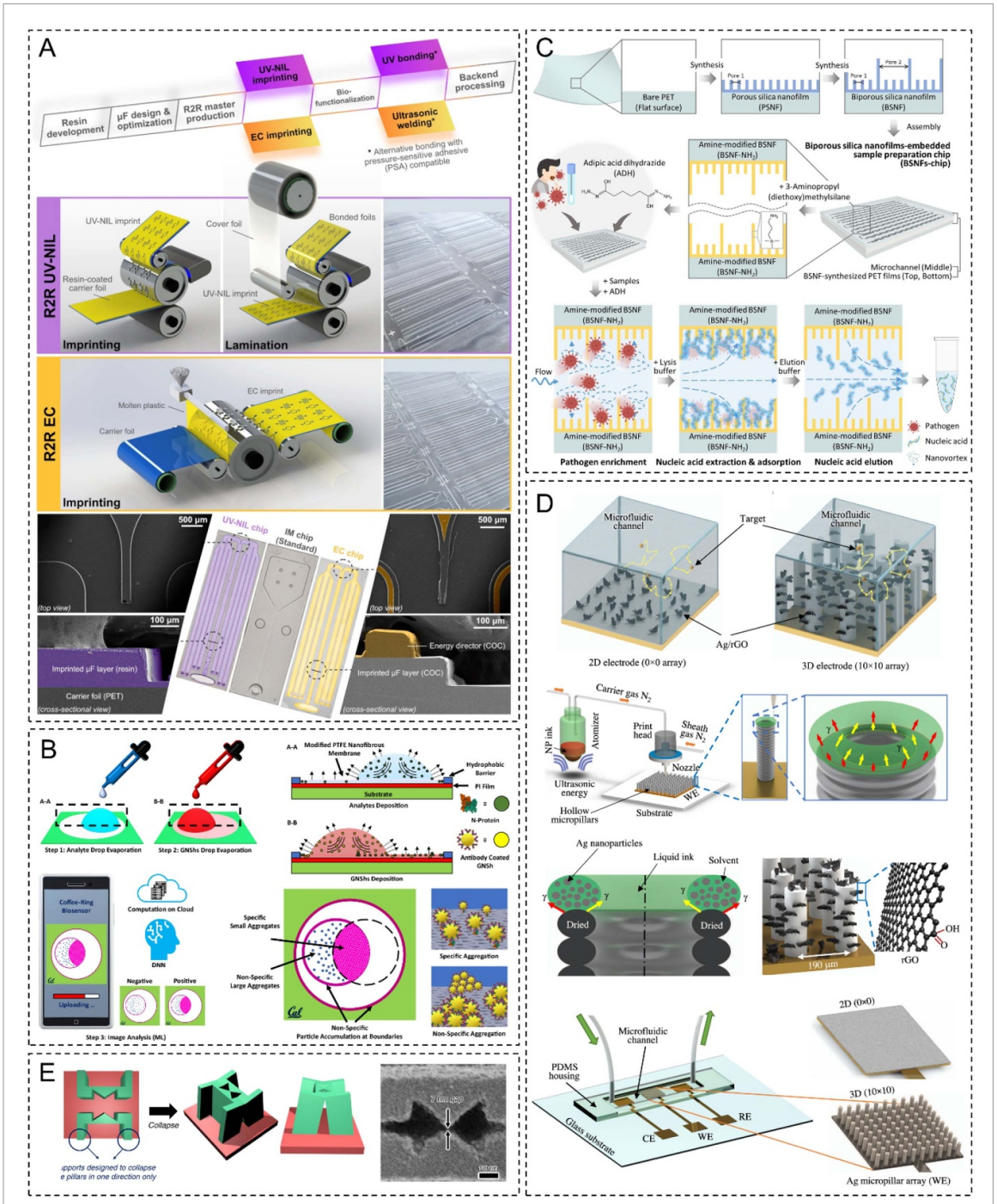


Figure 4. Representative scalable, hybrid, and three-dimensional nanofabrication approaches for biosensor-oriented platforms. (A) Roll-to-roll-compatible UV-NIL and extrusion-coating manufacture of foil-based lateral-flow chips for COVID-19 serology, illustrating scalable polymer diagnostic-chip production. Adapted from [36], Copyright© 2025 MDPI. (B) Lithography-free plasmonic coffee-ring biosensing combining evaporation-driven biomarker preconcentration, gold-nanoshell assembly, smartphone imaging, and deep-learning-assisted analysis. Adapted from [91], Copyright© 2025, Springer Nature. (C) PET microfluidic sample-preparation chip incorporating biporous silica nanofilms for pathogen enrichment, nucleic-acid extraction, and PCR-free detection. Adapted from [115], Copyright© 2024 Springer Nature. (D) Aerosol-jet-printed three-dimensional Ag micropillar electrodes coated with reduced graphene oxide and integrated into a PDMS microfluidic dopamine sensor. Adapted from [117], Copyright© 2021 Springer Nature. (E) Capillary-collapse lithography for ordered sub-10 nm plasmonic bowtie gaps relevant to SERS and nanosensing. Adapted from [131], Copyright© 2020 Springer Nature.

Evaporation-driven colloidal deposition provides a particularly simple lithography-free route for simultaneously concentrating analytes and forming plasmonically active particle assemblies. Behrouzi *et al*, for example, developed a lithography-free coffee-ring biosensor in which evaporation-driven assembly concentrated protein biomarkers into asymmetric gold-nanoshell patterns that were quantified using smartphone imaging and deep learning, as shown in figure 4(B) [91]. Such approaches are highly attractive for inexpensive disposable sensing, although random hotspot distributions remain a major source of

particle-to-particle and batch-to-batch variability [92]. Dewetting provides a more substrate-integrated lithography-free route. Thin Au, Ag, or bimetallic films reorganize into nanoislands or particles through thermal, laser-induced, or solid-state processing, with morphology controlled by film thickness, annealing conditions, substrate properties, and multilayer design. Dewetted Au nanoislands have supported self-referenced LSPR detection of protein adsorption, while solid-state dewetting on tapered optical fibers has been used to tune nanoisland morphology for SERS sensing [93, 94]. Hybrid multilayer strategies can further improve hotspot engineering, as demonstrated by Au/Al_2O_3/Au nanoarchitectures and Ag-dewetted Au nanoparticle arrays [95, 96].

Template assistance provides greater spatial control than random colloidal assembly or dewetting while avoiding serial nanoscale writing. Nanosphere lithography uses self-assembled colloidal masks to produce large-area nanoprisms, nanoholes, and related periodic plasmonic structures, providing greater optical uniformity than random films [97]. Other template systems enable more complex architectures, e.g. anodic-aluminum-oxide-derived templates have produced three-dimensional bimetallic plasmonic nanopillars for serum biomarker profiling, while nanocup-array metasurface sensors have been combined with catalytic signal amplification for portable cancer-biomarker detection [98, 99]. Block-copolymer templating provides an additional route to nanoscale particle and pore organization and is discussed in section 4.3, where the emphasis is on the underlying self-assembly mechanism and its biosensor applications. Random films and dewetted structures offer low-cost hotspot generation but generally lower spatial uniformity, whereas template-assisted arrays improve reproducibility at the cost of additional processing and defect-control requirements. For practical biosensing, either route must ultimately combine controlled morphology with reproducible biofunctionalization, antifouling behavior, and quantitative calibration.

4.3. Soft lithography and polymer-based micro/nanofabrication for biochips

Soft lithography occupies a different role from high-resolution nanopatterning because its primary value lies in integrating nanostructured transducers with fluid handling and biological samples. polydimethylsiloxane (PDMS) replica molding remains widely used for fabricating microchannels, chambers, valves, mixers, droplet generators, and cell-culture compartments because PDMS combines optical transparency, elasticity, gas permeability, and straightforward bonding to glass, silicon, or polymer substrates [14, 34, 100]. Microfluidic integration can directly determine biosensor performance by controlling sample volume, analyte transport, incubation, washing, and multiplexing. Patterned plasmonic arrays integrated with microfluidics have been used for SPR, LSPR, SPR imaging, and SERS analysis, while microfluidic electrochemical platforms provide controlled transport over modified electrodes with reduced reagent consumption [101, 102]. Channel geometry itself influences mass transport: decreasing channel height can enhance molecular recruitment, while stopped-flow and diffusion-controlled formats provide spatiotemporal control over BioFET and multiplexed assays [103, 104]. Soft-lithographic integration also supports portable biosensing. A print-and-stick microfluidic SPR platform coupled to smartphone imaging enabled point-of-care β2-microglobulin detection, illustrating how simplified polymer assembly can reduce the cost and complexity of conventional optofluidic devices [105]. More broadly, microfluidics can combine sample preparation, reaction control, and signal readout within compact diagnostic platforms [106].

Elastomeric microfluidics is similarly important for flexible and wearable devices because channels can conform to skin or tissue and route sweat, interstitial fluid, or reagents toward sensing zones. PDMS-based and related soft systems are widely used in wearable and implantable biointerfaces, while liquid-metal microfluidic architectures demonstrate how mechanically compliant channels can support stretchable sensing, including glucose detection [107, 108]. Organ-on-chip and cell-based biosensors exploit the same properties of PDMS for gas exchange, cell culture, optical observation, and integration with electrical or optical sensors [14]. However, PDMS also introduces well-known limitations, including small-molecule absorption, nonspecific adsorption, solvent swelling, evaporation, oligomer leaching, and hydrophobic recovery after plasma treatment, all of which can affect quantitative assays and drug-screening applications [109, 110]. These limitations motivate a transition toward thermoplastics such as COC, COP, PMMA, PC, and polyethylene terephthalate (PET), which offer better solvent resistance, lower small-molecule absorption, improved storage stability, and greater compatibility with scalable manufacturing. COC biochips have already been demonstrated for DNA hybridization assays, while reviews of thermoplastic microfluidics emphasize that molding, bonding, optical properties, and surface functionalization must be co-optimized for reproducible device manufacture [111–113].

Other polymer platforms, e.g. including UV-curable materials, polyacrylates, hydrogels, elastomers, and 3D-printed molds, further expand the design space. Polyacrylate microfluidics integrated with

nanostructured optical aptasensors have improved protein detection relative to PDMS-based configurations, while PET-based microfluidic sample-preparation chips containing biporous silica nanofilms have combined pathogen enrichment, nucleic-acid isolation, and PCR-free detection, as shown in figure 4(C) [114, 115]. Soft lithography and polymer processing therefore provide the integration layer that converts nanostructured transducers into practical biochips. PDMS remains highly effective for rapid prototyping, whereas thermoplastics and alternative polymers are increasingly important for scalable, disposable, and application-ready devices.

4.4. Three-dimensional fabrication and vertically integrated biosensor architectures

Three-dimensionality enters biosensor manufacturing in two distinct ways. First, additive and direct-write fabrication methods, including aerosol-jet printing, multiphoton lithography, stereolithography, and digital light processing, can directly produce non-planar structures that are difficult to realize using conventional planar processing. Second, established micro- and nanofabrication processes can be used to construct vertically integrated or high-aspect-ratio device architectures, [116] such as micropillar electrodes and stacked nanosheet FETs. These approaches should be distinguished because the former are primarily evaluated by resolution, material compatibility, throughput, and post-processing requirements, whereas the latter are justified by whether three-dimensional geometry provides a measurable sensing advantage, such as increased active area, improved analyte access, enhanced optical interaction, or greater sensing functionality within a limited footprint. Aerosol-jet printing illustrates how a three-dimensional fabrication process can directly improve electrochemical sensor architecture. Ali *et al* fabricated Ag micropillar electrodes coated with reduced graphene oxide (rGO) and integrated them into a PDMS microfluidic device for dopamine sensing (figure 4(D)) [117]. The vertically extended electrode geometry increases the electrochemically active surface area without a proportional increase in device footprint, illustrating a direct fabrication-enabled advantage of three-dimensional electrode design. More broadly, porous and high-aspect-ratio electrodes can increase receptor loading and analyte-accessible surface area, although these benefits must be balanced against reproducibility of morphology, functionalization, and mass transport [118]. Notably, flexible nanotube-array microelectrodes have enabled real-time H_2O_2 monitoring from living cells and human specimens [119].

For semiconductor biosensors, vertically stacked and gate-all-around architectures can increase effective sensing area and channel width within a compact lateral footprint. TCAD analysis of a vertically stacked nanosheet gate-all-around FET predicted higher biosensing sensitivity than nanowire and vertically stacked nanowire FET architectures, primarily owing to its larger channel width and multiple sensing channels [120]. More recently, a fabricated three-dimensional stacked silicon nanosheet FET with 8 nm interlayer cavities was specifically designed to mitigate Debye shielding through complementary sensing from opposing surfaces. The device demonstrated DNA detection in 1× PBS and approximately tenfold higher sensitivity than a planar device at high DNA concentration, providing experimental evidence that three-dimensional device architecture can improve FET sensing under high-ionic-strength conditions [121]. Such architectures, however, demand precise multilayer fabrication, dielectric control, surface functionalization, alignment, and process uniformity. Three-dimensional optical and plasmonic architectures provide a related geometry-driven advantage, with vertically extended or porous SERS substrates increasing analyte-accessible surface area and distributing electromagnetic hotspots throughout the sensing volume relative to planar substrates;[122] the template-assisted and self-assembly routes used to fabricate many such structures are discussed in sections 3.2 and 4.

Multiphoton lithography, or two-photon polymerization, enables freeform three-dimensional microstructures inaccessible to planar processing. Organic semiconductor composites have been patterned into functional 3D architectures for flexible electronics and biosensing, while two-photon-written structures followed by metallization or PEDOT:PSS electrodeposition have produced conductive bioelectronic microarchitectures [39, 123]. The main advantage is simultaneous control of geometry and biointerface architecture, although throughput and printable material choices remain limited. Stereolithography and digital light processing occupy a complementary manufacturing regime, sacrificing the resolution of multiphoton lithography in exchange for larger build volumes, faster fabrication, and lower infrastructure requirements. This trade-off is particularly useful when three-dimensional fabrication is required primarily for fluid handling or system integration rather than for defining the nanoscale transducer itself. For example, cleanroom-free stereolithography combined with hot embossing has enabled multiplexed miRNA biosensing platforms, illustrating how additive manufacturing can simplify the production of integrated diagnostic architectures [124–126]. Resin biocompatibility, post-curing, surface roughness, dimensional accuracy, and reliable fabrication of enclosed channels remain important manufacturing constraints.

Three-dimensional architectures are also attractive for tissue-interfacing and implantable bioelectronics because flat devices couple imperfectly to curved and heterogeneous biological surfaces. Vertical arrays, porous scaffolds, and tissue-conformal structures can improve contact area, reduce interfacial impedance, and enhance signal quality. Consequently, three-dimensional morphology, surface chemistry, and mechanical integration must be considered as a single nano-biointerface design problem [127]. The manufacturing challenges associated with 3D biosensors depend on whether complexity arises from the fabrication method or from the device architecture. Multiphoton lithography is limited primarily by serial writing speed and material choice, whereas SLA and DLP require control of resin biocompatibility, post-curing, surface quality, and enclosed-channel fidelity. Vertically integrated semiconductor architectures instead impose stringent requirements on multilayer alignment, dielectric control, dimensional uniformity, and surface functionalization. Across all approaches, additional three-dimensional surface area is beneficial only when it remains accessible to analytes and can be functionalized, calibrated, and reproduced across devices and batches. Three-dimensional complexity is therefore justified when it provides a measurable sensing or integration advantage that outweighs the additional fabrication and quality-control burden.

4.5. Emerging hybrid routes: capillary, electrohydrodynamic, edge, and magnetically assisted patterning

Several emerging methods use capillary, electric, magnetic, or edge-defined forces to create micro/-nanostructures that are difficult to obtain using conventional lithography. These techniques remain less standardized than NIL or soft lithography and should therefore be viewed primarily as specialized enabling routes. Capillary-force-based patterning exploits liquid filling, evaporation, mold confinement, or surface-tension-driven deformation. Applications include structured biomaterial surfaces, colloidal assembly, and low-cost polymer patterning [71, 128]. Biosensor-related demonstrations include colloidal crystal assembly for SPR sensing, nanoporous Au patches for wearable glucose detection, and capillary-collapse lithography producing ordered sub-10 nm plasmonic bowtie gaps, as shown in figure 4(E) [129–131]. Electrohydrodynamic lithography and printing use electric fields to deform polymer films or deposit functional inks and nanomaterial suspensions. Their contactless and digitally tunable nature is attractive for hierarchical micro/nanostructures, printed electronics, and flexible sensors, although uniformity, dielectric breakdown, material compatibility, and process stability remain important limitations [132]. Direct biosensor examples include electrohydrodynamically patterned SERS micropillars and MXene FET biosensors for aflatoxin B1 detection,[133, 134] making this the most immediately biosensor-relevant method within this group. Edge-defined lithography generates nanoscale features from the boundaries of larger pre-patterned structures, enabling nanogaps, nanowires, nanochannels, and edge electrodes without serially defining the entire device. Such methods remain specialized but are relevant to flow-through electroanalysis, nanofluidics, and selected biosensor architectures [13, 135, 136]. Magnetically assisted lithography and magnetorheological drawing are even less mature for biosensor manufacturing. Magnetic fields can align particles, ferrofluids, composites, or responsive polymers into anisotropic structures, offering remote control and soft-material compatibility. Current demonstrations are stronger in smart materials, soft robotics, microneedles, and cell manipulation than in biosensing, although magnetically patterned piezoresistive composites and spatially magnetized soft machines illustrate potential future routes for biointerfaces and fluidic control [137–139]. These emerging routes currently serve specialized rather than general-purpose manufacturing roles, with broader adoption dependent on improved reproducibility, uniformity, and biosensor-level validation.

5. Bottom-up and self-assembled biosensor architectures

Bottom-up and self-assembled nanofabrication provides a complementary route to lithographic, replication-based, and polymer-processing methods by exploiting programmed or spontaneous interactions among nanoparticles, polymers, biomolecules, and supramolecular building blocks. Colloidal assembly, DNA base pairing, block-copolymer phase separation, peptide/protein self-assembly, and responsive molecular interactions can generate hierarchical architectures that are difficult or costly to reproduce using purely top-down fabrication. For biosensors, their main value lies in chemical programmability, solution processability, molecular-scale organization, and compatibility with biological recognition. Colloidal assemblies generate plasmonic hotspots; DNA nanostructures position functional components with molecular precision; block copolymers provide nanopatterned or nanoporous templates; and responsive biointerfaces can couple molecular recognition directly to structural change. Their principal limitations are correspondingly different from those of deterministic lithography, including batch variability, structural heterogeneity, stability, defect control, and device integration. This section

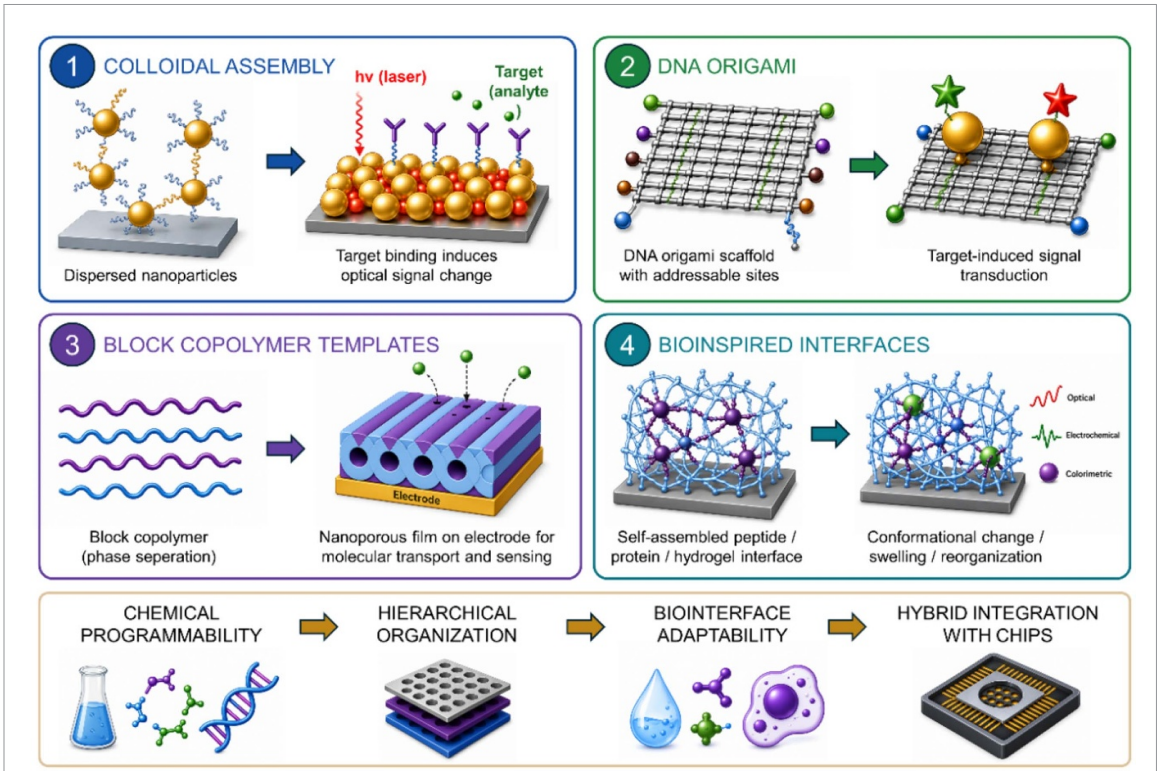


Figure 5. Bottom-up and self-assembled biosensor architectures. The schematic summarizes colloidal nanoparticle assemblies, DNA origami, block-copolymer-derived nanoporous templates, and responsive biointerfaces as chemically programmable routes to plasmonic hotspots, molecular-scale component positioning, controlled nanoporous transport, and dynamic sensing interfaces.

therefore treats bottom-up fabrication as a complementary strategy for introducing molecular precision and biological adaptability into manufacturable biosensor architectures, as summarized in figure 5.

5.1. Colloidal assembly and plasmonic nanoparticle superstructures

Colloidal assembly is one of the most established bottom-up routes for plasmonic biosensing. Au, Ag, and hybrid nanoparticles organize through ligand-mediated, electrostatic, capillary, interfacial, or biomolecular interactions into films, clusters, arrays, and higher-order superstructures. Because the nanoparticles simultaneously provide optical transduction and chemically addressable surfaces, they can be functionalized with antibodies, aptamers, nucleic acids, peptides, enzymes, or antifouling ligands while being assembled into structures with collective plasmonic behavior [140, 141]. A representative example was reported by Qi *et al*, who developed a template-assisted colloidal assembly strategy using elastomeric PDMS molds patterned with hexagonal triskelion cavities to organize Au and Ag nanoparticles into highly ordered plasmonic superlattices (figure 6(A)). The triskelion geometry was first optimized by FDTD simulations, using a lattice parameter of 500 nm, an arm width of 75 nm, and a vertex spacing of 400 nm, and subsequently transferred to patterned PDMS molds. During fabrication, 1.5 μl of PEG-SH-functionalized Au or Ag colloidal suspension stabilized with CTAC was confined between the PDMS stamp and a glass substrate over a 16 mm2 patterned area and allowed to self-assemble through solvent evaporation for 4–6 h. This approach enabled the formation of large-area triskelion arrays from Au nanospheres with diameters of 27, 45, and 54 nm, Ag nanospheres with diameters of 20, 27, 32, and 36 nm, and Au nanorods measuring 60 $\times$ 15 nm, demonstrating the versatility of template-assisted assembly across different colloidal compositions, sizes, and morphologies. The resulting superlattices exhibited strong collective plasmonic coupling and tunable chiroptical behavior, with g-factors reaching 0.40 for Ag nanoparticle arrays and 0.18 for Au nanoparticle arrays under normal incidence, while changes in nanoparticle size and morphology enabled systematic tuning of the optical response across the visible and near-infrared spectral regions [142].

Their sensing performance arises primarily from interparticle plasmonic coupling. Nanoscale gaps concentrate electromagnetic fields and enhance SERS, LSPR, fluorescence, and colorimetric responses, with performance governed by nanoparticle geometry, composition, spacing, ligand thickness, assembly order, and dielectric environment. Water-oil interfacial assembly has produced densely packed nanoparticle monolayers with accessible enhancing surfaces for quantitative SERS, while ordered cluster arrays and

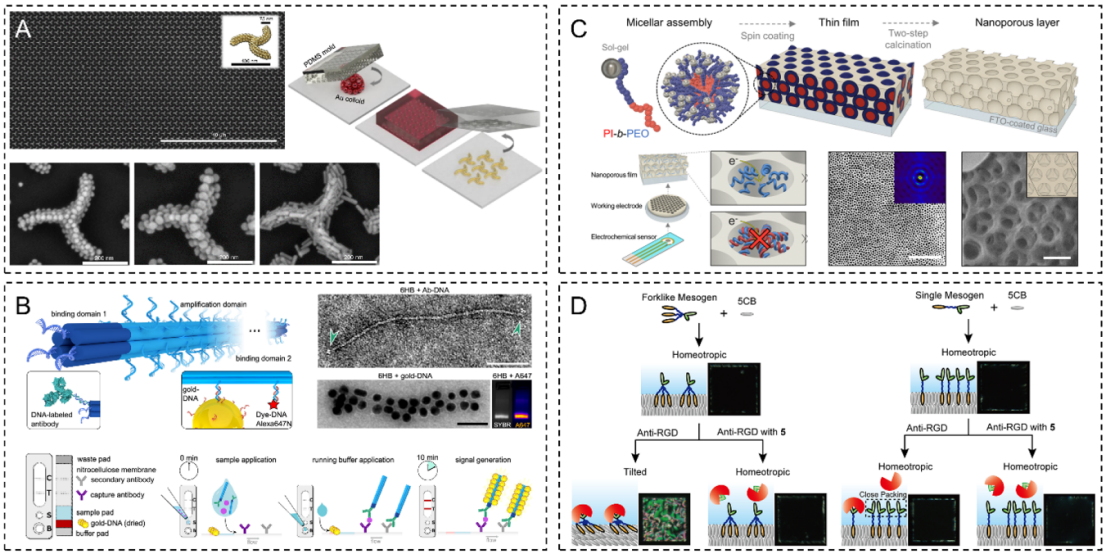


Figure 6. Representative bottom-up and self-assembled nanofabrication strategies for biosensor architectures. (A) Template-assisted colloidal self-assembly of Ag nanospheres, Au nanospheres, and Au nanorods into ordered triskelion plasmonic superlattices using patterned PDMS molds. Adapted from [142], Copyright© 2025 Springer Nature. (B) DNA-origami-assisted lateral-flow signal amplification using a programmable six-helix bundle scaffold for spatial organization of antibodies, Au nanoparticles, and fluorescent reporters. Adapted from [43], Copyright© 2025 Springer Nature. (C) Block-copolymer-directed fabrication of an ordered nanoporous electrochemical sensing interface using PI-b-PEO templating, sol–gel co-assembly, spin coating, and calcination, with SEM/FIB characterization of the pore network. Adapted from [164], Copyright© 2025 The Royal Society of Chemistry. (D) Responsive peptide-conjugated liquid-crystal interfaces that translate anti-RGD binding into a measurable molecular-ordering transition. Adapted from [174], Copyright© 2023 American Chemical Society.

superlattices enable tuning of both near- and far-field coupling [143, 144]. Target-responsive assembly adds a further sensing mechanism because analyte recognition can actively alter nanoparticle organization. DNA hybridization, aptamer folding, antibody-antigen binding, enzymatic reactions, or competitive interactions can trigger aggregation, dispersion, or structural reconfiguration, producing measurable changes in color, extinction, LSPR, fluorescence, or SERS. DNA-directed protein anchoring on functionalized Au nanoparticles illustrates how biomolecular programmability can control both recognition and plasmonic signal generation [145]. Such formats are particularly attractive for low-cost point-of-care detection because molecular recognition can be converted directly into an optical response.

The main limitation is reproducibility. Random aggregation can produce intense hotspots but poor spatial uniformity, whereas ordered assemblies require strict control of particle concentration, ligand chemistry, solvent conditions, drying dynamics, and substrate interactions. Colloidal instability, nonspecific adsorption, hotspot heterogeneity, and storage degradation further complicate quantitative use. Accordingly, current strategies increasingly favor ordered or confined assemblies that jointly control nanoscale spacing, surface chemistry, and collective optical response.

5.2. DNA Origami and Biomolecular Nanofabrication

DNA origami and related DNA nanostructures provide exceptionally programmable bottom-up fabrication because sequence-specific base pairing can encode geometry, addressability, and molecular positioning. DNA origami scaffolds, tiles, tetrahedra, branched structures, and dynamic devices can organize nanoparticles, fluorophores, enzymes, aptamers, antibodies, peptides, and other recognition elements with nanometer-scale control over spacing and orientation [42, 146, 147]. A representative example of this programmable nanofabrication strategy was reported by Ijäs *et al*, who developed a DNA origami-enabled signal amplification platform for lateral flow immunoassays (figure 6(B)). Their approach employed a 490 nm-long six-helix bundle DNA origami scaffold incorporating two antibody-binding domains and a central amplification domain containing 180 programmable DNA overhangs for the attachment of fluorescent dyes or DNA-functionalized Au nanoparticles. Detection antibodies were conjugated to the terminal binding domains, whereas multiple signal labels were assembled onto the amplification domain through sequence-specific DNA hybridization, enabling precise control over both label stoichiometry and nanoscale spatial organization. The resulting DNA origami nanostructure was subsequently integrated into a conventional LFIA platform, where multivalent label recruitment significantly enhanced signal generation while preserving the standard assay workflow. This work demonstrates how

DNA origami can function simultaneously as a programmable structural scaffold, a molecular assembly platform, and a signal amplification architecture for highly sensitive biosensing [43].

This precision is particularly valuable in optical and plasmonic biosensors. DNA origami can organize metallic nanoparticles into dimers, trimers, nanoantennas, chiral assemblies, and plasmonic cavities while positioning fluorophores, Raman reporters, or targets within regions of strong field enhancement. DNA-origami nanoantennas have enabled single-antibody detection through plasmon-enhanced fluorescence, while gold nanobipyramid assemblies have been used for selective recognition of thioflavin T [148, 149]. DNA-guided Au nanoparticle organization has also been integrated with fiber-optic SPR sensing, demonstrating compatibility with device-level optical readout [150]. Unlike static templates, DNA nanostructures can also participate directly in signal transduction. Target binding can induce opening, closing, strand displacement, fluorophore–quencher separation, or plasmonic reconfiguration. A DNA-origami 'book' biosensor converted nucleic-acid recognition into structural and fluorescent signals, while reconfigurable DNA systems have been adapted to visual and smartphone-compatible detection [151–153].

DNA nanostructures also improve electrochemical interfaces by controlling probe density, accessibility, and reporter distance from electrodes. Target-capturing DNA origami tiles have enhanced DNA biosensor signals without enzymatic amplification, while modular origami-based electrochemical architectures have been adapted to both nucleic-acid and protein targets [154, 155]. Related DNA-origami–protein nanopores and DNA-defined plasmonic nanogaps further extend the approach toward programmable single-molecule sensing [156, 157]. Translation remains limited by structural stability, nuclease degradation, ionic-strength and Mg2+ dependence, purification complexity, oligonucleotide cost, and batch reproducibility. Integration with solid-state chips, microfluidics, portable readers, and physiological samples remains equally important [158–160]. DNA origami is therefore best positioned for biosensors in which molecular-scale spatial control or dynamic reconfiguration provides functionality that conventional lithography cannot readily reproduce.

5.3. Block copolymer, nanosphere, and nanoporous templates

Block-copolymer (BCP) self-assembly generates periodic nanostructures through microphase separation, producing lamellae, cylinders, spheres, gyroids, nanopores, nanodots, and nanowire-like domains. Compared with deterministic lithography, BCPs provide parallel nanoscale organization over larger areas, with feature dimensions controlled by polymer composition, molecular weight, volume fraction, and processing conditions [44,45]. In plasmonic biosensors, BCP domains can control nanoparticle density and aggregation. A PS-b-P4VP-templated fiber-optic LSPR biosensor used chemically distinct polymer domains to organize a dense Au nanoparticle monolayer, reducing aggregation while improving refractive-index sensitivity and DNA hybridization detection [161]. Aligned lamellar BCPs have also been converted into sub-10 nm-half-pitch Au nanowires, while nanoimprint-assisted BCP assembly demonstrates how top-down registration and molecular-scale ordering can be combined when device-level alignment is required [162, 163].

A representative example of block-copolymer-directed biosensor nanofabrication was reported by Fornerod *et al*, who developed an inorganic nanoporous electrochemical sensing interface through the co-assembly of PI-b-PEO micelles with an aluminosilicate sol–gel precursor (figure 6(C)). Following spin coating onto fluorine-doped tin oxide (FTO) electrodes and a two-step calcination process to remove the polymer template, the resulting approximately 150 nm-thick film exhibited 65 vol% accessible porosity and an average pore diameter of 44 $\pm$ 12 nm. GISAXS, SEM, and FIB characterization confirmed a highly ordered, interconnected inverse-opal-like nanopore architecture that provided a large accessible surface for probe immobilization while supporting molecular transport through the porous network. When integrated into an electrochemical nanopore-blockage platform for E. coli 16 S rRNA-derived DNA detection, target-induced modulation of nanopore transport enabled label-free detection within 20 min, with a limit of detection of 30 fM and a limit of quantification of 500 fM [164]. This example illustrates the broader value of BCP-derived nanoporous and mesoporous films for biosensing, in which controllable pore size, connectivity, and surface chemistry can be used to regulate molecular transport and probe loading; more generally, self-assembled mesoporous architectures offer high internal surface area, size-selective transport, and tunable chemical functionality for DNA-, enzyme-, and ionic-transport-based sensing [165, 166].

Related nanoporous templates, including anodic aluminum oxide, porous silicon, nanoporous gold, mesoporous silica, and porous polymer networks, extend the same concept of high surface area and controlled transport, although their fabrication and integration requirements differ [167, 168]. The principal challenge is that nanoscale periodicity does not guarantee deterministic device-level organization. Grain boundaries, orientation, long-range order, defect density, and registration remain important limitations,

while practical biosensor use additionally requires reproducible functionalization, antifouling behavior, and microfluidic integration. BCP and nanoporous templates are therefore most useful when high-density molecular organization and transport control can be coupled to robust device-level fabrication.

5.4. Responsive, bioinspired, and hierarchical self-assembled interfaces

Responsive and bioinspired interfaces extend bottom-up fabrication beyond static templates by allowing the material itself to participate in molecular recognition or signal generation. Peptides, proteins, small molecules, hydrogels, vesicles, liquid crystals, porous networks, and hybrid organic–inorganic systems can self-organize into hydrated and biologically active interfaces supporting optical, electrochemical, fluorescence, colorimetric, and field-effect sensing [169, 170]. Peptide- and protein-based assemblies are attractive because sequence programmability and biocompatibility can be combined with receptor presentation and surface functionalization. Nanofibers, nanotubes, amphiphiles, coiled-coil structures, and related scaffolds can immobilize enzymes, antibodies, aptamers, nanoparticles, or electroactive components. Self-assembled GA-repeat peptides, for example, have been used as scaffolds on MoS_2 electrochemical transistors while preserving transistor performance and enabling femtomolar streptavidin detection [171, 172].

Responsive assemblies provide a further advantage by converting biochemical recognition into structural change. Swelling, shrinking, aggregation, disassembly, conformational rearrangement, cleavage, or interfacial ordering can be triggered by pH, temperature, ions, enzymes, redox conditions, light, or target binding [173]. At liquid-crystal interfaces, peptide-conjugated mesogens have translated biomolecular binding into optical ordering transitions, illustrating how self-assembly can act as both fabrication mechanism and transduction principle [174]. A representative example was reported by Uchida *et al*, who developed peptide-conjugated forklike mesogens that spontaneously self-assembled at aqueous/liquid-crystal interfaces to create biomolecule-responsive sensing platforms (figure 6(D)). The authors designed amphiphilic mesogens incorporating an RGD peptide recognition motif together with multiple rigid mesogenic cores to control interfacial organization. The self-assembled interface induced homeotropic alignment of the liquid crystal, whereas specific binding of anti-RGD antibodies triggered an ordering transition from homeotropic to tilted alignment, producing a distinct optical response observable by polarized optical microscopy. In contrast, a single-mesogen analogue formed densely packed interfaces that prevented effective biomolecular recognition and therefore generated no measurable optical transition. This work demonstrates how molecular self-assembly can simultaneously determine interfacial architecture, recognition accessibility, and signal transduction, highlighting responsive biointerfaces as an effective bottom-up strategy for optical biosensing. [159].

Hierarchical hybrid assemblies combine biological recognition with conductivity, catalytic activity, transport, or signal amplification by incorporating metals, graphene, MXenes, metal oxides, MOFs, COFs, or other functional nanomaterials. A hierarchical porous MOF biocatalytic microreactor, for example, improved enzyme organization and enabled amplified miRNA-21 detection in cancer cells and patient serum [175]. Biomodified two-dimensional materials similarly illustrate how engineered biointerfaces can support optical, electrochemical, fluorescence, and photoelectrochemical sensing [176, 177]. Bioinspired surface engineering is particularly relevant in complex biological matrices, where hydrated coatings, membrane-inspired layers, peptide-functionalized interfaces, and biomimetic polymers can improve recognition while reducing nonspecific adsorption. Multiscale biohybrid interface design increasingly aims to combine biological function with engineered mechanical and physicochemical properties [178]. The main barriers are stability and reproducibility. Biomolecular assemblies may undergo morphology drift, degradation, or loss of activity, whereas responsive materials can become difficult to calibrate when swelling or structural transitions are affected by matrix composition. Hybrid systems add further complexity in sterilization, storage, material compatibility, and scale-up. Their translational value therefore depends on coupling dynamic biological function with stable immobilization, antifouling chemistry, reproducible fabrication, and practical device integration.

6. Flexible and wearable biosensor fabrication

Flexible and wearable biosensors represent an important direction in nanofabricated sensing because they extend biosensor operation from rigid laboratory platforms to mechanically compliant, skin-conformal, and continuously operating systems. Unlike conventional chip-based biosensors, wearable devices must function under bending, stretching, sweat exposure, body motion, and prolonged contact with biological surfaces. Their performance is therefore governed not only by the nanoscale sensing interface, but also by substrate mechanics, interfacial adhesion, biofluid handling, signal stability, packaging, and device-level integration. Recent progress has been driven by the convergence of flexible substrates,

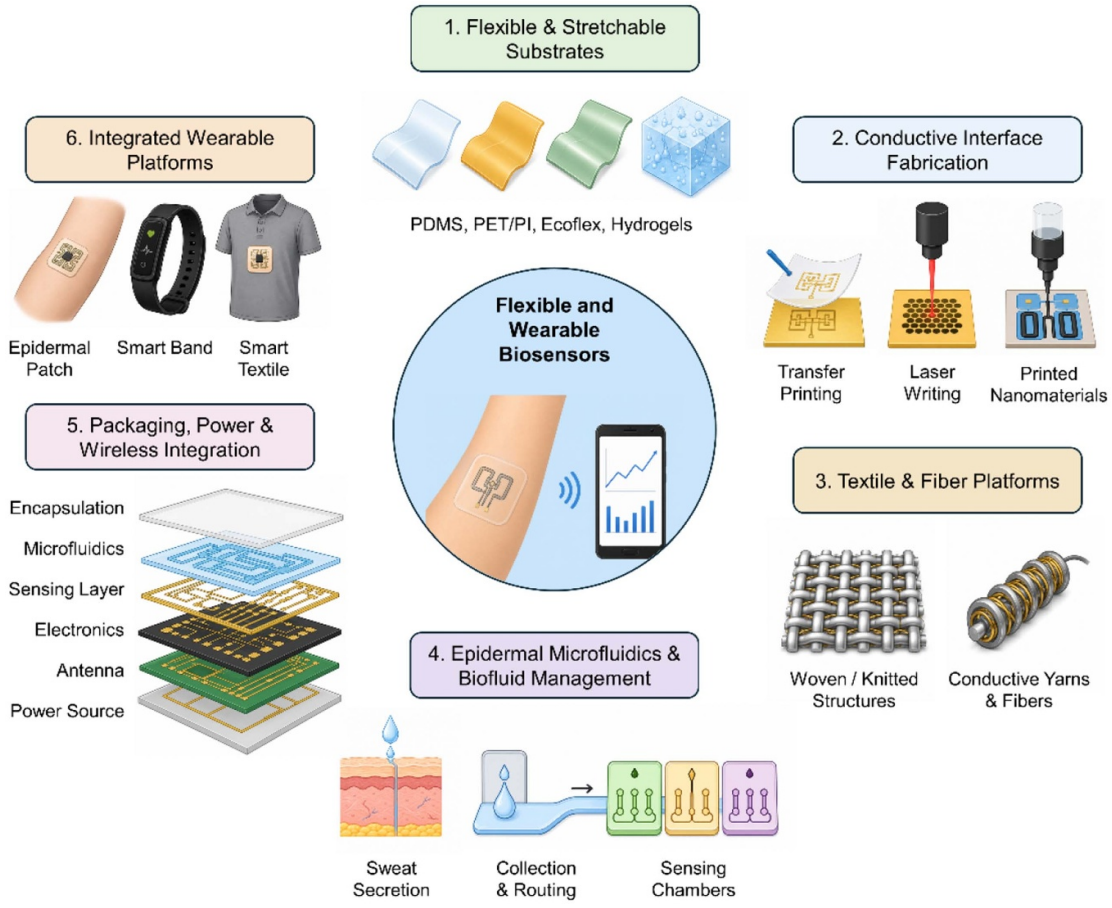


Figure 7. Overview of flexible and wearable biosensor fabrication strategies. The schematic summarizes flexible substrates, transfer- and laser-based conductive interfaces, printed nanomaterials, textile and fiber architectures, epidermal microfluidics, and multilayer integration of sensing modules with packaging, power, electronics, and wireless communication.

transfer-based patterning, laser-written conductive architectures, printed nanomaterial interfaces, textile-integrated sensing, and epidermal microfluidics. Materials such as PDMS, PET, polyimide (PI), Ecoflex, and hydrogels provide different levels of flexibility, stretchability, transparency, process compatibility, and biological compliance. At the same time, transfer printing, laser-induced graphene, screen and inkjet printing, solution-processed nanomaterial coatings, fiber-level functionalization, and stretchable interconnect design have enabled conductive, optical, and electrochemical sensing layers to be integrated onto deformable supports. These developments have expanded wearable biosensors beyond simple epidermal electrodes toward multifunctional systems capable of biochemical monitoring, controlled biofluid sampling, wireless communication, and prolonged skin-interfaced operation. However, flexible and wearable biosensor fabrication introduces challenges that are less prominent in rigid devices. Mechanical deformation can cause cracking, delamination, signal drift, or loss of electrical continuity, while biofluid sampling depends on secretion rate, evaporation, microfluidic routing, and stable skin contact. Scalable manufacturing additionally requires reproducible ink formulation, pattern fidelity, substrate compatibility, wash durability, encapsulation stability, biofunctionalization, and device-to-device uniformity. As summarized in figure 7, wearable biosensor fabrication extends beyond the sensing interface itself and requires the integration of compliant substrates, conductive interface fabrication, textile platforms, epidermal microfluidics, multilayer device integration, and application-specific wearable formats within a unified manufacturing framework.

6.1. Flexible and stretchable substrates

Among the substrate materials investigated in recent wearable biosensor fabrication, PDMS, PET, PI, Ecoflex, and hydrogels remain particularly important because they address different mechanical, optical, and biological requirements. PDMS provides optical transparency, elasticity, gas permeability, and compatibility with soft microfluidics. PET and PI offer mechanically robust, dimensionally stable, and process-compatible platforms for flexible electronics, printed biosensors, and wearable electrode arrays.

Ecoflex provides high stretchability for deformable skin-contact devices, whereas hydrogels offer hydrated and tissue-like interfaces that can improve biological compatibility. These materials should therefore be viewed as complementary substrate platforms rather than competing alternatives, with selection depending on the sensing mechanism, target biofluid or tissue, expected deformation range, fabrication process, and intended use environment.

PDMS remains one of the most widely used elastomeric substrates for soft microfluidic and epidermal biosensors. Its low elastic modulus enables conformal contact with irregular skin surfaces, while its optical transparency supports colorimetric, fluorescence, imaging-based, and optofluidic sensing formats. In wearable biosensors, PDMS-based structures are particularly useful for sweat collection channels, flexible reservoirs, encapsulation layers, and epidermal patches. However, PDMS also has important limitations. Hydrophobic recovery after plasma treatment can reduce long-term wettability, while its intrinsic hydrophobicity can hinder efficient fluid transport in sweat microfluidics [179]. Weak adhesion between PDMS and metallic thin films can further promote cracking or delamination during repeated deformation. Consequently, recent devices increasingly combine PDMS with surface modification, adhesion layers, hydrophilic channel treatments, composites, or multilayer encapsulation to preserve softness while improving analytical stability and durability [179–181].

PET and PI represent a different class of flexible substrates: they are less stretchable than elastomers but more suitable for mechanically stable electronic integration. PET offers optical transparency, low cost, chemical resistance, and compatibility with scalable film processing, making it useful for disposable biosensors, optical sensing patches, and printed electrochemical devices. Its limited stretchability, however, means that conductive coatings or patterned electrodes may crack under large tensile strain unless serpentine traces, island–bridge layouts, or elastomeric encapsulation are introduced. PI provides higher thermal stability, chemical resistance, and mechanical durability than PET, making it one of the most important substrates for flexible electronics and integrated biosensing systems [182]. Because PI can tolerate relatively high processing temperatures, it is compatible with thin-film metallization, flexible circuits, laser-induced graphene formation, and multifunctional bioelectronic platforms [183, 184]. PI is nevertheless not intrinsically stretchable, so PI-based wearable systems typically rely on serpentine conductors, kirigami-inspired geometries, island–bridge layouts, or elastomeric encapsulation to accommodate large body motion without mechanical failure [182, 185].

Ecoflex is particularly attractive when high stretchability and skin-like mechanical compliance are required. Its low modulus and high elongation at break allow devices to maintain conformal contact with highly deformable body regions during motion. This makes Ecoflex useful for electronic skin, soft strain sensors, motion-monitoring systems, rehabilitation devices, and stretchable biochemical sensing patches. In biochemical wearable devices, the low stiffness of Ecoflex can reduce interfacial stress between the device and skin and maintain stable contact during repeated stretching. However, its softness also complicates processing. Precise electrode patterning can be difficult because the substrate deforms during fabrication, and conductive layers often require adhesion promoters, embedded architectures, surface treatments, or composite formulations to prevent delamination under cyclic strain. Ecoflex is therefore frequently combined with conductive composites, liquid metals, hydrogels, stretchable nanomaterials, or multilayer elastomeric structures. Hybrid systems can also use relatively rigid PI islands to protect fragile components while elastomeric regions absorb strain, improving reliability under repeated deformation [185–187].

A representative example was reported by Kim *et al*, who developed a photo-patternable Ecoflex (PPE)-based strategy for fabricating intrinsically stretchable, multi-biochemical wearable sensors (figure 8(A)) [188]. In their process, conventional Ecoflex was modified with benzophenone-based photo-inhibition chemistry to enable direct UV patterning of the elastomeric encapsulation layer, thereby avoiding the alignment and lamination limitations associated with conventional soft-lithographic or mechanical patterning approaches. PPE was spin-coated at 700 rpm for 60 s, exposed to 365 nm UV light at 1.2 mW $cm^{-2}$for 10 min, annealed at 85 °C for 1 min, developed for 1 min, and finally cured at 100 °C for 1 h. The photo-patterned Ecoflex could be formed into openings down to approximately 200 μm resolution and remained mechanically intact when stretched to 200% strain. The complete wearable architecture combined an Ecoflex substrate, screen-printed Ag/Ecoflex stretchable conductors, PPE encapsulation, Au nanoparticle-modified electrodes, and distinct functional layers for glucose, lactate, pH, and humidity sensing. The encapsulated conductor maintained stable electrical characteristics up to 250% strain, retained performance after 1000 deformation cycles at 100% strain, and showed approximately 60% higher conductivity than a comparable PDMS-based electrode at 50% strain. At the device level, the biochemical sensors preserved stable operation under deformation up to 50% strain and after 1000 cycles at 20% strain, while the final patch was conformally mounted on the wrist for real-time

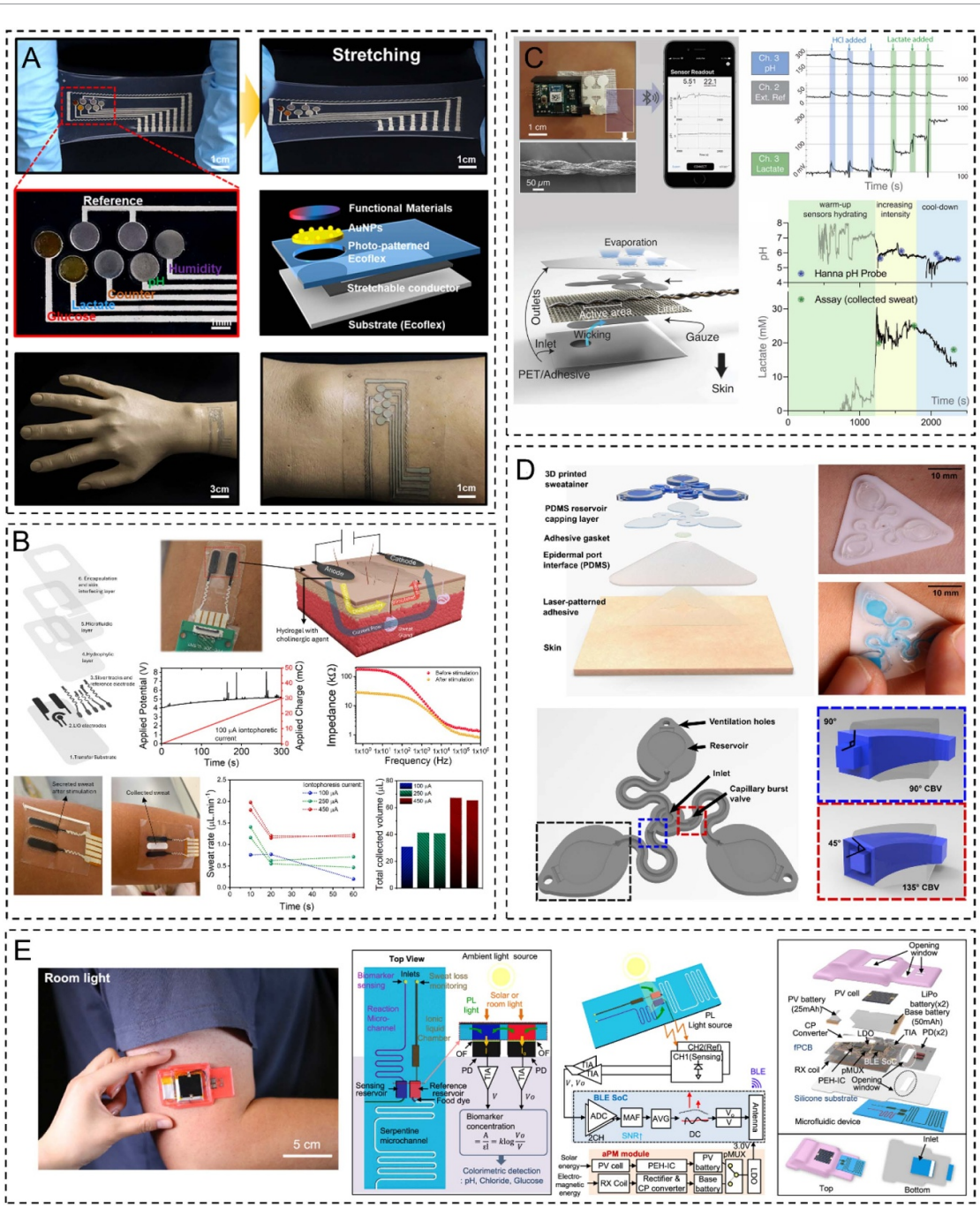


Figure 8. Representative fabrication and integration strategies for flexible and wearable biosensors. (A) Photo-patternable Ecoflex-based stretchable sweat sensor integrating Ag conductors, Au-nanoparticle-modified electrodes, selective encapsulation, and multiplexed detection of glucose, lactate, pH, and humidity. Adapted from [188], Copyright© 2023 Springer Nature. (B) Laser-induced graphene electrodes transferred to a flexible polyurethane platform and integrated with microfluidics, adhesive layers, iontophoretic sweat stimulation, and wearable electrochemical sensing. Adapted from [197], Copyright© 2025 The Royal Society of Chemistry. (C) Textile-integrated rGO sensing yarn combining pH and lactate electrodes, multilayer patch construction, wireless readout, and continuous on-body sweat monitoring. Adapted from [222], Copyright© 2024 Springer Nature. (D) DLP-printed three-dimensional epidermal 'sweatainer' incorporating sequential reservoirs, ventilation structures, capillary burst valves, and a conformal skin interface for passive sweat management. Adapted from [230], Copyright© 2023 AAAS. (E) Fully integrated wearable biosensor combining microfluidic sweat sensing, photovoltaic energy harvesting, rechargeable batteries, adaptive power management, flexible electronics, BLE communication, and soft encapsulation. Adapted from [240], Copyright© 2025 Springer Nature.

sweat monitoring. These results demonstrate how elastomer chemistry, direct photopatterning, stretchable conductive composites, and multilayer integration can be co-designed to improve mechanical reliability without sacrificing multiplexed biosensing functionality.

Hydrogels provide a distinct substrate class because their hydrated polymer networks can resemble the mechanical and physiological properties of biological tissues. Unlike dry polymer films, hydrogels form water-rich interfaces that can reduce mechanical mismatch with skin, wounds, or implanted

tissues while supporting analyte diffusion and biomolecular activity. Hydrogel-based biosensors have therefore been investigated for wound monitoring, implantable sensing, tissue-interfacing devices, and long-term physiological monitoring. Conductive hydrogels containing graphene, MXenes, CNTs, metallic nanoparticles, or conducting polymers further expand their use in electrochemical, strain-sensitive, and bioelectronic devices [189]. Hydrogel-based wearable patches have also enabled non-invasive glucose sensing from natural sweat, illustrating their potential as soft biochemical sensing interfaces [190]. Their main limitations are dehydration, swelling, relatively low mechanical strength, and long-term packaging requirements. Changes in hydration can alter both ionic conductivity and device dimensions, thereby affecting calibration and analytical reproducibility [191].

No single substrate satisfies all requirements for wearable biosensing. PDMS is well suited to soft microfluidics, epidermal patches, and optically accessible devices; PET and PI are preferred when flexible electronics, printed electrodes, dimensional stability, and process compatibility are required; Ecoflex is advantageous for highly stretchable systems; and hydrogels are uniquely suited to hydrated and tissue-like biointerfaces. Consequently, wearable biosensor fabrication is increasingly moving toward hybrid substrate architectures rather than single-material platforms. Elastomeric supports can be combined with hydrogel sensing layers, PI-based island–bridge circuits with stretchable substrates, PET-supported printed electrodes with compliant encapsulation, and PDMS microfluidics with nanostructured electrochemical or optical sensing surfaces. Such hybrid designs aim to combine mechanical compliance, fabrication compatibility, biointerface stability, and analytical performance within the same device [60, 181, 183].

6.2. Transfer, laser-written, and printed conductive interfaces

The fabrication of conductive interfaces on flexible and wearable substrates requires processes that preserve electrical and electrochemical performance while accommodating bending, stretching, skin contact, and repeated mechanical deformation. Unlike rigid chip-based biosensors, wearable platforms cannot rely exclusively on conventional wafer-level metallization or direct lithographic processing because polymeric, elastomeric, textile, and hydrogel-based substrates may deform, swell, absorb solvents, or exhibit heterogeneous surface morphology during fabrication. Consequently, recent wearable biosensor manufacturing increasingly relies on three complementary strategies: transfer-based integration of pre-fabricated structures, direct laser writing of conductive architectures, and additive deposition of functional nanomaterial inks. Although these approaches differ in how conductive structures are generated, they share the objective of integrating high-performance sensing interfaces onto mechanically compliant substrates while maintaining adhesion, pattern fidelity, and device reproducibility.

Transfer-based fabrication provides a bridge between high-resolution pattern definition and flexible substrate integration. Conductive films, nanowire networks, electrode arrays, or nanostructured sensing interfaces can first be fabricated on rigid donor substrates under optimized processing conditions and subsequently transferred to flexible receivers through conformal lamination, dry transfer, sacrificial release, peel-off, or adhesion-controlled printing. This strategy is particularly useful when the final substrate cannot tolerate photoresist processing, aggressive solvents, vacuum deposition, elevated temperatures, or plasma exposure. By separating pattern formation from final device assembly, transfer-based approaches preserve the precision of wafer-compatible fabrication while extending it to soft and unconventional wearable substrates [13, 192]. Dry-transfer photolithography illustrates how conventional lithographic precision can be adapted to mechanically compliant platforms. Instead of performing the complete resist-processing sequence directly on the final soft substrate, transferable resist layers can be formed separately and brought into conformal contact with the receiver. Chen *et al* demonstrated dry-transferable photoresist-enabled patterning for ultrathin flexible electronics, enabling high-resolution multiscale electrode architectures while maintaining pattern fidelity and mechanical reliability [193]. Although the platform is broader than biochemical biosensing alone, the fabrication principle is directly relevant to wearable biosensors requiring fine electrodes and interconnects on substrates that are incompatible with conventional wet lithography. Transfer printing provides a related route for integrating metallic films, nanowire networks, and conductive micro/nanostructures onto curved or compliant surfaces. High-resolution intaglio transfer printing of silver nanowire networks, for example, has produced flexible electrophysiological electrodes with high conductivity and stable electrical performance during repeated bending [194]. The same principle can be applied to biochemical biosensors because low-resistance interconnects and mechanically stable electrode interfaces are required regardless of the recognition mechanism.

Laser-induced graphene (LIG) and related laser-written architectures represent a second major fabrication route. In contrast to transfer processes, laser-based methods generate conductive patterns directly on or within the substrate through localized photothermal or photochemical conversion. The most

widely established example is LIG formation on polyimide, where laser irradiation converts the polymer surface into porous graphitic carbon. The process is mask-free, digitally programmable, compatible with ambient fabrication, and capable of generating electrodes with high electroactive surface area, making it particularly attractive for wearable electrochemical biosensing [195, 196]. A representative example was reported by Pinheiro *et al*, who developed a laser-written flexible biosensing platform by integrating transferred LIG electrodes into a multilayer wearable epidermal device (figure 8(B)). The fabrication strategy combined CO_2 laser-generated porous graphene electrodes with a water-assisted transfer process onto a polyurethane substrate, followed by assembly of hydrophilic, adhesive, and microfluidic layers to create a skin-conformal sensing platform. The integrated architecture incorporated iontophoretic sweat stimulation, epidermal microfluidic sampling, and electrochemical sensing within a single wearable system. Using a 10 min iontophoresis protocol, sweat generation was successfully induced at applied currents of 100, 250, and 450 μA, yielding approximately 31, 40, and 65 μl of sweat, respectively, while maintaining stable sweat transport through the integrated microfluidic network. The transferred LIG electrodes preserved excellent electrical performance after transfer, exhibiting a sheet resistance of $5.0 \pm 0.6\ \Omega\ \mathrm{sq}^{-1}$, an apparent conductivity of $25.5 \pm 2.6\ \mathrm{S\ cm}^{-1}$, and a 100% transfer yield, demonstrating that laser-written conductive architectures can be efficiently combined with multilayer wearable integration without compromising electrical properties. This work illustrates how laser-generated porous conductive interfaces can be transformed into fully integrated wearable biosensors through transfer-based fabrication, multilayer assembly, and epidermal device engineering [197].

A key advantage of LIG is the ability to tune both geometry and material properties through laser parameters. Wavelength, power, scanning speed, pulse duration, and line spacing can influence graphitization, porosity, wettability, conductivity, and electrochemical active area. PI is especially attractive because the substrate itself serves as the carbon precursor, eliminating separate conductive-film deposition or transfer. However, this direct conversion also makes device properties highly sensitive to processing conditions, so reproducible manufacturing requires control of laser fluence, substrate composition, ambient atmosphere, thermal history, and subsequent surface functionalization [198–200]. Wearable sweat sensing provides several representative demonstrations. Liao *et al* developed a PI-based LIG epidermal ion-selective platform for simultaneous monitoring of pH, Na^+, and K^+ with smartphone-connected wireless readout during physical activity [201]. Vivaldi *et al* similarly reported a largely laser-fabricated wearable platform combining LIG electrodes with a paper-based sweat collector for simultaneous measurement of uric acid, tyrosine, pH, and ionic impedance [202].

Laser-written interfaces have also been extended to glucose sensing through both enzymatic and non-enzymatic approaches. Metallic catalyst-modified LIG electrodes integrated with soft sweat microfluidics have enabled non-enzymatic glucose detection, whereas laser-induced interdigital graphene electrodes functionalized with rGO and glucose oxidase have supported flexible chemiresistive monitoring [203, 204]. These examples illustrate the evolution of LIG from a conductive support toward a multifunctional scaffold capable of incorporating catalytic materials, enzymes, microfluidic sampling, and on-body readout. Hybrid nanocomposite engineering further expands this functionality. Porous laser-written carbon can be combined with metallic nanoparticles, MXenes, conductive polymers, or metal–organic-framework-derived materials to improve catalytic activity, charge transfer, conductivity, or sensing stability. UV laser-written flexible electrodes containing MOF-derived Co/Co_3O_4/carbon composites, for example, exhibited lower impedance and improved electrochemical performance relative to bare LIG [205]. *In situ* formation of Ag nanoparticles within three-dimensional LIG architectures has also enabled self-powered glucose-sensing systems, demonstrating how direct laser writing can provide both structural patterning and a scaffold for functional nanocomposite formation [206].

Despite its processing simplicity, laser writing has important manufacturing limitations. Feature size is constrained by laser spot diameter, thermal diffusion, heat-affected zones, and substrate response. Stencil-assisted CO_2-laser processing has been explored to reduce minimum feature dimensions and improve higher-density sensor fabrication [207]. More generally, achieving uniform graphitization, conductivity, porosity, and surface chemistry over large areas remains challenging, particularly when moving from individual prototypes to high-throughput production. Mechanical fatigue, environmental stability, compatibility with substrates other than PI, and batch-to-batch reproducibility therefore remain central issues [200]. Printed, coated, and solution-processed nanomaterial interfaces provide a third fabrication strategy by depositing pre-synthesized conductive or catalytic materials onto flexible supports. Inkjet printing, screen printing, aerosol-jet printing, spray coating, blade coating, drop casting, and electrophoretic deposition can be used to form sensing layers under relatively mild processing conditions. Their manufacturing behavior depends not only on the intrinsic properties of graphene, MXenes, CNTs, metallic nanoparticles, or conducting polymers, but also on ink rheology, dispersion stability, wetting, drying, coating thickness, substrate adhesion, and post-processing [208–210].

Inkjet printing is particularly attractive for mask-free and material-efficient patterning because individual droplets can be digitally positioned to control electrode geometry and local film thickness. A fully inkjet-printed graphene-Prussian Blue platform on flexible PI demonstrated electrochemical peroxide and lactate sensing, illustrating how additive deposition can combine conductive and catalytic materials within a common manufacturing workflow [211]. Reliable printing nevertheless requires careful control of viscosity, surface tension, droplet formation, substrate wetting, coffee-ring effects, and curing conditions, especially when biological recognition elements or redox mediators are incorporated into the ink formulation. Screen printing offers lower spatial resolution but greater compatibility with high-throughput and low-cost manufacturing, particularly on textile, paper, and polymer substrates. Screen-printed textile electrodes have been demonstrated for non-invasive sweat glucose monitoring, while paper-based ionic-liquid/graphene electrodes modified with Prussian Blue/MXene composites have enabled enzymatic glucose sensing [212, 213]. Such platforms illustrate the manufacturing advantage of printing entire electrode layouts directly from functional inks, although film thickness, mesh resolution, ink formulation, curing, and substrate roughness can introduce device-to-device variability.

Graphene and its derivatives remain common components of printed wearable biosensors because they combine high surface area, electrical conductivity, chemical functionalizability, and solution processability. Graphene oxide, rGO, and hybrid graphene inks can promote electron transfer and provide sites for enzyme or receptor immobilization, but their performance depends strongly on dispersion quality, binder chemistry, functionalization, and substrate adhesion [210, 214]. Functionalized graphene oxide has, for example, been integrated into continuous capillary-flow platforms for wearable glucose and lactate monitoring [215]. MXenes provide another important class of printable conductive nanomaterials because of their metallic conductivity, layered morphology, hydrophilicity, and compatibility with aqueous formulations. MXene-based interfaces have been incorporated into paper patches, hydrogels, stretchable electrodes, and textile platforms for glucose and multiparameter sweat sensing [216, 217]. A Ga@MXene wearable biosensor combined conductive MXene networks with a stretchable hydrogel matrix for sweat glucose monitoring, illustrating the compatibility of two-dimensional nanomaterials with hydrated and mechanically compliant sensing platforms [218]. Their major manufacturing limitation is chemical stability: oxidation and prolonged electrolyte exposure can degrade conductivity and sensing performance. Embedding MXenes within hydrogels or composite matrices, combining them with conductive polymers or metallic nanoparticles, and improving encapsulation are therefore important stabilization strategies [218, 219].

CNTs and metallic nanostructures further broaden the composition of printed wearable interfaces. CNTs are frequently incorporated into hybrid inks to improve electrical percolation, film integrity, flexibility, and strain tolerance, whereas Prussian Blue nanoparticles, Au nanoparticles, Ag nanowires, metal oxides, and liquid metals can provide elecftrocatalytic activity, optical functionality, or enhanced electrical conductivity. Prussian Blue-modified graphene and MXene electrodes, for example, have been used to improve peroxide-mediated enzymatic detection, while printed metal-oxide structures have supported flexible electrochemical sensing [213, 220]. These hybrid interfaces nevertheless introduce additional manufacturing variables, including particle aggregation, oxidation, phase separation, binder compatibility, adhesion loss, and fatigue during repeated deformation. Transfer-based integration, laser writing, and additive printing therefore represent complementary rather than competing routes for wearable biosensor fabrication. Transfer processes are particularly useful when high-resolution structures must be integrated onto substrates that cannot be patterned directly; laser writing provides mask-free formation of porous conductive interfaces; and printing enables scalable deposition of nanomaterial-based sensing layers over large and unconventional surfaces.

6.3. Textile and fiber-based wearable biosensors

Textile- and fiber-based biosensors extend wearable sensing beyond planar polymer films by integrating sensing functionality directly into fibers, yarns, woven fabrics, knitted structures, and garments. Their main manufacturing advantage is that mechanical compliance, air permeability, large-area coverage, and established textile-processing infrastructure can be combined with biochemical, electrochemical, optical, or electrophysiological sensing. Conductive functionality can be introduced through fiber spinning, wet spinning, electrospinning, weaving, embroidery, screen or inkjet printing, dip or spray coating, and deposition of graphene, carbon nanotubes (CNTs), MXenes, conductive polymers, or metallic nanostructures. Fiber-level manufacturing provides a route to highly integrated wearable sensing architectures. Rather than depositing separate electrodes onto a finished textile, functional materials can be incorporated during fiber formation or assembled directly around a fiber core. Zhang *et al* demonstrated this

approach using functionalized CNT strips helically arranged around a pre-stretched polymer fiber to create an all-in-one electrochemical sensing fiber. The device simultaneously measured pH, K^+, Na^+, glucose, lactate, and uric acid using approximately 1 μl of sweat and retained operation under strains of up to 300% [221]. This architecture illustrates an important advantage of fiber-based manufacturing: sensing, mechanical compliance, and multianalyte functionality can be embedded into the fiber itself rather than assembled as separate planar layers.

A representative example of textile-integrated biosensor fabrication was reported by Napier *et al*, who developed a multifunctional electrochemical sensing yarn by braiding rGO-based functional fibers into a single wearable textile platform (figure 8(C)) [222]. The rGO fibers were fabricated by dry spinning graphene oxide followed by chemical reduction, producing conductive fibers with electrical conductivity of approximately 18 kS m^{-1}, tensile strength exceeding 200 MPa, Young's modulus above 6 GPa, and elongation at break greater than 9%. Four functional fibers, e.g. a Pt nanoparticle-modified lactate working electrode, PtNP-rGO counter electrode, Ag/AgCl reference electrode, and ferrocene-functionalized pH sensing fiber, were braided into a single electrochemical yarn before integration into a multilayer textile patch consisting of linen fabric, patterned gauze, filter paper, PET/adhesive encapsulation, and wireless readout electronics. The fabricated lactate sensor achieved a limit of detection of 0.7 mM, a sensitivity of 3.8 μA mM^{-1} cm^{-2}, and retained approximately 97% of its initial response after more than 2 h of continuous operation. Wireless on-body validation during cycling demonstrated continuous real-time monitoring of sweat lactate and pH with good agreement to commercial analytical measurements, highlighting how fiber fabrication, textile integration, multilayer packaging, wireless electronics, and physiological validation can be combined into a single wearable manufacturing strategy. Core–shell and nanofiber-based structures provide another strategy for improving the electrical and mechanical properties of wearable fibers. Aramid-nanofiber/MXene coaxial fibers, for example, have achieved conductivities of approximately 3.0×10^5 S m^{-1} together with high tensile strength and toughness, while the aramid shell improves resistance to chemical and environmental degradation [223]. Although such fibers are not exclusively biochemical biosensors, they illustrate how conductive 2D materials can be structurally protected within mechanically robust fiber architectures. Electrospinning offers a related route to high-surface-area and highly oriented fibrous structures. High-strength PAN nanofiber yarns with tensile strengths exceeding 700 MPa have been fabricated by combining electrospinning with controlled alignment, while Ag-nanowire coating can subsequently impart conductivity [224]. These fabrication concepts are directly relevant to wearable biosensors because high surface area, mechanical durability, and stable electrical pathways are critical for maintaining signal integrity in deformable textile environments.

Coating and printing provide a simpler route when conventional textiles are used as the structural substrate. Commercial conductive fabrics can be converted into biochemical sensing electrodes without custom fiber synthesis. Chowdhury *et al* functionalized commercially available conductive textiles with glucose oxidase or glucose dehydrogenase and demonstrated sweat glucose sensing, with the best-performing configuration reaching a detection limit of 41.3 μM [225]. This approach is manufacturing-relevant because it avoids complex fiber production and instead uses readily available e-textiles as standardized electrode supports. However, the analytical performance remains dependent on enzyme immobilization, local conductivity, fabric porosity, and reproducibility of the textile surface. Solution-based functionalization also enables conductive or catalytic nanomaterials to be immobilized onto natural fibers. Du *et al* used a modified cyanotype process to deposit Prussian Blue nanoparticles of approximately 18 nm onto silk fibers for electrochemical H_2O_2 sensing [226]. The process preserved the mechanical properties of silk while providing stable electrochemical functionality, and the resulting fiber retained electrical performance after 100 home-laundry cycles. This is a particularly important result from a manufacturing perspective because washability remains one of the least consistently demonstrated properties in textile biosensors. It also illustrates that low-cost chemical functionalization can provide an alternative to vacuum deposition or lithographic processing when large-area or garment-integrated sensing is required.

Screen printing and related additive methods are also attractive because they are already compatible with high-throughput textile processing. Metallic or carbon-based inks can be patterned directly onto woven or knitted fabrics, followed by deposition of catalytic nanoparticles or biorecognition layers. Lim *et al* screen-printed Ag-based electrodes on PET/cotton fabrics and subsequently electrodeposited Au nanoparticles to improve surface properties and biocompatibility [227]. The resulting textile electrodes achieved an initial signal-to-noise ratio of approximately 12.5 for electrophysiological measurements and retained functionality over 15 washing cycles, although the signal-to-noise ratio decreased to approximately 7.2 after repeated laundering. While this platform is electrophysiological rather than molecular, the durability data are highly relevant to biochemical textile sensors because the same conductive networks and interconnects must withstand laundering and mechanical wear. Washability and mechanical

durability remain central challenges in textile biosensor fabrication. Conductive coatings that remain stable during bending can still fail during washing due to abrasion, detergent exposure, swelling, oxidation, or delamination. Electrospun PVDF coatings on CNT yarns provide an example of how interfacial engineering can improve long-term robustness. Such yarns retained functionality after 10 washing cycles, approximately 1200 rubbing cycles, and up to 200 000 mechanical fatigue cycles [228]. These results indicate that coating adhesion and fiber-material interfacial strength may be as important as initial electrical conductivity when textile devices are intended for repeated wear. However, laundering protocols vary substantially across studies, preventing direct comparison of durability metrics and highlighting the need for more standardized testing.

6.4. Epidermal microfluidics and biofluid management

Rather than functioning as isolated sensing electrodes, modern wearable devices integrate flexible substrates, microfluidic channels, biochemical recognition layers, wireless electronics, and sometimes active sampling mechanisms into unified epidermal biointerfaces. From a manufacturing perspective, the analytical performance of these systems depends as much on reliable biofluid handling as on the sensitivity of the sensing material itself [229]. Sweat remains the most extensively investigated biofluid for wearable biosensing because it can be collected non-invasively and contains a wide range of physiologically relevant biomarkers, including electrolytes, metabolites, amino acids, hormones, vitamins, drugs, and inflammatory mediators. However, sweat collection presents several engineering challenges. Sweat secretion varies considerably with body location, hydration level, temperature, physical activity, and individual physiology. Under resting conditions, secretion rates may be insufficient for continuous monitoring, whereas high perspiration during exercise can dilute analytes, accelerate evaporation, and promote mixing between newly secreted and previously accumulated sweat. Epidermal microfluidic systems therefore perform several essential functions simultaneously, including controlled sweat collection, directional transport, separation of fresh and aged sweat, regulation of sample residence time, and minimization of evaporation and external contamination.

The fabrication of epidermal microfluidics has evolved considerably during the past few years. Early wearable devices often relied on simple reservoirs positioned directly above sensing electrodes, providing limited control over sample transport and renewal. More recent systems employ multilayer microchannels, passive capillary networks, burst valves, sweat-routing chambers, venting structures, and three-dimensional epifluidic architectures that guide sweat across multiple sensing regions without external pumps. These designs require precise control over channel dimensions, surface wettability, sealing quality, adhesive layer thickness, and mechanical compliance because inadequate fluidic design can result in air entrapment, leakage, backflow, evaporation, delayed sensor response, or analyte cross-contamination. A representative example was reported by Wu *et al*, who developed a DLP-printed epidermal microfluidic 'sweatainer' platform that integrates three-dimensional fluid-control elements with a conformal skin interface for passive sweat collection and sequential sample management (figure 8(D)) [230]. The device consisted of a 3D-printed photocurable-resin microfluidic network combined with a 200 μm-thick PDMS reservoir capping layer, a 60 μm biomedical adhesive gasket, and a 400 μm-thick PDMS epidermal port containing a laser-patterned sweat-collection opening of approximately 180 mm^2. The microfluidic architecture incorporated rectangular channels measuring approximately 600 μm in width and 400 μm in height, together with ventilation structures and geometry-controlled capillary burst valves that regulate flow into sequential collection reservoirs. The complete device was designed to collect up to approximately 50.8 μl of sweat while maintaining a fluid-tight skin interface and resisting uncontrolled fluid displacement during mechanical handling. By exploiting additive manufacturing to define non-planar valve geometries and integrated fluid-routing structures, the platform demonstrates how three-dimensional fabrication can expand the design space of epidermal microfluidics beyond conventional planar soft-lithographic architectures.

Several representative studies demonstrate how nanostructured sensing interfaces can be successfully integrated with epidermal microfluidics. Wang *et al* reported an integrated wearable electrochemical platform for continuous monitoring of metabolites and nutrients in sweat by combining graphene electrodes functionalized with molecularly imprinted polymers and redox-active nanoparticles with iontophoresis-based sweat induction, microfluidic sampling, onboard calibration, signal processing, and wireless communication [231]. Rather than optimizing only the sensing chemistry, this work emphasized complete system integration, illustrating how sensing performance depends on coordinated interaction between biofluid sampling, transport, calibration, and electronic readout. A similar systems-level design philosophy is evident in the Stressomic platform, which integrates laser-engraved graphene electrodes decorated with gold nanodendrites, iontophoretic sweat stimulation, microfluidic burst valves, and wireless electronics for multiplexed monitoring of cortisol, epinephrine, and norepinephrine [232]. Such

platforms demonstrate that wearable biosensor fabrication has progressed beyond isolated nanomaterial development toward highly integrated analytical systems in which microfluidics and sensing are designed simultaneously.

Laser-based manufacturing also contributes to epidermal microfluidic integration. Fully laser-fabricated wearable devices have combined laser-induced graphene electrodes with laser-patterned or paper-based sweat collectors to enable simultaneous monitoring of uric acid, tyrosine, pH, and ionic impedance [202]. Besides eliminating conventional photolithography, laser processing enables electrode fabrication and fluidic integration within the same manufacturing workflow, reducing assembly complexity and improving alignment between sensing and sampling components. Bioinspired microfluidic architectures have further improved passive sweat collection and transport. Liao *et al* developed epidermal microchannels inspired by the vein structure of Ginkgo biloba leaves, enabling rapid and time-sequenced collection of sweat for glucose and lactate analysis [233]. Shin *et al* reported hierarchically graded microchannels combined with superhydrophobic–superhydrophilic Janus membranes that enabled directional capillary transport, minimized evaporation, and supported multiday sweat collection without external pumping [234]. These examples illustrate how channel geometry, wettability gradients, and biomimetic fluid routing can significantly improve sample renewal and analytical reproducibility while reducing power consumption. Although fluidic design is essential, successful epidermal integration also depends on mechanical compatibility with the skin. Wearable devices must maintain intimate contact during bending, stretching, sweating, and prolonged use without causing discomfort or irritation. Adhesive layers, encapsulation materials, stretchable interconnects, breathable substrates, and flexible electronics must therefore be designed together so that they preserve both reliable skin attachment and uninterrupted sweat transport. Poor mechanical integration can lead to leakage, motion artifacts, delamination, unstable electrode contact, and degradation of analytical performance despite highly sensitive sensing materials.

Despite substantial progress, epidermal microfluidic biosensors continue to face significant manufacturing challenges. Sweat secretion remains inherently variable and often insufficient during sedentary conditions, requiring iontophoresis, exercise, thermal stimulation, or highly efficient passive microfluidic designs. Long-term operation is further complicated by enzyme degradation, biofouling, evaporation, salt crystallization, pH fluctuations, mechanical deformation, and gradual deterioration of skin adhesion. From a manufacturing perspective, reproducible assembly of multilayer microfluidics together with sensing interfaces, membranes, adhesives, encapsulation layers, and electronic components remains considerably more challenging than fabrication of individual sensing elements. Furthermore, interpretation of sweat biomarker concentrations remains complicated because sweat composition does not always correlate directly with blood chemistry, making calibration dependent on sweat rate, sampling location, and individual physiological differences.

6.5. Packaging, power, and wireless integration

Consequently, packaging has evolved from a passive protective layer into an active component of wearable system design, where mechanical reliability, electrical stability, and user comfort must be optimized together. Recent wearable platforms increasingly adopt a co-design strategy in which sensing materials, encapsulation, power management, and communication modules are developed as an integrated architecture rather than assembled independently [235, 236]. Encapsulation is central to long-term device reliability because it must simultaneously protect conductive traces and electronic components from sweat, mechanical damage, and environmental degradation while preserving access of the sensing region to biological fluids. Unlike rigid biosensors enclosed within conventional packages, wearable systems require encapsulation layers that remain stretchable, breathable, and conformal during repeated body motion. Kim *et al* demonstrated this concept using photo-patternable Ecoflex as both a flexible substrate and an encapsulating material capable of electrically isolating neighboring sensing channels while preserving mechanical stretchability and skin conformity [188]. Similarly, monolithically integrated textile wristbands have shown that electronic interconnects can be encapsulated without sacrificing the intrinsic porosity and air permeability of fabrics, enabling waterproof operation together with wireless epidermal biosensing [237]. These examples illustrate that packaging has become a functional design element rather than simply a protective coating.

Mechanical integration presents another major challenge because wearable devices combine components with widely different mechanical properties. Flexible sensing layers are often coupled to comparatively rigid batteries, integrated circuits, connectors, antennas, or communication modules that concentrate mechanical stress during bending and stretching. To reduce strain localization, recent devices

employ serpentine interconnects, stretchable conductors, soft encapsulation layers, multilayer packaging, and mechanically isolated rigid islands that protect fragile electronic components while maintaining overall flexibility [238]. Nevertheless, prolonged exposure to sweat, repeated deformation, and adhesive fatigue can gradually weaken electrical connections or promote moisture penetration into electronic components. Despite their importance for practical deployment, long-term shelf life, sterilization compatibility, connector durability, and moisture resistance remain insufficiently quantified in most wearable biosensor studies. Wireless communication has become an essential component of modern wearable biosensors because continuous physiological monitoring requires reliable transmission of analytical data to external devices. Bluetooth Low Energy (BLE) and near-field communication (NFC) remain the dominant communication technologies, although each introduces different manufacturing considerations. NFC enables battery-free or near-battery-free operation through inductive coupling but requires close proximity between the wearable sensor and the reader. BLE supports longer communication distances and continuous real-time monitoring but requires greater energy consumption together with more complex electronic circuitry [239]. As a result, communication strategy directly influences battery size, packaging architecture, thermal management, and overall device flexibility.

A representative example of system-level integration was reported by Park *et al*, who developed a light-adaptive wearable biosensing platform, combining epidermal microfluidics, flexible electronics, photovoltaic energy harvesting, electromagnetic wireless charging, rechargeable batteries, adaptive power management, and BLE communication within a single skin-interfaced architecture (figure 8(E)). The modular design coupled a detachable PDMS-based sweat-sensing unit to a flexible electronic platform, while the power-management circuitry dynamically selected between harvested, wirelessly supplied, and stored energy according to operating conditions. Notably, the photoluminescent encapsulation supported approximately 60 min of operation in darkness following 2 min of UV charging, illustrating how packaging, energy harvesting, power management, sensing, and wireless communication can be co-designed rather than treated as independent subsystems (10.1038/s41467-025-60911-1) [240].

Power supply remains one of the major limitations for flexible wearable biosensors because conventional lithium batteries are relatively bulky, rigid, and mechanically incompatible with soft substrates. Consequently, recent research has increasingly focused on self-powered and energy-harvesting systems that reduce dependence on rigid batteries. Biofuel cells, triboelectric nanogenerators, piezoelectric harvesters, supercapacitors, and hybrid energy systems have all been explored as alternative power sources for wearable biosensors [241, 242]. Although many of these technologies remain at the proof-of-concept stage, they illustrate how energy harvesting may eventually become integrated into wearable biosensor fabrication rather than added as an external component. A representative example is a battery-free sweat sensing platform that combined triboelectric and electromagnetic energy harvesting with wireless biochemical sensing. During running, human motion charged onboard capacitors from approximately 2.2–3.3 V within 33–60 s, after which Bluetooth transmission of Na^+ and K^+ measurements was sustained during approximately 35 min of continuous exercise. This study demonstrates that human-motion energy can support practical biochemical sensing, while also emphasizing the need for ultralow-power electronics and energy-efficient wireless communication to maximize operational lifetime.

Manufacturing strategies increasingly seek compatibility between sensing components and electronic integration. Screen-printable functional nanomaterials have been investigated for enzyme-based biofuel cells, allowing energy generation and electrochemical sensing to be fabricated using similar additive manufacturing processes [209]. Likewise, multilayer printing approaches have enabled simultaneous fabrication of conductive interconnects, sensing electrodes, and wireless circuitry through carefully engineered inks and oxidation-resistant sintering processes [243]. Such approaches reduce assembly complexity while improving compatibility among conductive materials, encapsulation layers, sensing interfaces, and electronic components, making them attractive for scalable wearable manufacturing. Despite substantial progress, packaging and electronic integration remain among the least standardized aspects of wearable biosensor fabrication. Moisture ingress, sweat-induced corrosion, antenna deformation, battery thickness, connector reliability, persistent skin adhesion, sterilization, storage stability, and scalable multilayer assembly are discussed far less frequently than sensing performance, even though they often determine real-world device lifetime.

6.6. Manufacturing reliability, testing, and reporting

Conductive films, nanomaterial coatings, interconnects, enzyme layers, and microfluidic structures may crack, delaminate, or lose electrical continuity under cyclic deformation. Continuous exposure to sweat, saliva, interstitial fluid, or wound exudate subjects biorecognition layers to variations in pH, ionic strength, hydration, temperature, and biofouling. Evaporation, salt crystallization, variable secretion rates, and degradation of enzymes or other recognition elements can introduce signal drift, making co-design

of sensing chemistry, surface functionalization, microfluidics, and encapsulation essential for stable operation. Transfer printing, laser writing, screen printing, inkjet printing, textile processing, and additive manufacturing each introduce process-specific sources of variation related to alignment, ink rheology, nanomaterial dispersion, graphitization, coating thickness, or substrate heterogeneity. Mechanical mismatch between rigid electronic components and soft substrates, unstable electrical connections, inadequate encapsulation, or poor integration between sensing and microfluidic layers can compromise device reliability even when individual sensing elements perform well. Future progress will depend on improved process control, application-relevant durability testing, and integrated device architectures that combine scalable fabrication with mechanical robustness and long-term operational stability.

7. AI-assisted and process-aware biosensor manufacturing

Artificial intelligence is increasingly entering biosensor nanofabrication not only as a tool for signal interpretation, but also as an enabling layer for design, process optimization, defect inspection, material synthesis, and manufacturing control. In this review, AI-assisted biosensor manufacturing refers to data-driven workflows that connect fabrication parameters, nanoscale structure, material properties, process variability, and device performance. This distinction is important because practical translation depends not only on analytical sensitivity, but also on reproducibility, yield, defect tolerance, scale-up, and compatibility with biofunctionalization and device integration. Modern biosensor fabrication involves strongly coupled processes, including lithography, etching, deposition, nanoimprinting, printing, laser writing, nanomaterial synthesis, soft microfluidics, surface functionalization, and packaging. Small changes in nanogap size, etch depth, electrode morphology, surface roughness, coating density, or interfacial chemistry can alter optical resonance, electrical response, drift, or calibration. These multivariable process–structure–performance relationships are difficult to optimize through manual trial-and-error alone. Current AI applications therefore cluster around four manufacturing functions: fabrication-aware optimization, defect and variability control, AI-assisted synthesis of biosensor-enabling materials, and closed-loop experimental workflows. Importantly, much of the strongest evidence remains biosensor-enabling rather than biosensor-exclusive, so AI should presently be viewed as a process-support layer rather than a replacement for nanofabrication expertise or experimental validation.

7.1. Fabrication-aware design and process optimization

AI-assisted design in biosensor nanofabrication should not be viewed only as a route to structures with higher simulated optical or electrical performance. From a manufacturing perspective, the more important objective is fabrication-aware design: identifying geometries and process conditions that retain high performance while remaining compatible with realistic feature-size limits, lithographic bias, etch profiles, material deposition, surface functionalization, and fabrication variability. This distinction is critical because idealized inverse-designed structures may contain narrow nanogaps, sharp corners, high-aspect-ratio features, disconnected elements, or process windows that cannot be reproduced reliably. Nanophotonic biosensors provide a natural application for this approach. Conventional design typically relies on FDTD, FEM, RCWA, eigenmode calculations, or related full-wave simulations. These methods are accurate but become computationally demanding when many geometric and material parameters must be optimized simultaneously. Machine-learning surrogate models and inverse-design frameworks can learn structure–response relationships and rapidly screen candidate structures after an initial simulation dataset has been generated. Recent reviews describe the use of neural networks, topology optimization, adjoint methods, evolutionary algorithms, reinforcement learning, and generative models for nanophotonic inverse design [244]. For biosensors, however, optimization objectives should extend beyond resonance wavelength or quality factor to include linewidth, refractive-index sensitivity, analyte-accessible near-field overlap, field enhancement, fabrication tolerance, and compatibility with liquid-phase operation and surface functionalization. Fabrication-aware optical design also depends on the accuracy of the material models supplied to simulation. Recent systematic spectroscopic-ellipsometry measurements of MBE-grown AlxGa1 − xAs, independently constrained by high-resolution x-ray diffraction and photoluminescence, demonstrate the need for composition- and wavelength-specific refractive-index data when small index errors can alter modal confinement, coupling, and resonance predictions [245]. Inverse lithography provides a particularly direct link between AI design and manufacturability. Modern AI-assisted inverse-lithography workflows use CNNs, GANs, support-vector-based models, and hybrid physics-AI methods to predict mask-to-wafer transformations and correct geometries

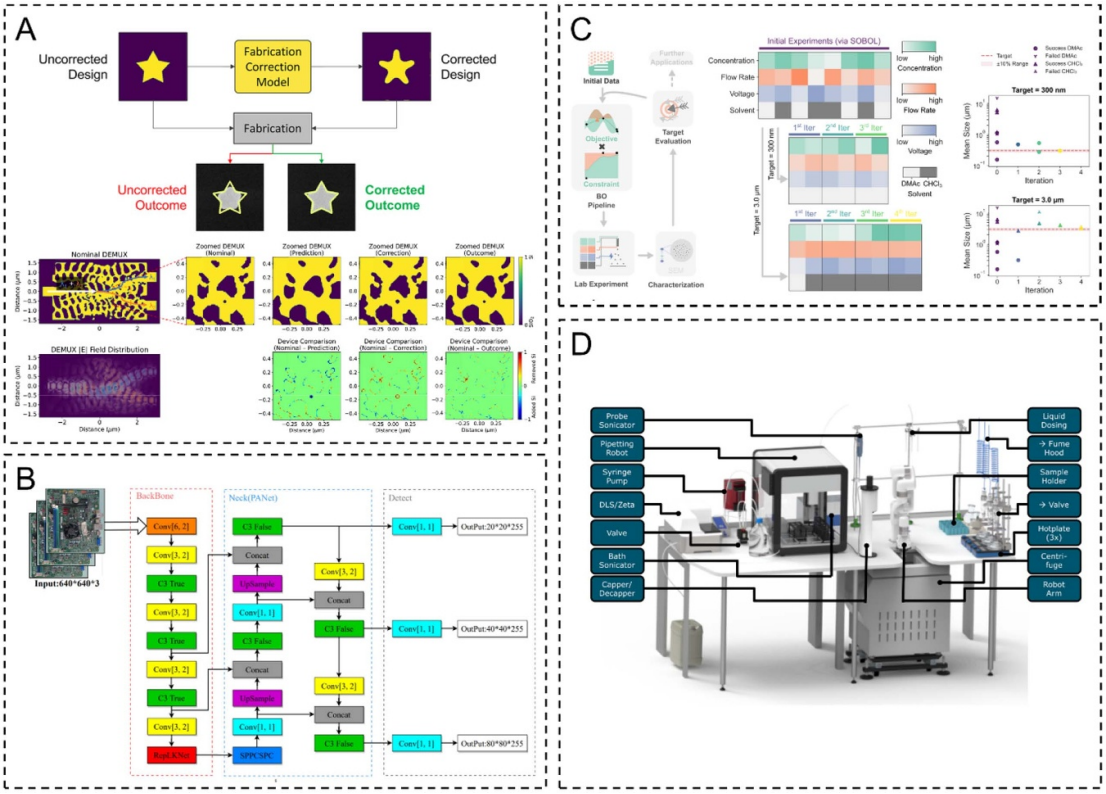


Figure 9. Representative artificial intelligence strategies for process-aware biosensor manufacturing. (A) Deep-learning-assisted prediction and pre-compensation of fabrication-induced distortions in inverse-designed nanophotonic devices, reducing structural error and fabrication-induced spectral shifts. Adapted from [248], Copyright© 2023 American Chemical Society. (B) Deep-learning-based manufacturing inspection pipeline for automated defect localization and classification using a multi-scale YOLO architecture. Reproduced from [258], Copyright© 2024 Springer Nature. (C) Constrained composite Bayesian optimization (CCBO) for target-driven electrospray synthesis of polymeric particles, integrating feasibility-aware optimization, experimental feedback, and convergence toward predefined particle sizes. Adapted from [268], Copyright© 2025 Royal Society of Chemistry. (D) MINERVA self-driving laboratory integrating robotic synthesis, purification, in-line characterization, process scheduling, and machine-learning feedback within a closed-loop experimental workflow. Adapted from [283], Copyright© 2025 American Chemical Society.

before fabrication [246]. This is directly relevant to plasmonic, metasurface, photonic-crystal, and FET-based biosensors because their functional structures are often defined through the same exposure, development, etching, and deposition constraints as semiconductor devices. The objective is no longer simply to generate an optically optimal geometry, but to generate a geometry that still produces the intended structure after the complete fabrication process.

A representative application of fabrication-aware AI is the use of deep-learning models to predict and compensate for process-induced structural distortions in nanophotonic devices (figure 9(A)). Models trained on SEM-derived data can learn the relationship between intended and fabricated geometries and predict systematic deviations such as over-etching, under-etching, corner rounding, and loss of fine structural features [247]. Building on this predictive capability, tandem deep-learning frameworks have been used to generate pre-compensated layouts that account for fabrication bias before processing, enabling the resulting structures to more closely reproduce the intended geometry and optical response without modifying the underlying fabrication process [248]. This progression from predicting fabrication errors to correcting them at the design stage is particularly relevant to nanophotonic biosensors, where relatively small geometric deviations can shift resonance positions, alter near-field localization, broaden high-Q features, and introduce device-to-device variability. However, these studies primarily provide biosensor-enabling evidence from integrated nanophotonics rather than direct demonstrations of biosensor manufacturing, and the pre-compensation literature cited here includes a preprint; such approaches should therefore be regarded as an emerging strategy for fabrication-aware biosensor design rather than an established manufacturing solution.

Fabrication robustness can also be incorporated directly into optimization objectives. Deep-learning-optimized photonic crystal nanobeam cavities have been designed to tolerate fabrication errors including surface roughness, structural slant, and positioning variation [249]. Although demonstrated outside biosensing, the principle is directly relevant to photonic biosensors, particularly high-Q resonators for

which extremely narrow linewidths may offer little practical advantage if the response varies strongly across nominally identical fabricated devices. This shifts inverse design from maximizing ideal performance toward finding a region of design space in which performance remains acceptable under realistic fabrication distributions. An adjacent example in hybrid III–V/silicon photonics demonstrates this design-for-manufacturing logic by jointly optimizing epitaxial composition, waveguide geometry, supermode confinement, a CMOS-compatible 220 nm silicon device layer, and tolerance to fabrication-induced deviations [250–252].

AI-assisted process optimization extends this logic from geometry to the manufacturing process itself. In continuous nanomanufacturing, machine learning has been proposed for soft sensing, multimodal metrology, yield modeling, process monitoring, and real-time control, particularly in roll-to-roll and large-area nanopatterning systems [253]. These concepts are relevant to biosensors fabricated by NIL, roll-to-roll replication, printing, laser processing, or other scalable routes because such processes contain interacting variables that cannot always be optimized effectively through one-factor-at-a-time experiments. Bayesian optimization is particularly useful when fabrication experiments are expensive or slow. In projection multi-photon 3D printing, Gaussian-process-based Bayesian optimization combined with active learning reduced geometric error to approximately the measurement-limited regime within only four optimization iterations, demonstrating how adaptive experimental design can substantially reduce process-development effort [254]. This concept is relevant to two-photon polymerization and micro-3D-printing of biosensor architectures, where laser power, scan speed, exposure dose, material formulation, voxel dimensions, and post-processing conditions interact strongly.

A similar strategy has been applied to plasma etching. Bayesian-optimized continuous plasma etching following Langmuir–Blodgett colloidal lithography was used to fabricate silicon monolithic structures with high-aspect-ratio cavities while reducing the experimental burden associated with etch-process development [255]. Although not developed as a biosensor platform, such optimization is directly transferable to silicon nanowires, nanopores, photonic structures, and micro/nanofluidic architectures where etch depth, sidewall angle, surface roughness, and aspect ratio affect device performance. Large-area replication processes provide another target. Grey relational analysis combined with artificial neural networks has been used for multi-geometry optimization of a roll-to-roll nanoimprint module, linking process parameters to dimensional outcomes in continuous replication [256]. For biosensor manufacturing, this is particularly relevant to replicated plasmonic, photonic, and polymeric sensor surfaces, where scalability is meaningful only if nanoscale fidelity and device response remain stable over large areas and across repeated production cycles.

7.2. Defect prediction, fabrication variability, and quality control

This has been demonstrated in silicon nanowire FET arrays, where fabrication and surface-modification variability produce sensor-to-sensor electrical differences, and in plasmonic and nanophotonic platforms, where variations in nanogap width, roughness, periodicity, or etch depth can shift optical response [15,28]. AI-assisted inspection provides a route from sparse manual quality control toward automated analysis of high-volume metrology data. Semiconductor manufacturing offers the most mature examples, particularly for SEM-based defect classification and localization using deep-learning models [257]. Similar workflows are directly relevant to nanofabricated biosensors containing nanoholes, nanopillars, nanogaps, etched nanowires, photonic crystals, metasurfaces, or replicated NIL structures. A representative example is shown in figure 9(B), where deep-learning-based object detection is used for automated manufacturing inspection. Although developed outside biosensor fabrication, the same approach could be adapted to detect incomplete pattern transfer, broken conductive traces, dimensional deviations, and other defects relevant to biosensor quality control [258]. Optical inspection offers a complementary strategy when large areas must be screened more rapidly than is practical with SEM. Computational imaging combined with neural-network analysis has enabled detection of deep-subwavelength defects with classification performance above 90%, including defects approaching approximately $\lambda/16$ in scale [259, 260]. Such approaches could be particularly useful for centimeter-scale plasmonic, photonic, and nanoimprinted biosensor substrates.

Limited annotated training data remain an important constraint. Synthetic data provide one solution: Shinde *et al* generated artificial SEM images of photolithographic line defects and trained YOLOv8 for automated detection, achieving approximately 96% mAP and detecting 84.6% of bridge defects and 78.3% of break defects in real SEM images [261]. Transfer learning and semi-supervised approaches may further reduce the need for large labeled datasets, which is particularly relevant for biosensor architectures with relatively small device-specific defect libraries. Defect mechanisms also depend strongly

on fabrication method. NIL can introduce incomplete filling, residual-layer variation, air trapping, demolding damage, and local pattern-density effects. A recent physics-informed/data-driven NIL framework combined process simulation, CNN-based virtual metrology, and uncertainty-aware prediction to estimate spatial defect risk before fabrication [262]. Printed and flexible biosensors present different failure modes, including line breaks, short circuits, pinholes, thickness nonuniformity, and delamination. Related anomaly-detection approaches developed for PCB inspection have achieved approximately 98% detection performance with false-pass rates below 1.7% and provide a methodological basis for inspection of printed electrochemical electrodes, textile interconnects, and flexible sensing layers [263].

Quality control can also move upstream from post-process defect detection toward predictive quality. Models that integrate process parameters, tool logs, metrology, and historical production data may identify process drift before visible failure occur [264]. This is especially important for biosensors because functional degradation may arise from subtle changes in film thickness, porosity, nanoparticle density, oxide quality, hydrogel state, or receptor loading without producing an obvious macroscopic defect.

High-resolution physical and electronic characterization provides a complementary route for establishing the process-structure-performance relationships required for meaningful quality control. Cross-sectional scanning tunneling microscopy and spectroscopy (X-STM/STS), for example, can simultaneously resolve buried nanoscale morphology and spatially dependent electronic properties, including local density of states and wavefunction distributions in semiconductor nanostructures [265]. In recent III–V-on-silicon laser manufacturing work, atomic-scale X-STM/STS has been combined with dislocation-filter engineering and matched device fabrication to track defect evolution through the epitaxial structure and relate growth optimization to the performance of the resulting devices [266]. Although these studies are not biosensor demonstrations, they illustrate how advanced metrology can connect fabrication history, nanoscale structure, and device-relevant functionality—a principle directly applicable to manufacturing-oriented biosensor quality control. The major limitation is that current AI inspection studies rarely connect structural abnormalities directly to biosensor performance. Most models determine whether a structure is anomalous but do not predict whether the deviation alters resonance wavelength, electrochemical current, impedance, calibration slope, limit of detection, or real-sample accuracy. Future biosensor quality-control datasets should therefore pair fabrication and structural metrology with functional sensing measurements from the same devices.

7.3. AI-assisted nanomaterial synthesis for biosensor-enabling materials

Nanomaterials are central to many nanofabricated biosensors. Plasmonic Au and Ag nanoparticles provide LSPR and SERS enhancement, quantum dots enable fluorescence, metal and metal-oxide nanoparticles contribute electrocatalytic activity, graphene, CNTs, and MXenes form conductive sensing interfaces, while hydrogels and polymer coatings improve mechanical compatibility, antifouling behavior, and biomolecule immobilization. Because their performance depends strongly on size, morphology, crystallinity, surface chemistry, and synthesis history, reproducible nanomaterial synthesis has become an essential manufacturing requirement rather than a purely materials-science challenge. Conventional synthesis requires simultaneous optimization of numerous interacting parameters, including precursor concentration, temperature, pH, ligand chemistry, residence time, flow rate, and purification. AI-assisted synthesis addresses this multidimensional optimization problem using Bayesian optimization, surrogate modeling, active learning, reinforcement learning, robotic experimentation, and in-line characterization. Microfluidic synthesis is particularly well suited to these approaches because reaction conditions can be tightly controlled while spectroscopic characterization is performed continuously [267].

A representative example is presented in figure 9(C), where constrained composite Bayesian optimization autonomously guides electrospray synthesis toward predefined particle-size targets while satisfying practical processing constraints [268]. Rather than optimizing a single variable, the framework balances experimental feasibility with target particle size, demonstrating how AI can efficiently navigate multidimensional synthesis spaces while reducing experimental effort. Among biosensor materials, plasmonic nanoparticles represent one of the clearest applications. Their optical response depends critically on particle size, morphology, aspect ratio, tip sharpness, and surface chemistry. Self-driving laboratories combining microfluidics, in-line spectroscopy, and machine learning have demonstrated automated optimization of plasmonic nanoparticle synthesis, [269] while robotic platforms integrating automated synthesis, UV–vis characterization, and closed-loop optimization have achieved Au nanorod synthesis with resonance deviations of approximately $\leqslant$1.1 nm after 735 autonomous experiments [270]. Evolution-guided Bayesian optimization has similarly enabled multi-objective optimization of Ag nanoparticle synthesis, balancing optical performance with experimental efficiency [271].

Comparable strategies have also been demonstrated for quantum dots, where reinforcement-learning-based AlphaFlow and transfer-learning-assisted Bayesian optimization enable autonomous optimization of multistep synthesis routes and target optical properties [272, 273]. Beyond optical materials, AI-assisted synthesis is increasingly being applied to electrocatalytic nanoparticles, conductive inks, hydrogels, and antifouling polymers relevant to electrochemical, printed, wearable, and implantable biosensors [274–278]. Despite this progress, current AI-assisted synthesis primarily optimizes material-level properties rather than final biosensor performance. Future workflows should therefore extend optimization beyond nanoparticle size or optical response to include deposition, surface functionalization, storage stability, and analytical performance under realistic operating conditions.

7.4. Toward closed-loop and autonomous biosensor manufacturing

Closed-loop manufacturing represents the highest level of AI integration in biosensor fabrication by connecting design, synthesis, fabrication, inspection, characterization, and optimization within an iterative design–make–test–learn workflow [279]. Instead of optimizing individual fabrication steps independently, autonomous systems continuously update subsequent experimental decisions using feedback from previous manufacturing and characterization results. Current demonstrations are strongest at the nanomaterial level. AI-enabled robotic synthesis platforms have successfully combined automated experimentation with machine-learning-guided optimization [280–282]. A representative example is shown in figure 9(D), where robotic synthesis, automated purification, in-line characterization, scheduling, and machine-learning-based decision making are integrated into a unified autonomous laboratory capable of iterative experimental optimization [283]. Reinforcement learning further extends this concept by optimizing sequential experimental decisions. Systems such as AlphaFlow autonomously determine reagent addition, reaction sequence, and processing conditions through continuous experimental feedback [272]. Similar strategies could eventually be applied to biosensor fabrication steps including lithography, surface activation, receptor immobilization, antifouling-layer deposition, and microfluidic processing.

The next challenge is extending closed-loop optimization from nanomaterial synthesis to complete biosensor manufacturing. In principle, fabrication could be coupled with in-line optical inspection, SEM analysis, Raman mapping, profilometry, electrical characterization, impedance spectroscopy, and functional biosensing measurements, allowing AI to detect process drift, predict manufacturing yield, and adjust fabrication parameters in real time [253]. Unlike conventional nanomanufacturing, however, biosensors require optimization of both structural fidelity and biological function. Successful closed-loop manufacturing must therefore integrate functional metrics such as sensitivity, selectivity, response time, calibration stability, antifouling performance, drift, regeneration, and real-sample recovery rather than relying solely on dimensional or optical measurements. Digital twins could eventually unify design files, process histories, microscopy, surface chemistry, material characterization, and analytical performance into predictive manufacturing models, although such comprehensive biosensor manufacturing twins remain largely conceptual.

Several challenges continue to limit fully autonomous biosensor production. Current systems typically optimize isolated materials or fabrication steps, biological processes introduce additional variability, manufacturing datasets remain fragmented, and optimization often focuses on proxy variables without directly demonstrating improved biosensor performance. Consequently, the most realistic near-term strategy is modular autonomy, in which AI-assisted nanoparticle synthesis, process optimization, quality inspection, hydrogel or ink formulation, and feedback-driven manufacturing are implemented as interoperable modules before being integrated into complete autonomous production workflows.

7.5. Application-driven AI selection for biosensor design and nanofabrication

The increasing diversity of AI-assisted design and manufacturing approaches raises an important practical question regarding which computational strategy is most appropriate for a specific biosensor design or fabrication problem. Method selection should therefore be guided by the intended task, the type and amount of available data, the computational cost of data generation, and the degree of interpretability required. Artificial neural networks (ANNs) and deep neural networks (DNNs) are particularly suitable for learning nonlinear relationships between multiple geometrical or processing variables and device responses, whereas tree-based ensemble methods such as random forests and gradient-boosting algorithms are effective for structured datasets containing parameters such as feature size, pitch, gap width, height, exposure dose, or etching conditions. When interpretation of the model is required, feature-attribution approaches such as SHAP can further identify the variables that most strongly influence the predicted response. For nanofabrication, this information is particularly valuable because influential design variables can be translated into critical dimensional tolerances and prioritized during process optimization and quality control [284, 285].

A representative example is the machine-learning-assisted analysis of plasmonic coaxial cylindrical pillar/ring nanoarrays reported by Wang *et al* FDTD simulations were used to investigate the relationships between geometrical parameters and optical properties, including plasmonic resonance, local electric-field enhancement, and *Q*-factor. Machine-learning analysis, including XGBoost prediction, was subsequently used to evaluate these multidimensional structure–property relationships. Among the investigated geometrical variables, structure height and gap width were particularly effective for optimizing field enhancement and *Q*-factor [285]. This example illustrates how physics-based simulations can provide training data for machine-learning models, which can then accelerate exploration of the design space and identify the geometrical variables that require the greatest control during fabrication. For biosensor development, this approach can reduce the number of candidate geometries requiring experimental fabrication while providing a rational basis for defining critical process tolerances.

The appropriate computational strategy changes when the objective shifts from device design to experimental process optimization. Bayesian optimization is particularly useful when fabrication experiments are expensive, slow, or material intensive because new experimental conditions can be selected iteratively from previous observations rather than through exhaustive parameter sweeps. Recent studies have applied Bayesian optimization to SERS-related substrate and nanomaterial synthesis, where fabrication variables such as nanoparticle concentration and coating or synthesis conditions were optimized with respect to optical response, spatial uniformity, and reproducibility [286, 287]. Interpretability can also complement this process: SHAP analysis of an AI-assisted silver nanoparticle synthesis workflow identified silver nitrate concentration and seed flow rate as influential variables controlling spectral characteristics [287]. Such examples illustrate how AI can move beyond performance prediction toward identifying experimentally controllable parameters that directly inform fabrication decisions.

Inverse-design approaches provide another important route for application-driven AI selection. Neural surrogate models, deep generative models, and hybrid deep-learning/optimization frameworks can efficiently explore large nanophotonic design spaces that would otherwise require extensive numerical simulation [284, 288]. Importantly, recent approaches increasingly incorporate manufacturability into the optimization problem rather than maximizing ideal optical performance alone. Target-driven active learning has, for example, been used to generate metasurface geometries while maintaining compatibility with practical feature-size and deposition constraints, thereby providing a direct link between computational optimization and experimentally realizable structures [289]. More broadly, fabrication-aware and tolerance-aware inverse design is particularly relevant to biosensors in which small deviations in nanogap width, resonator dimensions, surface morphology, or periodicity can significantly alter resonance position, field enhancement, sensitivity, or device-to-device reproducibility.

AI method selection should therefore reflect the manufacturing question being addressed rather than relying on a single universally preferred algorithm. Prediction of complex structure–property relationships may favor neural networks, interpretable analysis of structured geometrical or process data may favor tree-based models combined with feature-attribution methods, and expensive experimental optimization may favor Bayesian approaches. Image-based deep learning can support automated inspection and quality control when microscopy or other imaging data are available, while inverse-design and active-learning frameworks are more appropriate when the objective is to identify manufacturable structures within large design spaces. The practical distinctions among these approaches are summarized in table 3.

Looking forward, agentic AI represents a further transition from individual predictive and optimization models toward computational systems capable of coordinating multiple specialized tasks. Lupoiu *et al* recently introduced a multi-agentic framework for autonomous freeform metasurface design in which specialized agents interact with surrogate electromagnetic solvers, optimization tools, other agents, and human designers to translate design objectives into optimized photonic structures [290]. Although agentic AI has not yet been established as an end-to-end strategy for biosensor manufacturing, this work provides a relevant conceptual direction for future systems in which simulation, nanostructure optimization, fabrication constraints, metrology, and experimental feedback could be coordinated within an integrated computational workflow. Such systems should nevertheless remain coupled to experimental validation, particularly for biosensors in which biological variability, surface functionalization, and real-sample performance cannot be captured solely through structural or electromagnetic optimization.

Table 3. Practical selection of AI/ML approaches for biosensor design and nanofabrication.

Design/manufacturing need	Suitable AI/ML approach	Typical input	Main advantage	Design/fabrication output	References
Predict nonlinear structure-performance relationships	ANN/DNN	Geometry, material, and process parameters	Captures complex nonlinear relationships and enables rapid surrogate prediction	Predicted optical/electrical response and candidate design space	[284, 288]
Identify critical design and fabrication variables	XGBoost + SHAP	Gap width, height, pitch, diameter, and other structured parameters	Provides predictive modeling together with interpretable parameter importance	Critical dimensions and fabrication tolerances	[285]
Optimize expensive fabrication or synthesis experiments	Bayesian optimization	Process parameters and experimental feedback	Efficiently explores multidimensional process spaces with fewer experiments	Optimized fabrication or synthesis conditions	[286, 287]
Generate fabrication-feasible nanostructures	Inverse design/active learning	Target optical/electrical response and fabrication constraints	Searches large design spaces while incorporating manufacturability	Candidate geometries compatible with fabrication limits	[284, 289]
Automated inspection and quality control	CNN-based image analysis	SEM, AFM, or optical microscopy images	Enables automated analysis of high-volume metrology data	Defect detection, classification, and process monitoring	Section 6.2 Refs.
Coordinate autonomous multi-step design	Agentic AI	Design objectives, constraints, simulation and optimization tools	Coordinates specialized models and computational tools	Iteratively optimized design workflow	[290]

8. Translational challenges and future directions in nanofabricated biosensors

Despite major advances in deterministic top-down patterning, scalable replication, bottom-up assembly, flexible and wearable fabrication, and AI-assisted manufacturing, translation of nanofabricated biosensors remains constrained by factors extending well beyond transducer sensitivity. Practical deployment requires reproducible fabrication, scalable production, stable biofunctionalization, robust packaging, quality-controlled manufacturing, and reliable operation in complex samples. Recent commercialization analyses similarly identify lot-to-lot consistency, shelf life, manufacturing scale-up, quality systems, and real-matrix validation as persistent barriers [291, 292].

8.1. Reproducibility, scalability, and manufacturing quality

Differences in nanogap width, etch depth, sidewall roughness, metal thickness, nanoparticle density, electrode morphology, or array periodicity can directly alter optical, electrical, or electrochemical response. At the same time, surface functionalization, receptor density, analyte transport, sample matrix, and readout conditions introduce additional variability, making reproducibility a coupled fabrication-chemistry problem. Top-down silicon nanowire FET biosensors illustrate this challenge clearly. Variations in nanowire dimensions, oxide properties, fabrication conditions, surface modification, and electrical readout can produce substantial sensor-to-sensor differences in threshold voltage, transconductance, noise, and biosensing response [28]. Similar considerations apply to transistor-based point-of-care platforms, where manufacturing yield, integration, and shelf stability remain important constraints on deployment [293]. Consequently, performance from an optimized single device provides limited information unless the corresponding variability across devices and fabrication batches is also quantified. Plasmonic, SERS, and nanophotonic biosensors face analogous challenges. Their response depends on nanogap geometry, hotspot density, particle morphology, resonance linewidth, metal roughness, and large-area structural uniformity. Heterogeneous hotspot distributions can limit quantitative reproducibility even when strong local enhancement is achieved. For practical plasmonic sensing, substrate-to-substrate variation, spatial signal uniformity, calibration stability, and fabrication yield are therefore as important as maximum field enhancement or limit of detection [15].

The biological layer introduces an additional source of variability. Enzyme activity, antibody orientation, aptamer density, blocking efficiency, reagent dispensing, drying conditions, and storage history can substantially affect sensor response even when the underlying nanostructure is well controlled.

Translation-focused analyses therefore emphasize that scale-up must include biological reagents, substrates, supply chains, quality systems, and storage stability rather than focusing exclusively on the transducer [291]. Each scalable fabrication route also introduces method-specific sources of variation. NIL and roll-to-roll processing are affected by mold wear, residual layers, registration, demolding, and defect propagation; printed platforms depend strongly on ink rheology, wetting, drying, and nanomaterial dispersion; and flexible or additive manufacturing must additionally control adhesion, material homogeneity, and mechanical deformation. Recent mass-produced nanowell biosensors illustrate this shift by combining large-array fabrication, batch manufacturing, reproducible device characteristics, and clinical validation within the same production-oriented workflow [294]. Such examples move beyond isolated nanofabrication demonstrations toward manufacturing-ready biosensor engineering. Scale-up must therefore be accompanied by predefined quality-control criteria and manufacturing-oriented reporting. In addition to sensitivity and limit of detection, translational studies should report fabrication yield, device-to-device and batch-to-batch variability, calibration stability, storage stability, recovery, response time, drift, and failure rates. AI-assisted metrology may support this transition by linking fabrication data with device performance, but conventional statistical process control and standardized functional testing remain equally important.

8.2. Biofunctionalization, packaging, and real-sample validation

Even highly reproducible nanostructures cannot become practical biosensors without stable and selective biointerfaces. Biofunctionalization must integrate antibodies, aptamers, nucleic acids, enzymes, peptides, molecularly imprinted receptors, or other recognition elements while preserving both transducer performance and biological activity. Receptor density, orientation, accessibility, blocking efficiency, antifouling chemistry, and long-term stability therefore become manufacturing parameters in their own right. This requirement is particularly important for electrochemical, optical, and field-effect biosensors because the recognition layer directly influences electron transfer, optical near-field interaction, surface charge response, fouling, and analyte accessibility. Bioelectrode studies consequently emphasize that electrode morphology and surface chemistry must be co-optimized with receptor immobilization to maintain sensitivity, selectivity, and operational stability [118]. Biofouling remains a major obstacle to real-sample operation. Biological and environmental matrices contain proteins, lipids, salts, cells, and other species that can adsorb nonspecifically, block target access, increase background, and introduce drift. Antifouling strategies based on PEG/OEGMA-type polymers, zwitterionic materials, hydrogels, peptide coatings, and biomimetic interfaces can reduce nonspecific adsorption, but they must retain efficient receptor coupling and analyte transport. Functionalized polymer brushes and zwitterionic coatings have demonstrated improved low-fouling performance and baseline stability under biologically relevant conditions, [295, 296] while related approaches have been explored in electrochemical–SPR platforms operating in blood, serum, and milk [297].

Biosensors must be combined with sample-delivery structures, microfluidics, membranes, adhesives, reagents, electronics or optics, power, and user interfaces without compromising the sensing surface. Packaging failures can produce leakage, evaporation, corrosion, contamination, optical misalignment, unstable electrical contact, or reagent degradation. These requirements are particularly demanding for wearable systems, where packaging must also tolerate repeated motion, moisture, and prolonged skin contact. Storage stability is similarly underreported in many proof-of-concept studies. Enzymes, antibodies, hydrogels, redox mediators, nanomaterials, and polymer coatings may change during drying, temperature cycling, humidity exposure, sterilization, or prolonged storage. Translation-oriented biosensor studies therefore increasingly emphasize dry-down chemistry, packaging, shelf life, and user workflow alongside analytical performance [298]. Performance in buffer or artificially spiked solutions may not predict behavior in authentic biological, environmental, or food samples because matrix components alter viscosity, ionic strength, adsorption, enzyme activity, optical background, electrochemical interference, and analyte transport. Practical studies should therefore use matrix-matched calibration, relevant concentration ranges, appropriate positive and negative controls, and comparison with established analytical methods where applicable.

Clinically oriented biosensors additionally require progression from analytical to diagnostic validation. Limit of detection and analytical sensitivity alone cannot establish clinical utility; appropriate patient cohorts, independent controls, reference-method comparison, and diagnostic sensitivity and specificity are required. Recent translational studies continue to emphasize validation in sufficiently large and biologically realistic sample populations as a prerequisite for meaningful clinical adoption [299]. The key implication is that real-sample operation should influence sensor design from the beginning rather

than serve only as a final proof-of-concept experiment. Antifouling layers, sample preparation, calibration strategy, microfluidic routing, reagent stabilization, and packaging should therefore be co-designed with the nanostructured transducer.

8.3. Future directions: toward integrated, standardized, and manufacturing-ready biosensors

A first priority is the transition from isolated sensing elements to fully integrated biosensing platforms. Future devices will increasingly combine sensing interfaces, microfluidics, electronics, packaging, wireless communication, and user workflow within a unified architecture, particularly for wearable, implantable, and point-of-care applications [300]. Hybrid printing has already enabled assembly-free fabrication of integrated microfluidic biosensors with sub-100 μm resolution, incorporated electrodes and fluidic channels, and lactate detection down to 442 nM across a physiologically relevant 1–10 mM range [301]. Such examples illustrate how manufacturing integration can reduce assembly complexity while preserving analytical functionality. Cross-sector co-packaged photonics programs provide a useful manufacturing analogue because they integrate component fabrication, chiplet assembly, optical/electrical interfaces, thermal constraints, packaging, and foundry compatibility within one system architecture [116]. A second priority is manufacturing-aware design from the earliest stages of device development. Rather than optimizing only sensitivity or signal enhancement, future biosensors should incorporate fabrication tolerance, production yield, batch reproducibility, and material compatibility as explicit design constraints. Wafer-scale graphene–CMOS biosensor fabrication has already demonstrated yields exceeding 99% with device-to-device variation below 30%, illustrating that manufacturing metrics can be optimized alongside sensing performance [293]. Similar considerations increasingly guide material selection in field-effect transistor biosensors, where compatibility with scalable semiconductor processing may be more important for translation than single-device performance alone [302].

Standardization will be equally important. Device yield, batch variability, calibration procedures, shelf life, real-sample recovery, and quality-control criteria remain inconsistently reported across biosensor studies. Integrated photonic biosensor literature similarly identifies the absence of standardized fabrication protocols, benchmarks, packaging strategies, and design guidelines as a major obstacle to commercialization [80]. Manufacturing-oriented reporting should therefore accompany conventional analytical metrics and include device-to-device variability, batch reproducibility, yield, calibration stability, storage stability, and validation across independent production runs. Quality control should also move upstream into the manufacturing process. Embedded monitoring can identify process deviations before final device testing and reduce both material waste and performance variability. Babamiri *et al* demonstrated this concept during electrofabrication of molecularly imprinted polymer biosensors, reporting reductions in relative standard deviation of 79% for agmatine detection and 87% for GFAP sensing, together with improved detection success rates [303]. Similar in-line strategies could be extended to nanophotonic, plasmonic, semiconductor, printed, and flexible biosensors. Biosensors should increasingly be judged not only by sensitivity under optimized conditions, but by their ability to provide reproducible measurements after realistic manufacturing, storage, handling, and sample exposure [298]. This shift is reflected in wearable and implantable biosensors based on printable core–shell nanoparticles that have enabled continuous monitoring of metabolites, vitamins, and therapeutic drugs in patient and animal studies using scalable inkjet printing [304].

Regulatory and quality-management considerations should likewise be introduced earlier in the development cycle. Material selection, fabrication route, process documentation, supply-chain strategy, immobilization chemistry, storage conditions, and quality-control procedures should be considered together rather than addressed only after analytical optimization [305]. The choice between semiconductor fabrication, roll-to-roll processing, additive manufacturing, or hybrid approaches should therefore be guided not only by achievable resolution, but also by intended production volume, process robustness, biofunctionalization reproducibility, long-term stability, and regulatory requirements [291]. Collectively, these trends define a translational pathway in which manufacturing, biointerface engineering, quality assurance, regulatory readiness, and application-specific validation are optimized together, as summarized in figure 10.

8.4. From laboratory prototypes to commercial biosensor manufacturing

Translation of nanofabricated biosensors from laboratory prototypes to commercial products requires manufacturing criteria that extend beyond analytical sensitivity and limit of detection. At the commercialization stage, device-to-device reproducibility, process yield, batch consistency, cost, packaging, calibration, regulatory compliance, and compatibility with high-throughput manufacturing become increasingly important. Consequently, fabrication strategies that provide exceptional performance at laboratory scale may remain difficult to translate if critical dimensions, surface properties, or sensing responses

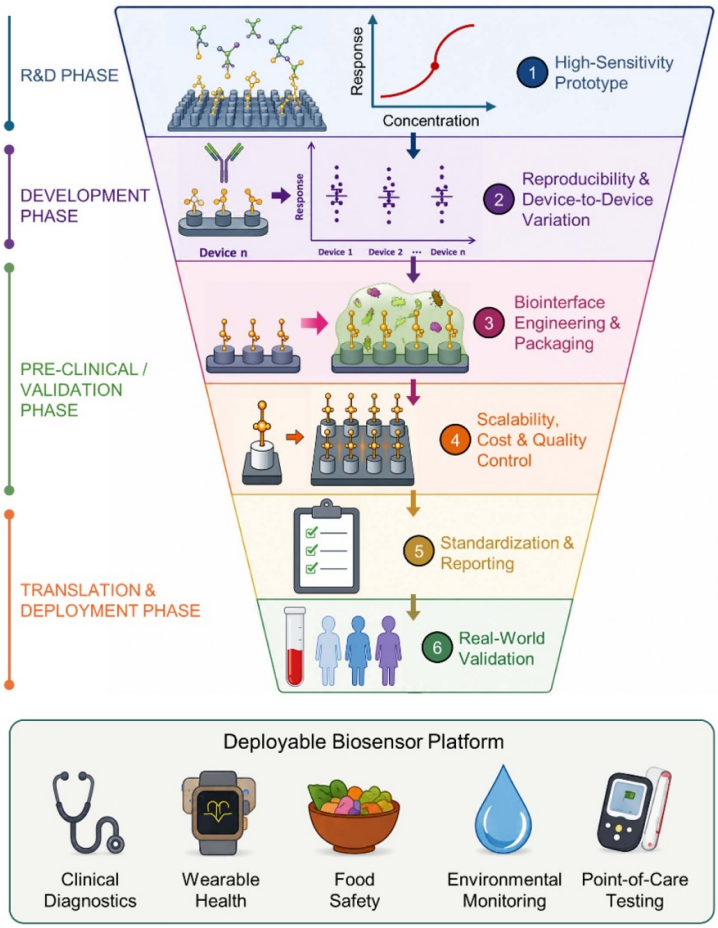


Figure 10. Translational funnel for nanofabricated biosensors. The schematic summarizes the progression from high-performance laboratory prototypes toward deployable biosensors through improved device reproducibility, stable biofunctionalization, scalable manufacturing, quality control, standardized validation, regulatory readiness, and real-world application testing.

cannot be reproduced across large numbers of devices. Commercial translation therefore requires the sensing architecture and its fabrication process to be considered as an integrated manufacturing system rather than as independent optimization problems.

Silicon nanowire field-effect transistor (SiNW-FET) biosensors illustrate this transition particularly clearly. Their compatibility with top-down semiconductor processing provides a potential route toward wafer-scale fabrication and integration, but process variability remains a major challenge because variations in nanowire geometry and fabrication conditions can produce substantial sensor-to-sensor differences [28, 306]. Controlled top-down fabrication has consequently become important not only for defining nanoscale features but also for improving electrical uniformity and analytical consistency. For example, controllable fabrication of SiNW arrays on silicon-on-insulator substrates has been shown to reduce current fluctuations and improve device uniformity, illustrating how process control can directly support manufacturing reproducibility [307]. CMOS-compatible fabrication further provides a route for integrating nanoscale sensing elements with established semiconductor processing and device-level architectures [308]. These examples demonstrate that the translational significance of top-down nanofabrication lies not only in dimensional precision but also in its potential to provide standardized and reproducible device production.

Wearable biosensors provide a more mature example of translation from sensing technology to commercial healthcare systems. Continuous glucose-monitoring platforms associated with companies such as Abbott, Dexcom, and Medtronic demonstrate that commercial viability depends not only on sensing performance but also on scalable and affordable manufacturing, long-term reliability, regulatory compliance, and interoperability with digital health ecosystems [309]. At the device level, this transition requires integration of the sensing interface with sampling, calibration, packaging, electronics, wireless communication, and user-facing readout. Emerging wearable platforms similarly illustrate this system-level shift

through the integration of microfluidic sampling, electrochemical sensing, calibration, wireless transmission, and smartphone-based interfaces. Thus, for wearable biosensors, successful translation increasingly depends on manufacturing and integrating the complete sensing system rather than optimizing the nanostructured sensing interface alone.

In contrast, single-molecule/nanopore and nanoparticle-based sensing illustrate technologies for which manufacturing translation remains less mature. Nanopore-FET architectures offer a potential path toward parallelized and scalable semiconductor fabrication for single-molecule detection, but recent literature remains focused primarily on device design, sensitivity enhancement, and manufacturability rather than established commercial biosensor production [310, 311]. Nanoparticle-enabled biosensors face a different manufacturing challenge: maintaining particle size, surface chemistry, functionalization, and analytical response across synthesis batches and production scales. Reviews of nanomaterial-assisted biosensors therefore identify reproducibility, validation, certification, cost, and batch variability as persistent barriers to commercialization [312, 313]. Continuous-flow and microfluidic synthesis strategies provide a relevant manufacturing direction because particle formation can be controlled under reproducible mixing conditions and scaled through parallelization rather than simply increasing batch volume.

Collectively, these examples show that the principal bottleneck in biosensor translation often shifts from achieving high analytical performance to reproducing that performance reliably at manufacturing scale. The relevant fabrication strategy must therefore be evaluated not only according to achievable resolution or sensitivity, but also according to process variability, yield, material consistency, integration complexity, quality control, and production cost. Technologies compatible with established manufacturing infrastructures, such as semiconductor processing for FET-based sensors, or with scalable system integration, as demonstrated by commercial wearable platforms, currently provide clearer routes toward translation. For emerging nanopore and nanoparticle-based systems, advances in parallel fabrication, automated synthesis, process monitoring, and standardized quality control will be important for narrowing the gap between laboratory demonstrations and reproducible commercial devices.

8.5. Materials availability and sustainability in biosensor nanofabrication

Sustainability is becoming an increasingly important consideration in biosensor nanofabrication as devices move toward large-scale and, in many cases, disposable production. High-performance biosensors frequently rely on noble metals such as Au, Ag, and Pt because of their favorable plasmonic, electrical, catalytic, and surface-functionalization properties. However, material cost, limited availability, and inefficient utilization can become increasingly relevant at manufacturing scale. These considerations are motivating strategies that reduce noble-metal loading, improve material utilization, or replace noble metals with alternative materials such as carbon-based structures, metal oxides, and other functional nanomaterials where compatible with the required sensing mechanism [314–316].

Environmental impact also originates from the fabrication process itself. Conventional micro- and nanofabrication can involve multiple lithography, deposition, etching, cleaning, and surface-modification steps that require substantial energy input and the use of photoresists, solvents, surfactants, etchants, and other process chemicals. Consequently, sustainability should be considered alongside resolution, throughput, and reproducibility when selecting a fabrication strategy. Material-efficient deposition, surfactant-free processing, additive manufacturing, and ambient- or low-temperature fabrication provide potential routes for reducing chemical consumption and process complexity while retaining the functional properties required for biosensing [317, 318].

The environmental burden is particularly relevant for single-use point-of-care, wearable, and microfluidic biosensors, where large-scale deployment can generate substantial quantities of polymeric and electronic waste. Petroleum-derived substrates and components that are difficult to recycle therefore introduce an additional manufacturing consideration beyond device performance. Renewable and biodegradable materials, including paper, cellulose and nanocellulose, chitosan, zein, and other biopolymer-based substrates, are increasingly being investigated as alternatives for disposable sensing platforms. For example, biodegradable zein nanofibers have been demonstrated as substrates for disposable SERS biosensors, while nanocellulose-coated paper has been investigated for point-of-care glucose detection [319, 320].

More broadly, sustainable biosensor manufacturing requires consideration of the complete device life cycle rather than substitution of a single material or fabrication step. Green nanoparticle synthesis, renewable substrates, additive and low-temperature processing, reduced use of hazardous chemicals, and design for recyclability or biodegradation can reduce environmental burden, but these approaches must still satisfy requirements for analytical performance, reproducibility, shelf life, scalability, and cost. Lifecycle assessment can therefore complement conventional manufacturing metrics by considering material

consumption, energy and water use, fabrication, and end-of-life pathways. Combining such environmental assessment with techno-economic analysis may ultimately provide a more meaningful basis for selecting scalable nanofabrication strategies for future biosensor manufacturing.

9. Conclusion

Nanofabrication has transformed biosensor development from the optimization of individual nanoscale structures into a broader manufacturing challenge that integrates patterning, materials engineering, biofunctionalization, fluid handling, and device assembly. Top-down lithography provides precise and deterministic control of sensing architectures, whereas scalable replication, transfer-based manufacturing, bottom-up self-assembly, additive fabrication, and flexible processing extend these capabilities toward larger-area, lower-cost, and application-compatible platforms. Increasingly, the most effective strategies combine these approaches rather than relying on a single fabrication route.

The next stage of biosensor nanofabrication will depend less on achieving smaller features or higher analytical sensitivity alone and more on translating nanoscale functionality into reproducible and manufacturable devices. Control of batch-to-batch variability, surface chemistry, biofouling, packaging, storage stability, and device-level integration must therefore advance alongside nanostructure design. AI-assisted process optimization and standardized quality-control frameworks may further accelerate this transition by linking fabrication parameters with structural characteristics and analytical performance. Ultimately, progress toward clinically and commercially relevant biosensors will require nanofabrication strategies that balance precision, scalability, reproducibility, biological compatibility, and system-level integration within robust manufacturing workflows.

Data availability statement

No new data were created or analysed in this study.

Author contributions

Meryem Beyza Avci
Conceptualization (equal), Writing – original draft (equal), Writing – review & editing (equal)

Furkan Kocer
Conceptualization (equal), Writing – original draft (equal), Writing – review & editing (equal)

Seda Nur Topkaya
Conceptualization (equal), Writing – original draft (equal), Writing – review & editing (equal)

Konstantinos Papatryfonos 0000-0002-1944-2752
Conceptualization (equal), Writing – original draft (equal), Writing – review & editing (equal)

Arif E Cetin 0000-0002-0788-8108
Conceptualization (equal), Funding acquisition (equal), Writing – original draft (equal), Writing – review & editing (equal)

References

[1] n.d. Biochips Market Growth Analysis-Size and Forecast 2024–2028 (available at: www.technavio.com/report/biochips-market-analysis)
[2] Lakhera P, Chaudhary V, Bhardwaj B, Kumar P and Kumar S 2022 *Biosens. Bioelectron. X* **11** 100218
[3] Blin G 2021 *Development* **148** dev186387
[4] Yadav A, Dogra P, Sagar P, Srivastava M, Srivastava A, Kumar R and Srivastava S K 2025 *Spectrochim. Acta A* **335** 126002
[5] Zoory M J and Altimime S M 2020 *Optik* **200** 163383
[6] Liu R, Cao L, Liu D, Wang L, Saeed S and Wang Z 2023 *Nanomaterials* **13** 1818
[7] Kumar A and Whitesides G M 1993 *Appl. Phys. Lett.* **63** 2002
[8] Chou S Y, Krauss P R and Renstrom P J 1995 *Appl. Phys. Lett.* **67** 3114
[9] Park M, Harrison C, Chaikin P M, Register R A and Adamson D H 1997 *Science* **276** 1401
[10] Maruo S, Nakamura O and Kawata S 1997 *Opt. Lett.* **22** 132
[11] Kasi D G, de Graaf M N S, Motreuil-Ragot P A, Frimat J-P M S, Ferrari M D, Sarro P M, Mastrangeli M, van den Maagdenberg A M J M, Mummery C L and Orlova V V 2021 *Micromachines* **13** 49

[12] Liu Z, Zhou Y, Lu J, Gong T, Ibáñez E, Cifuentes A and Lu W 2024 *Biomark. Res.* **12** 153
[13] Fruncillo S, Su X, Liu H and Wong L S 2021 *ACS Sens.* **6** 2002
[14] Alghannam F, Alayed M, Alfihed S, Sakr M A, Almutairi D, Alshamrani N and Fayez N A 2025 *Biosensors* **15** 76
[15] Altug H, Oh S-H, Maier S A and Homola J 2022 *Nat. Nanotechnol.* **17** 5
[16] Zhu C, Ekinci H, Pan A, Cui B and Zhu X 2024 *Microsystems Nanoeng.* **10** 52
[17] Rippa M *et al* 2022 *ACS Appl. Mater. Interfaces* **14** 4969
[18] Sloyan K, Melkonyan H, Apostoleris H, Dahlem M S, Chiesa M and Ghaferi A A 2021 *Nanotechnology* **32** 472004
[19] Höflich K *et al* 2023 *Appl. Phys. Rev.* **10** 041311
[20] Yang W, van Dijk M, Primavera C and Dekker C 2021 *iScience* **24** 103237
[21] Ignatane L, Ignatans R, Prikulis J, Trausa A, Tipaldi C F, Vanags E, Zubkins M, Smits K and Sarakovskis A 2024 *Nanomaterials* **14** 1784
[22] Roa S, Redondo C, Akinoglu G E, Pedano M L, Maguregui M, Sirena M and Morales R 2024 *Mater. Today Chem.* **38** 102101
[23] Koc N, Belarouci A, Oktem E and Aksu S 2024 *ACS Appl. Mater. Interfaces* **16** 32516
[24] Jiang K, Xie M, Tang Z, Zhang X and Yang D 2025 *Sensors* **25** 5906
[25] López-Muñoz G A, Cortés-Reséndiz A, Ramón-Azcón J and Rydosz A 2022 *Front. Sens.* **3** 945525
[26] Zhao H, Cao X, Dong Q, Song C, Wang L and Gao L 2023 *Nanoscale Adv.* **5** 1291
[27] Sharma E, Rathi R, Misharwal J, Sinhmar B, Kumari S, Dalal J and Kumar A 2022 *Nanomaterials* **12** 2754
[28] Tintelott M, Pachauri V, Ingebrandt S and Vu X T 2021 *Sensors* **21** 5153
[29] Xu J *et al* 2024 *Appl. Phys. Rev.* **11** 021411
[30] Karimi K, Fardoost A, Mhatre N, Rajan J, Boisvert D and Javanmard M 2024 *Micromachines* **15** 1274
[31] Fan J, Men Y, Tseng K H, Ding Y, Ding Y, Villarreal F, Tan C, Li B and Pan T 2018 *Biomicrofluidics* **12** 034107
[32] Chung H, Park J and Boriskina S V 2022 *Nanophotonics* **11** 1427
[33] Miranda I, Souza A, Sousa P, Ribeiro J, Castanheira E M S, Lima R and Minas G 2021 *J. Funct. Biomater.* **13** 2
[34] Venzac B 2025 *Lab Chip* **25** 2129
[35] Xu J, Harasek M and Gföhler M 2025 *Polymers* **17** 455
[36] Khumwan P *et al* 2025 *Biosensors* **15** 229
[37] Maize K, Mi Y, Cakmak M and Shakouri A 2023 *Adv. Mater. Technol.* **8** 2200173
[38] Crapnell R D and Banks C E 2024 *Anal. Methods* **16** 2625
[39] Ruggiero A, Criscuolo V, Grasselli S, Bruno U, Ausilio C, Bovio C L, Bettucci O and Santoro F 2022 *Chem. Commun.* **58** 9790
[40] Qu Y, Shen F, Peng H, Chen G, Wang L and Sun L 2024 *JACS Au* **4** 903
[41] Rahmani P, Goodlad M, Zhang Y, Li Y and Ye T 2022 *ACS Appl. Mater. Interfaces* **14** 47359
[42] He Z, Shi K, Li J and Chao J 2023 *iScience* **26** 106638
[43] Ijäs H, Trommler J, Nguyen L, van Rest S, Nickels P C, Liedl T and Urban M J 2025 *Nat. Commun.* **16** 3216
[44] Sytu M R C, Cho D H and Hahm J 2024 *Polymers* **16** 1267
[45] Hu X-H and Xiong S 2022 *Front. Nanotechnol.* **4** 762996
[46] Li L, Du F, Zong X, Cui L and Liu Y 2022 *Appl. Opt.* **61** 6924
[47] Ku C-A, Yu C-Y, Hung C-W and Chung C-K 2023 *Nanomaterials* **13** 2853
[48] Purwidyantri A and Prabowo B A 2022 *IEEE Nanotechnol. Mag.* **16** 20
[49] Balasa I G, Cesca T, Kalinic B, Piccotti D, Scian C and Mattei G 2021 *Appl. Surf. Sci.* **556** 149802
[50] Li D, Wu A, Wan Q and Li Z 2021 *Sci. Rep.* **11** 14929
[51] Geng G, Zhang Z, Li C, Pan R, Li Y, Yang H and Li J 2022 *Micromachines* **13** 856
[52] Hang Y, Boryczka J and Wu N 2022 *Chem. Soc. Rev.* **51** 329
[53] Vairaperumal T, Selvaraj D, Sasikumar G K and Liu P-Y 2026 *TrAC Trends Anal. Chem.* **203** 119003
[54] Cedrún-Morales M *et al* 2026 *J. Mater. Chem. C* **14** 5607
[55] Shafi N, Bhat A M, Parmar J S, Sahu C and Periasamy C 2022 *Silicon* **14** 9237
[56] Sung D and Koo J 2021 *Biomed. Eng. Lett.* **11** 85
[57] Yaman S, Avci M B, Kurul F, Topkaya S N and Cetin A E 2023 *Sensors Actuators A* **363** 114685
[58] Qaiser N, Suryaprabha T, Vetrano F, Hwang B and Elatab N 2026 *npj Flex. Electron.* **10** 23
[59] Park S, Kim S, Lee S, Tsukruk V V, Park S and Lim H 2025 *Adv. Electron. Mater.* **11** 202500010
[60] Xie L, Yang K, Wang M, Hou W and Ren Q 2025 *Biosensors* **15** 611
[61] Zhang T, Duolikun K, Zhang Z, Feng B, Liu K, Sun J and Zhao W 2026 *Coord. Chem. Rev.* **568** 218362
[62] Irannejad N and Rezaei B 2022 *Electrochemical Sensors* (Elsevier) pp 177–212
[63] Butler D and Ebrahimi A 2022 *Biosens. Bioelectron.* **208** 114198
[64] Lee J *et al* 2025 *Nat. Photon.* **19** 938
[65] Bhardwaj H, Hashmi Z, Singh A K, Kumar G, Lakshmi G B V S and Solanki P R 2025 *Nanoscale Adv.* **7** 196
[66] Wang P *et al* 2024 *Nat. Commun.* **15** 887
[67] Nowduri B, Britz-Grell A, Saumer M and Decker D 2023 *Nanotechnology* **34** 165301
[68] Oh D K, Lee T, Ko B, Badloe T, Ok J G and Rho J 2021 *Front. Optoelectron.* **14** 229
[69] Milenko K, Dullo F T, Thrane P C V, Skokic Z and Dirdal C A 2023 *Nanomaterials* **13** 1598
[70] Basu P, Verma J, Abhinav V, Ratnesh R K, Singla Y K and Kumar V 2025 *Int. J. Mol. Sci.* **26** 3027
[71] Stokes K, Clark K, Odetade D, Hardy M and Oppenheimer P G 2023 *Discov. Nano* **18** 153
[72] Jaiswal A, Rastogi C K, Rani S, Singh G P, Saxena S and Shukla S 2023 *iScience* **26** 106374
[73] Cheng X, Liang D, Jiang M, Sha Y, Liu X, Liu J, Cao Q and Shi J 2025 *Micromachines* **16** 667
[74] Papatryfonos K *et al* 2017 *J. Appl. Phys.* **121** 053101
[75] Papatryfonos K, de Oliveira E R C and Lanzillotti-Kimura N D 2024 *Proc. SPIE* 40
[76] Rodriguez A, Papatryfonos K, de Oliveira E R C and Lanzillotti-Kimura N D 2023 *Phys. Rev. B* **108** 205301
[77] Papatryfonos K, Rodriguez A, de Oliveira E R C and Lanzillotti-Kimura N D 2024 *Proc. SPIE* **12991** 25
[78] Papatryfonos K, Joshi S, Merghem K, Bouchoule S, Guilet S, Gratiet L L, Martinez A and Ramdane A 2014 *26th Int. Conf. Indium Phosphide and Related Materials* (IEEE) pp 1–2
[79] Hu J *et al* 2023 *Biosensors* **13** 645
[80] Butt M A, Akca B I and Mateos X 2025 *Nanomaterials* **15** 731
[81] Wang W, Arzubiaga L, Shayesteh M, Fenner S, Clark O and Charlton M D B 2025 *J. Vac. Sci. Technol. A* **43** 023405
[82] Mendoza-Castro J H, Vorobev A S, Iadanza S, Lendl B, O'Faolain L and Grande M 2024 *Opt. Express* **32** 13197

[83] Gharib G, Bütün İ, Muganlı Z, Kozalak G, Namlı İ, Sarraf S S, Ahmadi V E, Toyran E, van Wijnen A J and Koşar A 2022 *Biosensors* **12** 1023
[84] Zheng P, Wu L, Raj P, Kim J H, Paidi S K, Semancik S and Barman I 2024 *Adv. Sci.* **11** 202405910
[85] Unno N and Mäkelä T 2023 *Nanomaterials* **13** 2031
[86] Song L, Chen J, Xu B B and Huang Y 2021 *ACS Nano* **15** 18822
[87] Ahn J, Jang H, Jeong Y, Choi S, Ko J, Hwang S H, Jeong J, Jung Y S and Park I 2024 *Adv. Sci.* **11** 202303704
[88] Tahir U, Kim J I, Javeed S, Khaliq A, Kim J-H, Kim D-I and Jeong M Y 2022 *Nanomaterials* **12** 480
[89] Park Y, Kim J, Yang Y, Oh D K, Kang H, Kim H and Rho J 2025 *Adv. Sci.* **12** 202409371
[90] Cao Y, Ma D, Li H, Cui G, Zhang J and Yang Z 2025 *Chips* **4** 10
[91] Behrouzi K, Fard Z K, Chen C-M, He P, Teng M and Lin L 2025 *Nat. Commun.* **16** 4597
[92] Ferrari E 2023 *Biosensors* **13** 411
[93] Melgarejo K, Del Barrio M, Benito-Peña E, Mirea T and Barrios C A 2025 *Plasmonics* **20** 9951
[94] Zheng D, Kashif M F, Piscopo L, Collard L, Ciracì C, De Vittorio M and Pisanello F 2024 *ACS Photonics* **11** 3774
[95] Pandey P, Seo M-K, Shin K H, Lee Y-W and Sohn J I 2022 *Nanomaterials* **12** 401
[96] Guan T *et al* 2024 *ACS Appl. Mater. Interfaces* **16** 40286
[97] Colombelli A, Lospinoso D, Rella R and Manera M G 2022 *Nanomaterials* **12** 547
[98] Kim W H, Lee S, Jeon M J, Lee K J, Park J, Park D W, Park S and Sim S J 2025 *Adv. Sci.* **12** 202414688
[99] Li R, Fan H, Zhou H, Chen Y, Yu Q, Hu W, Liu G L and Huang L 2023 *Adv. Sci.* **10** 202301658
[100] Ayoib A *et al* 2024 *Int. J. Nanoelectron. Mater.* **17** 143
[101] Liu Y and Zhang X 2021 *Micromachines* **12** 826
[102] Feng X, Zhao J, Wu S, Kan Y, Li H and Zhang W 2025 *Chemosensors* **13** 200
[103] Kang S and Davis J J 2025 *Chem. Sci.* **16** 6965
[104] Tintelott M, Gharpure P, Coffinier Y, Vu X T, Vlandas A, Ingebrandt S and Pachauri V 2023 *Phys. Fluids* **35** 042016
[105] Xiao C, Eriksson J, Suska A, Filippini D and Mak W C 2022 *Anal. Chim. Acta* **1201** 339606
[106] Sekhwama M, Mpofu K, Sudesh S and Mthunzi-Kufa P 2024 *Discov. Appl. Sci.* **6** 458
[107] Wang Z, Shah A, Lee H and Lee C H 2025 *Lab Chip* **25** 4542
[108] Zhang Y, Duan H, Li G, Peng M, Ma X, Li M and Yan S 2022 *J. Nanobiotechnol.* **20** 246
[109] Shakeri A, Khan S and Didar T F 2021 *Lab Chip* **21** 3053
[110] Grant J, Özkan A, Oh C, Mahajan G, Prantil-Baun R and Ingber D E 2021 *Lab Chip* **21** 3509
[111] Rodrigues R G, Condelipes P G M, Rosa R R, Chu V and Conde J P 2023 *Micromachines* **14** 1837
[112] Shakeri A, Khan S, Jarad N A and Didar T F 2022 *Materials* **15** 6478
[113] Shakeri A, Jarad N A, Khan S and Didar T F 2022 *Anal. Chim. Acta* **1209** 339283
[114] Arshavsky-Graham S, Enders A, Ackerman S, Bahnemann J and Segal E 2021 *Microchim. Acta* **188** 67
[115] Jeon E *et al* 2024 *Nat. Commun.* **15** 1366
[116] Papatryfonos K *et al* 2021 *Appl. Sci.* **11** 6098
[117] Ali M A, Hu C, Yuan B, Jahan S, Saleh M S, Guo Z, Gellman A J and Panat R 2021 *Nat. Commun.* **12** 7077
[118] Kalita N, Gogoi S, Minteer S D and Goswami P 2023 *ACS Meas. Sci. Au* **3** 404
[119] Sun Y *et al* 2023 *npg Asia Mater.* **15** 6
[120] Li C, Liu F, Han R and Zhuang Y 2021 *IEEE Access* **9** 63602
[121] Li Y *et al* 2024 *Biosensors* **14** 144
[122] Zhou X, Liu S, Xiang H, Li X, Wang C, Wu Y and Li G 2025 *Biosensors* **15** 555
[123] Dadras-Toussi O, Khorrami M, Titus A S C L S, Majd S, Mohan C and Abidian M R 2022 *Adv. Mater.* **34** 202200512
[124] Milton L A, Viglione M S, Ong L J Y, Nordin G P and Toh Y-C 2023 *Lab Chip* **23** 3537
[125] Luo Z, Zhang H, Chen R, Li H, Cheng F, Zhang L, Liu J, Kong T, Zhang Y and Wang H 2023 *Microsyst. Nanoeng.* **9** 103
[126] Lu H, Rakhymzhanov A, Buttner U and Alsulaiman D 2024 *ACS Omega* **9** 38096
[127] Cho Y, Choi Y, Jang Y and Seong H 2025 *Adv. Healthcare Mater.* **14** 202500189
[128] Suh K, Park M C and Kim P 2009 *Adv. Funct. Mater.* **19** 2699
[129] Wang H *et al* 2020 *Small* **16** 201905480
[130] Bae C W, Toi P T, Kim B Y, Lee W I, Lee H B, Hanif A, Lee E H and Lee N-E 2019 *ACS Appl. Mater. Interfaces* **11** 14567
[131] Kim I, Mun J, Hwang W, Yang Y and Rho J 2020 *Microsyst. Nanoeng.* **6** 65
[132] Lv G, Tian H, Shao J and Yu D 2022 *RSC Adv.* **12** 9681
[133] Gomes P D C, Hin-Chu M, Rickard J J S and Oppenheimer P G 2024 *Adv. Sci.* **11** 202306068
[134] Siva S, Bodkhe G A, Cong C, Kim S and Kim M 2024 *Chem. Eng. J.* **479** 147492
[135] Moore F, Schmueser I, Terry J G and Mount A R 2025 *Faraday Discuss.* **257** 360
[136] Hirbodvash Z, Houache M S E, Krupin O, Khodami M, Northfield H, Olivieri A, Baranova E A and Berini P 2021 *Chemosensors* **9** 277
[137] Liu W C, Chou V H Y, Behera R P and Ferrand H L 2022 *Nat. Commun.* **13** 5015
[138] Meng X, Li S, Shen X, Tian C, Mao L and Xie H 2024 *Nat. Commun.* **15** 10442
[139] Panina L V, Gurevich A, Beklemisheva A, Omelyanchik A, Levada K and Rodionova V 2022 *Cells* **11** 950
[140] Borah R, Ag K R, Minja A C and Verbruggen S W 2023 *Small Methods* **7** 2201536
[141] Hou S, Bai L, Lu D and Duan H 2023 *Acc. Chem. Res.* **56** 740
[142] Qi X, Pérez L A, Mendoza-Carreño J, Garriga M, Alonso M I and Mihi A 2025 *Nat. Commun.* **16** 1687
[143] Ye Z, Li C, Chen Q, Xu Y and Bell S E J 2021 *Nanoscale* **13** 5937
[144] Scarabelli L, Vila-Liarte D, Mihi A and Liz-Marzán L M 2021 *Acc. Mater. Res.* **2** 816
[145] Alsadig A, Abbasgholi-NA B, Vondracek H, Medagli B, Fortuna S, Posocco P, Parisse P, Cabrera H and Casalis L 2022 *Nanomaterials* **13** 78
[146] Dass M, Gür F N, Kołątaj K, Urban M J and Liedl T 2021 *J. Phys. Chem. C* **125** 5969
[147] Dey S *et al* 2021 *Nat. Rev. Methods Prim.* **1** 13
[148] Pfeiffer M, Trofymchuk K, Ranallo S, Ricci F, Steiner F, Cole F, Glembockyte V and Tinnefeld P 2021 *iScience* **24** 103072
[149] Kaur C, Kaur V, Rai S, Sharma M and Sen T 2023 *Nanoscale* **15** 6170
[150] Tsang E, Scarpellini C, Dillen A, Jeminejs A, Von t. sivertsen M, Sutherland D S, Lammertyn J and Gothelf K V 2025 *Small Methods* **9** 202502111
[151] Domljanovic I, Loretan M, Kempter S, Acuna G P, Kocabey S and Ruegg C 2022 *Nanoscale* **14** 15432

[152] Sun S, Shu X, Chen X, Wang F, Qiang X-L, Xiao Q-R and Shi X-L 2025 *RSC Adv.* **15** 34473
[153] Kido S, Takahashi N, Miyazaki H, Kono S, Saito K and Kuzuya A 2025 *ACS Omega* **10** 43300
[154] Williamson P, Piskunen P, Ijäs H, Butterworth A, Linko V and Corrigan D K 2023 *ACS Sens.* **8** 1471
[155] Jeon B, Guareschi M M, Stewart J M, Wu E, Gopinath A, Arroyo-Currás N, Dauphin-Ducharme P, Plaxco K W, Lukeman P S and Rothemund P W K 2025 *Proc. Natl Acad. Sci.* **122** e2311279121
[156] Shen Q *et al* 2023 *J. Am. Chem. Soc.* **145** 1292
[157] Ghamari S, Chiarelli G, Kołątaj K, Subramanian S, Acuna G P and Vollmer F 2025 *Nanophotonics* **14** 253
[158] Fang Y, Chen X, Qi Q, Lin M and Liang Q 2026 *Adv. Sci.* **13** 202513357
[159] Hao Z, Kong L, Ruan L and Deng Z 2024 *Nanomaterials* **14** 1968
[160] Niu R, Tao M and Chao J 2025 *Chemistry* **7** 165
[161] Lu M, Peng W, Lin M, Wang F and Zhang Y 2021 *Nanomaterials* **11** 616
[162] Singh M *et al* 2022 *ACS Appl. Mater. Interfaces* **14** 12824
[163] Zhang J, Chen Y, Li G, Sun Z, Meng Z and Wong W-Y 2025 *Sci. China Chem.* **68** 2027
[164] Fornerod M J J, Alvarez-Fernandez A, Füredi M, Rajendran A A, Prieto-Simón B, Voelcker N H and Guldin S 2025 *Nanoscale Horiz.* **10** 760
[165] Alvarez-Fernandez A, Maiz J, Faustini M, Stefik M, Soler-Illia G J A A and Guldin S 2026 *Acc. Mater. Res.* **7** 88
[166] Chung Y-H and Oh J K 2024 *Biosensors* **14** 542
[167] Ju J and Hayward R C 2024 *ACS Appl. Mater. Interfaces* **16** 34079
[168] Abeysekera I, Bosire R, Masese F K, Ndaya D and Kasi R M 2024 *Soft Matter* **20** 6834
[169] Kim J, Kang J H, Kwon W H, Lee I, Park S J, Kim C-H, Jeong W, Choi J S and Kim K 2023 *Biomater. Res.* **27** 127
[170] Deng D, Chang Y, Liu W, Ren M, Xia N and Hao Y 2023 *Biosensors* **13** 773
[171] Li T, Lu X-M, Zhang M-R, Hu K and Li Z 2022 *Bioact. Mater.* **11** 268
[172] Noguchi H, Nakamura Y, Tezuka S, Seki T, Yatsu K, Narimatsu T, Nakata Y and Hayamizu Y 2023 *ACS Appl. Mater. Interfaces* **15** 14058
[173] Mu R, Zhu D, Abdulmalik S, Wijekoon S, Wei G and Kumbar S G 2024 *Bioact. Mater.* **35** 181
[174] Uchida J, Niwa A, Hasome M, Makiura R, Abbott N L and Kato T 2023 *ACS Appl. Mater. Interfaces* **15** 36657
[175] Yan Y, Guo L, Geng H and Bi S 2023 *Small* **19** 202301654
[176] Miller M A and Medina S 2024 *WIREs Nanomed. Nanobiotechnol.* **16** e1966
[177] Wang R, Wang X, Wang Y and Wei G 2025 *Biosensors* **15** 328
[178] Wang Y *et al* 2025 *Mater. Today Bio* **35** 102382
[179] Lu F, Yang J H and Koh A 2025 *Lab Chip* **25** 6550
[180] Dorsainvil J S, Batayneh J, McDonald M, Pachter N, Patel S, Manashirov D, Hookway T and Koh A 2025 *Adv. Mater. Technol.* **10** 202500342
[181] Inukonda S M and Panda S 2025 *npj Flex. Electron.* **9** 100
[182] Zhang T, Chai Y, Wang S, Yu J, Jiang S, Zhu W, Fang Z and Li B 2023 *Sensors* **23** 9743
[183] Wang H, Zhao Z, Liu P and Guo X 2022 *npj Flex. Electron.* **6** 26
[184] Zou Y *et al* 2023 *Polymers* **15** 3553
[185] Lee B, Cho H, Jeong S, Yoon J, Jang D, Lee D K, Kim D, Chung S and Hong Y 2022 *J. Inf. Disp.* **23** 163
[186] Pietsch M, Schlisske S, Held M, Maag P and Hernandez-Sosa G 2022 *Flex. Print. Electron.* **7** 025007
[187] Gul O, Song M, Gu C-Y, Ahn J, Lee K, Ahn J, Kim H J, Kim T-S and Park I 2025 *Nat. Commun.* **16** 1337
[188] Kim S, Kang J, Lee I, Jang J, Park C B, Lee W and Bae B-S 2023 *npj Flex. Electron.* **7** 33
[189] Li J, Ding Q, Wang H, Wu Z, Gui X, Li C, Hu N, Tao K and Wu J 2023 *Nano-Micro Lett.* **15** 105
[190] Lin P-H, Sheu S-C, Chen C-W, Huang S-C and Li B-R 2022 *Talanta* **241** 123187
[191] Duan H, Peng S, He S, Tang S, Goda K, Wang C H and Li M 2025 *Adv. Sci.* **12** 202411433
[192] Wen B, Yang J, Hu C, Cai J and Zhou J 2024 *Adv. Mater. Interfaces* **11** 202300856
[193] Chen L, Liu P, Feng B, Shu Z, Liang H, Chen Y, Dong X, Xie J and Duan H 2023 *Adv. Mater.* **35** 202303513
[194] Kim H H, Kim K, Yang J and Choi M K 2024 *Adv. Mater. Technol.* **9** 202301262
[195] Wang M, Yang Y and Gao W 2021 *Trends Chem.* **3** 969
[196] Wang H, Zhao Z, Liu P and Guo X 2022 *Biosensors* **12** 55
[197] Pinheiro T, de Almeida H V, Nunes D, Martins R and Fortunato E 2025 *Mater. Horizons* **12** 8194
[198] Devi M, Wang H, Moon S, Sharma S and Strauss V 2023 *Adv. Mater.* **35** 202211054
[199] Le K-V *et al* 2025 *Nanoscale Horiz.* **10** 2688
[200] Li Z, Huang L, Cheng L, Guo W and Ye R 2024 *Small Methods* **8** 202400118
[201] Liao J, Zhang X, Sun Z, Chen H, Fu J, Si H, Ge C and Lin S 2022 *Biosensors* **12** 397
[202] Vivaldi F, Dallinger A, Poma N, Bonini A, Biagini D, Salvo P, Borghi F, Tavanti A, Greco F and Di Francesco F 2022 *APL Bioeng.* **6** 036104
[203] Zhu J *et al* 2021 *Biosens. Bioelectron.* **193** 113606
[204] Sun H, Song S, Zhao G, Wang X and Liu G 2023 *Adv. Mater. Interfaces* **10** 202300281
[205] De Chiara B *et al* 2025 *ACS Appl. Mater. Interfaces* **17** 3772
[206] Kang L, Jiang J, Liu S, Ai J, Hong J, Tang C, Jun S C, Yamauchi Y and Zhang J 2025 *Small* **21** 202412044
[207] Clark K M, Nekoba D T, Viernes K L, Zhou J and Ray T R 2024 *Biosens. Bioelectron.* **264** 116649
[208] Jamshidnejad-Tosaramandani T, Kashanian S, Omidfar K and Schiöth H B 2025 *Biosensors* **15** 451
[209] Veenuttranon K, Kaewpradub K and Jeerapan I 2023 *Nano-Micro Lett.* **15** 85
[210] Panáček D, Urban M, Silvestri A, Dědek I, Nalepa M, Merkoçi A, Prato M and Otyepka M 2026 *Small* **22** 202513028
[211] Boček Ž, Zubak M and Kassal P 2025 *Biosensors* **15** 28
[212] Khosravi S, Soltanian S, Servati A, Khademhosseini A, Zhu Y and Servati P 2023 *Biosensors* **13** 684
[213] Niamsi W, Larpant N, Kalambate P K, Primpray V, Karuwan C, Rodthongkum N and Laiwattanapaisal W 2022 *Biosensors* **12** 852
[214] Song J *et al* 2025 *Mater. Today Bio* **32** 101667
[215] Poletti F, Zanfrognini B, Favaretto L, Quintano V, Sun J, Treossi E, Melucci M, Palermo V and Zanardi C 2021 *Sens. Actuators B* **344** 130253
[216] Myndrul V, Coy E, Babayevska N, Zahorodna V, Balitskyi V, Baginskiy I, Gogotsi O, Bechelany M, Giardi M T and Iatsunskyi I 2022 *Biosens. Bioelectron.* **207** 114141
[217] Wang L, Li M, Ya S, Tian H, Li K, Zhang Q, Li Y, Wang H and Hou C 2025 *Biosensors* **15** 531

[218] Zhang W, Jiang S, Yu H, Feng S and Zhang K 2025 *iScience* **28** 111737
[219] Nguyen T T, Zhou L, Kong J, Luo A, Hao Z and Zhang J 2025 *Biosensors* **15** 804
[220] Gunasekaran N K, Jalajamony H M, Adhinarayanan S, De S, Adu R, Strobel S, Ramesh G T and Fernandez R E 2025 *Sci. Rep.* **15** 22380
[221] Zhang A *et al* 2024 *Sci. China Mater.* **67** 251
[222] Napier B, Matzeu G and Omenetto F G 2024 *Commun. Mater.* **5** 246
[223] Liu L-X, Chen W, Zhang H-B, Ye L, Wang Z, Zhang Y, Min P and Yu Z-Z 2022 *Nano-Micro Lett.* **14** 111
[224] Shao Q, Xing B, Du Z and Yu W 2024 *Polymers* **16** 3137
[225] Chowdhury M-U-S, Roy S, Aryal K P, Leung H and Pandey R 2024 *ACS Mater. Au* **4** 592
[226] Du S, Tan Y, Chen J, Wei Y, Qu Z, Li J, Zhang J and Zhou W 2024 *Compos. Commun.* **52** 102122
[227] Lim T, Zhang H and Lee S 2021 *APL Mater.* **9** 091113
[228] Busolo T, Szewczyk P K, Nair M, Stachewicz U and Kar-Narayan S 2021 *ACS Appl. Mater. Interfaces* **13** 16876
[229] Pour S R S, Calabria D, Emamiamin A, Lazzarini E, Pace A, Guardigli M, Zangheri M and Mirasoli M 2024 *Biosensors* **14** 29
[230] Wu C-H, Ma H J H, Baessler P, Balanay R K and Ray T R 2023 *Sci. Adv.* **9** adg4272
[231] Wang M *et al* 2022 *Nat. Biomed. Eng.* **6** 1225
[232] Tu J *et al* 2025 *Sci. Adv.* **11** eadx6491
[233] Liao C, Li S, Yang C, Du C, Yao H, Han Z, Stachewicz U and Liu Y 2025 *Talanta* **287** 127683
[234] Shin S *et al* 2025 *Sci. Adv.* **11** eadw9024
[235] Min J, Tu J, Xu C, Lukas H, Shin S, Yang Y, Solomon S A, Mukasa D and Gao W 2023 *Chem. Rev.* **123** 5049
[236] Brasier N *et al* 2024 *Nature* **636** 57
[237] Ma X *et al* 2023 *Sci. Adv.* **9** eadj2763
[238] Liu G, Lv Z, Batool S, Li M, Zhao P, Guo L, Wang Y, Zhou Y and Han S 2023 *Small* **19** 2207879
[239] Xu J, Fang Y and Chen J 2021 *Biosensors* **11** 245
[240] Park C *et al* 2025 *Nat. Commun.* **16** 5808
[241] Song Y, Mukasa D, Zhang H and Gao W 2021 *Acc. Mater. Res.* **2** 184
[242] Chen R-S, Gao M, Chu D, Cheng W and Lu Y 2024 *Nano Energy* **128** 109960
[243] Kwon Y, Kim J, Kim H, Kang T W, Lee J, Jang S S, Lee Y and Yeo W-H 2024 *ACS Appl. Mater. Interfaces* **16** 68016
[244] Kim J, Kim J, Kim J, Hyeong Y, Neseli B, You J, Shim J, Shin J, Park H and Kurt H 2025 *Nanophotonics* **14** 121
[245] Papatryfonos K *et al* 2021 *AIP Adv.* **11** 025327
[246] Yang Y, Liu K, Gao Y, Wang C and Cao L 2025 *Light: Sci. Appl.* **14** 250
[247] Gostimirovic D, Xu D-X, Liboiron-Ladouceur O and Grinberg Y 2022 *ACS Photonics* **9** 2623
[248] Gostimirovic D, Grinberg Y, Xu D-X and Liboiron-Ladouceur O 2023 *ACS Photonics* **10** 1953
[249] van Haagen S, Nur S and Ishihara R 2025 *ACS Appl. Opt. Mater.* **3** 998
[250] Smith P R, Papatryfonos K and Selviah D R 2025 *Nanomaterials* **15** 1645
[251] O' Brien P, Marris-Morini D and Van Thourhout D 2026 *Proc. SPIE* **14100** 65
[252] Sciamanna M, Mørk J and Lin F-Y 2026 *Proc. SPIE* **14090** 42
[253] Venkatesan S, Cullinan M A and Baldea M 2025 *Rev. Chem. Eng.* **41** 311
[254] Johnson J E, Jamil I R, Pan L, Lin G and Xu X 2025 *Light Sci. Appl.* **14** 56
[255] Osipov A, Fumina A, Belyanov I, Speshilova A, Endiiarova E and Gerdt A 2026 *ACS Omega* **11** 23945
[256] Nguyen T S, Gafurov A N, Jo J, Lee T-M, Lee S-H and Kim K 2023 *Polymers* **15** 2909
[257] Dehaerne E, Dey B, Blanco V and Davis J 2025 *J. Micro/Nanopatterning, Mater. Metrol.* **24** 020901
[258] Shen M *et al* 2024 *Sci. Rep.* **14** 19287
[259] Zhu J, Liu J, Xu T, Yuan S, Zhang Z, Jiang H, Gu H, Zhou R and Liu S 2022 *Int. J. Extrem. Manuf.* **4** 032001
[260] Liu J *et al* 2025 *Int. J. Extrem. Manuf.* **7** 015601
[261] Shinde P P, Pai P P, Adiga S P, Mayya K S, Seo Y, Hwang M, Go H and Park C 2025 *Heliyon* **11** e43377
[262] Chien J and Lee E 2026 *Micromachines* **17** 674
[263] Kim J, Ko J, Choi H and Kim H 2021 *Sensors* **21** 4968
[264] Tercan H and Meisen T 2022 *J. Intell. Manuf.* **33** 1879
[265] Papatryfonos K, Rodary G, David C, Lelarge F, Ramdane A and Girard J-C 2015 *Nano Lett.* **15** 4488
[266] Papatryfonos K, Girard J, Tang M, Deng H, Seeds A J, David C, Rodary G, Liu H and Selviah D R 2025 *Adv. Photonics Res.* **6** 2400082
[267] Chen X and Lv H 2022 *npg Asia Mater.* **14** 69
[268] Wang F, Parhizkar M, Harker A and Edirisinghe M 2025 *Digit. Discov.* **4** 3066
[269] Wu T *et al* 2025 *Nat. Commun.* **16** 1473
[270] Gao F *et al* 2025 *Nat. Commun.* **16** 7558
[271] Low A K Y *et al* 2024 *npj Comput. Mater.* **10** 104
[272] Volk A A, Epps R W, Yonemoto D T, Masters B S, Castellano F N, Reyes K G and Abolhasani M 2023 *Nat. Commun.* **14** 1403
[273] Hu H, Wang H, Huang X, Geng Y, Xu J and Yuan Z 2025 *Small* **21** e04547
[274] Han C, Dong X, Zhang W, Huang X, Gong L and Su C 2025 *Nanomaterials* **15** 631
[275] Konstantopoulos G, Koumoulos E P and Charitidis C A 2022 *Nanomaterials* **12** 2646
[276] Wei D, Wang Z, Lin H, Yin X P and Wang Y 2026 *ACS Omega* **11** 10971
[277] Li Z, Song P, Li G, Han Y, Ren X, Bai L and Su J 2024 *Mater. Today Bio* **25** 101014
[278] Jiang P, Dai Y, Hou Y, Stein J, Lin S S, Zhou C, Hou Y, Zhu R, Lee K and Yang L 2025 *BMEMat* **3** e70004
[279] Szymanski N J, Zeng Y, Huo H, Bartel C J, Kim H and Ceder G 2021 *Mater. Horizons* **8** 2169
[280] Jiang Y, Salley D, Sharma A, Keenan G, Mullin M and Cronin L 2022 *Sci. Adv.* **8** eabo2626
[281] Park J, Kim Y M, Hong S, Han B, Nam K T and Jung Y 2023 *Matter* **6** 677
[282] Fernandez-Cuesta I, West M M, Montinaro E, Schwartzberg A and Cabrini S 2019 *Lab Chip* **19** 2394
[283] Zaki M, Prinz C and Ruehle B 2025 *ACS Nano* **19** 9029
[284] Keawmuang H, Hu S, Badloe T, So S and Rho J 2025 *ACS Appl. Mater. Interfaces* **17** 33259
[285] Wang A, Hang Y, Wang J, Tan W and Wu N 2024 *J. Phys. Chem. C* **128** 12495
[286] Xu X, Zhu B, Zeng Y and Qi Y 2025 *Microchem. J.* **218** 115687
[287] Zhu S, Zhang J, He X, Ding L, Luo X and Wen W 2026 *Int. J. Mol. Sci.* **27** 3305
[288] Baek S J and Lee M 2025 *PeerJ. Comput. Sci.* **11** e2895

[289] Cui C, Zheng K, Liu J, Chen C and Sun X 2026 *Results Eng.* **30** 110173
[290] Lupoiu R, Shao Y, Dai T, Mao C, Edée K and Fan J A 2025 *Sci. Adv.* **11** eadx8006
[291] Zhou G and Liu H 2026 *Biosensors* **16** 112
[292] Carvalho J H S, Catai M A S, Bertolim L V, Freitas R C, Camargo J R, Brazaca L C and Janegitz B C 2026 *Biosensors* **16** 98
[293] Shi X, Pu H, Shi L L, He T-C and Chen J 2025 *Nanoscale* **17** 9804
[294] Park Y M *et al* 2026 *Adv. Sci.* **13** e22897
[295] Postma E J, Scheres L, de Beer S, Kuzmyn A R and Zuilhof H 2025 *Adv. Mater. Interfaces* **12** 2400955
[296] Smail S M, Laibinis P E and Weiss S M 2025 *ACS Omega* **10** 31932
[297] Vasilescu A, Gáspár S, Gheorghiu M, Polonschii C, Banciu R M, David S, Gheorghiu E and Marty J-L 2025 *Chemosensors* **13** 92
[298] Docherty N, Macdonald D, Gordon A, Dobrea A, Mani V, Fu Y, Pang S, Jimenez M and Corrigan D K 2025 *Chem. Commun.* **61** 13359
[299] Chhillar M, Bhatt P, Kukkar D and Yadav A K 2026 *Biosens. Biomol. Electron.* **1** 3
[300] Wu J, Liu H, Chen W, Ma B and Ju H 2023 *Nat. Rev. Bioeng.* **1** 346
[301] Du Y, Reitemeier J, Jiang Q, Bappy M O, Bohn P W and Zhang Y 2024 *Small* **20** 2304966
[302] Janićijević Ž and Baraban L 2025 *ACS Sens.* **10** 2431
[303] Babamiri B, Farrokhnia M, Mohammadi M and Nezhad A S 2025 *Sci. Rep.* **15** 8859
[304] Wang M *et al* 2025 *Nat. Mater.* **24** 589
[305] Ulucan-Karnak F, Kuru C İ and Akgöl S 2024 *Front. Nanotechnol.* **6** 1348308
[306] Coffer J L 2022 *Semiconducting Silicon Nanowires for Biomedical Applications* (Elsevier) pp 401–12
[307] Lu Z, Zhou H, Wang Y, Liu Y and Li T 2022 *Nano Res.* **15** 7468
[308] Delacour C, Veliev F, Crozes T, Bres G, Minet J, Ionica I, Ernst T, Briançon-Marjollet A, Albrieux M and Villard C 2021 *Adv. Eng. Mater.* **23** 2001226
[309] Sedighi A, Kou T, Huang H and Li Y 2026 *Nano-Micro Lett.* **18** 16
[310] Liang L, Qin F, Wang S, Wu J, Li R, Wang Z, Ren M, Liu D, Wang D and Astruc D 2023 *Coord. Chem. Rev.* **478** 214998
[311] Verhulst A S, Ruic D, Willems K and Van Dorpe P 2022 *IEEE Sens. J.* **22** 5732
[312] Wan K, Jiang S, Chen S, Xing Y, Wu J and Guo Y 2024 *Alex. Eng. J.* **102** 82
[313] Chicea D and Nicolae-Maranciuc A 2025 *Materials* **18** 1809
[314] Montes-García V, Squillaci M A, Diez-Castellnou M, Ong Q K, Stellacci F and Samorì P 2021 *Chem. Soc. Rev.* **50** 1269
[315] Choi H K, Lee M-J, Lee S N, Kim T-H and Oh B-K 2021 *Front. Chem.* **9** 672739
[316] Pandey M, Bhaiyya M, Rewatkar P, Zalke J B, Narkhede N P and Haick H 2025 *Adv. Healthcare Mater.* **14** 2500400
[317] Rafati N, Hashemzadeh H, Jafarzadeh S, Saievar-Iranizad E and Naderi-Manesh H 2024 *Microchem. J.* **207** 112233
[318] Adimule V, Manhas N and Nandi S 2024 pp 191–204
[319] Turasan H, Cakmak M and Kokini J 2022 *J. Appl. Polym. Sci.* **139** e52622
[320] Hossain L, De Francesco M, Tedja P, Tanner J and Garnier G 2022 *Front. Bioeng. Biotechnol.* **10** 1052242